#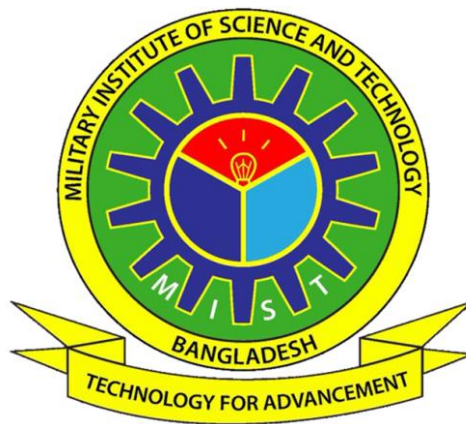 Numerical and Experimental Investigation of Non-Circular Free Jet with and without Peripheral Twist for Improvement in Mass Entrainment, Mixing and Turbulence Characteristics

Md. Touhidur Rahman Evan

(Bsc Eng , MIST)

A THESIS SUBMITTED FOR THE DEGREE OF MASTER OF
SCIENCE IN MECHANICAL ENGINEERING
DEPARTMENT OF MECHANICAL ENGINEERING
MILITARY INSTITUTE OF SCIENCE & TECHNOLOGY

2018

Approval

The thesis titled **"Numerical and Experimental Investigation of Non-Circular Free Jet with and without Peripheral Twist for Improvement in Mass Entrainment, Mixing and Turbulence Characteristics"**, Submitted by Md. Touhidur Rahman Evan **Roll no:** 1015180008(P) **Session**: April 2015 has been accepted in partial fulfillment of the requirement for the degree of Masters of Science (M.Sc.) in Mechanical Engineering.

BOARD OF EXAMINARS

1.   **Chairman**

   _____
   Wg Cdr Dr. Vikram Deshpande
   Instr Cl A
   Military Institute of Science and Technology

2.   **Member**

   _____
   Dr. M. A. Taher Ali
   Professor
   Military Institute of Science and Technology

3.   **Member**

   _____
   Dr. Md Shahnewaz Bhuiyan
   Associate Professor
   Military Institute of Science and Technology

4.   **Member**
   (Ex-officio)

   _____
   Col Md Humayun Kabir Bhuiyan
   Head of ME Dept
   Military Institute of Science and Technology

5.   **Member**
   (External)

   _____
   Dr. Maglub Al Nur
   Professor
   Bangladesh University of Engineering & Technology

Military Institute of Science & Technology

Declaration

I hereby declare that, this thesis is my original work and it has been written by me in its entirety. I have duly acknowledged all the sources of information which have been used in the thesis.

This thesis has also not been submitted for any degree in any university previously.

Md.Touhidur Rahman Evan

Acknowledgement

Abstract

Free jet flow is a basic flow configuration found in wide range of applications, majority of them being mixing, heating or cooling. The present study is therefore focused to improve the performance of the free turbulent jets within its 'developing zone' using two different mechanisms viz. (a) use of non-circular cross section jet and (b) introduction of swirl to jet by means of peripheral twist. The present research considers experimental and computational study of circular and non-circular turbulent jets (having Reynolds number 7.2×10^4 based on jet exit diameter). A 'jet modifier pipe', is used for the creation of circular and non-circular jets. Essentially, jet modifier pipe is small pipe through which circular jet is gradually changed to non-circular jet. Axial center line velocity, jet spread rate, potential core length and jet velocity profiles at various downstream locations are measured both experimentally and computationally. Turbulence intensity and tangential velocities at different downstream locations of the jet are determined numerically.

The comparison of local jet velocity along jet axis indicates that the deceleration of axial velocity for triangular jet is maximum while that for circular jet is minimum which is indicating maximum potential core length for circular jet. A consistent observation is also showcased by jets wherein, the potential core length for circular jet is maximum, while non-circular jets show lower core length. The peak turbulence intensity location is found closer to jet exit for triangular and rectangular jets which is an indicator of efficient mixing. Rectangular jets show saddle shape profile at downstream of the pipe exit. The rectangular jet possesses an upper hand in terms of jet performance characteristics from the point of mixing characteristics.

In order to improve the mixing characteristics of non-circular jets, a peripheral twist has been provided to jet modifier pipe. The parametric analysis included study of twist rate and length of jet modifier pipe. The study indicates that, increase in twist rate of jet modifier pipe increases tangential velocity of jet, with rectangular jet outperforming square and triangular jets. The twisted jet modifier pipe length has an opposite effect wherein, the smaller the length of pipe, the higher is the tangential velocity. In nut shell the computational and experimental studies indicate that the peripheral twist introduced to non-circular free jets are far superior to the circular free jet in the mixing process.

List of Figures

List of Tables

Nomenclature

Latin Letters	
Symbols	Meanings
R_e	Reynolds Number
M	Mach Number
T	Temperature
U_0	Bulk Mean Velocity
U_C	Centerline Velocity
L	Length
D	Circular jet exit Diameter
A	Area
b_u	Jet Half Width
C_{2u}	Virtual Origin
ΔP	Pressure Difference
G	Acceleration due to gravity
m_0	Mass Flow Rate
P_s	Mean Static Pressure
P_a	Atmospheric Pressure
X	X co-ordinate
Y	Y co-ordinate
Z	Z co-ordinate
$k\text{-}\varepsilon$	K-epsilon turbulence model
u'	The Root-Mean-Square (RMS), or Standard Deviation, of the turbulent velocity fluctuations over a specified period of time
U	The average of the velocity
s	Swirl number
u	Axial velocity component
v	Radial velocity component
w	Circumferential velocity component
Greek Letters	
μ	Kinematic Viscosity
ρ_a	Density of Air
ρ_w	Density of Water
τ	Shear Stress
θ	Inclination Angle
α	Thermal diffusivity

Chapter 1

Introduction

1.1 Preface

A jet is formed by a flow issuing from a nozzle into the ambient fluid, which can be at rest (free jet), in motion (co-flowing or, counter flowing jet) or, tangential to a solid surface (wall jet). It is one of the basic flow configurations that have been widely used in many practical applications such as fuel injections, combustor, jet engine propulsion exhaust etc. One of the most important considerations for jet flow is its entrainment and mixing process with its boundaries.

1.1.1 Jet Flow

A jet flow is generated when a fluid is discharged through an orifice, aperture or nozzle from a region of high pressure into a region of low pressure. Such flows occur in a variety of situations of diverse geometries and varied flow conditions. It is a typical phenomenon around us, which can be seen almost every day.

Various jet configurations evolved over the years and precise applications have been developed for particular fields. Examples include vertical take-off and landing of aircraft, film cooling of gas turbine blades and environmental problems such as pollutant dispersion from chimneys or, the discharge of effluents into the ocean etc. Typically, any jet has higher momentum compared to the surrounding fluid's ambient conditions. In case, the surrounding fluid medium (having certain viscosity) is made of the same fluid as the jet, the surrounding fluid is carried along with the jet in a process called entrainment.

1.1.1.1 Types of Jet Flow

Jet flows vary greatly depending on the values of Reynolds Number and Mach number. It can be classified as follows depending on the surrounding in which the jet is discharged.

- **Confined Jet:** The flow is discharged into an enclosed region bounded by a solid surface.

- **Free Jet:** The jet which is discharged to an ambient fluid where the flow is not

affected by any kind of solid surface is known as free jet.

Depending upon the exit geometry of the nozzle or orifice, the free jet flows can be divided into the following sub-categories;

- **Plane Jet:** Fluid is discharged from a plane nozzle into a large stagnant mass of the same fluid. The cross-section of the nozzle exit can be square or rectangular in shape.

- **Axisymmetric Jet:** Fluid is discharged from a circular nozzle or, orifice into a large stagnant mass of the same fluid.

- **Compound jet:** Compound jet can be created when a flow (discharged from a nozzle) at a high speed emerges in a stationary liquid. Any type of mentioned jet flows in a parallel moving stream of fluid is known as a compound jet.

- **Co-axial Jet:** In case of co-axial jets, the fluid is discharged from a nozzle through a co-axial path.

- **3D Free Jet:** Fluid discharges from triangular, rectangular, square, elliptic or wedge shape jet.

- *Wall Jet:* The jet flow, which is encountered by a vertical or inclined wall placed at a certain distance right from the exit of the nozzle or orifice, is called the wall jet.

The jet flows can again be classified, depending on the direction of streamline as Co-Flowing Jet and Counter Flowing Jet. When the jet flows in the same direction as the ambient fluid, is called co-flowing jet. When the jet flows in the opposite direction of the ambient fluid, is called counter flowing jet.

Similarly, depending on the velocity of the flow, jet can be divided into Subsonic and Supersonic Jet. Jet flow can also be classified as miscible and immiscible flow and so on.

1.1.2 Jet Flow Field

The time averaged jet velocity at the exit of a nozzle is a uniform, **hat shape profile**. Due to a large velocity difference between the jet and the ambient fluids, a **thin shear layer** is created. The shear layer is subjected to flow instabilities that eventually lead to the generation of strong turbulent fluctuations and it continuously grows downstream.

Such highly turbulent shear flow entrains ambient fluid into the jet and enhances the flow mixing.

Consequently, the shear layer and the jet spread laterally and the jet velocity continuously decreases in the downstream direction. Near the pipe or nozzle exit and along the central portion of the jet, a region with an almost uniform mean velocity is called the **potential core**. When the shear layers merge from all sides, the potential core eventually disappears.

The entrainment and the mixing process continue beyond the potential core region [2]. As such, the velocity distribution eventually results to a bell shape profile. This region is called self- similar region. The jet boundary line can be interpreted as the outmost location where the velocity approaches to zero.

1.2 <u>Motivation behind the Present Study</u>

Jet flow is typically one of the most common phenomena encountered both in engineering field and in nature. Most of the jet flows are typically turbulent in nature and are found in many applications ranging from daily activities to industrial applications. This extensive use of turbulent jet attracted the researchers from the middle of the 20th century to work on this flow field. Till now number of research works have been undertaken on different types of jet and alteration of its characteristics to improve performance of jets in terms of mixing.

Noncircular jets have seen to improve the mixing of various types of air-breathing engines and other combustors, to abate jet noise, to enhance supersonic mixing, cooling of the walls of the combustion chamber and blades of aero-engines. Therefore, it is very important to understand the physics behind the non-circular jets to optimize the mixing. Previous works show that noncircular free jets have shown better performance in terms of mass entrainment and mixing. The previous studies have considered the sharp edged and corner radii cross sectioned non-circular jets. Further, the previous studies have considered the abrupt changes of cross sections such as orifice plates. It has been found that no intentional introduction of swirl and its effects has taken place yet. In the present study, existence of peripheral twist near the edges of the non-circular jets is expected to introduce the additional swirl in the jet in addition to effect of shape change in jet cross

section. This is expected to enhance jet entrainment and mixing. This is also expected to create the fine-scale turbulence structure along the periphery of the jet. The even distribution of the fine-scale turbulence structures circumferentially could shorten the core length more effectively.

Therefore, in this study, characteristics of free circular and non-circular jets (triangular, rectangular and square cross section) with and without peripheral twist are investigated both numerically as well as experimentally. The numerical investigation (ANSYS software simulation) would involve thorough parametric study to characterize the circular and non-circular jets with and without peripheral twist. Comparison of the numerical and experimental results allows us to optimize the numerical methods extending the jet characteristics at higher speeds and throw light on different applications of twisted non-circular jets.

1.3 Objectives and Scopes

The main objective of this study is to understand the creation of non-circular jets and improvement of jet performance by numerical and experimental method. The objectives of the present research are:

1. To design and fabricate jet flow modifier pipe.
2. To generate the base jet parameters of circular and non-circular 3-D jets.
3. To analyze numerically the effects of peripheral twist to the non-circular free jets (triangular, rectangular and square).
4. To validate the base parameters experimentally generated for circular and non-circular jets in step 1 and 2 above and also to validate the hypothesis of enhancing the mixing performance.

1.4 Working Approach

Since the non-circular exit jet is compared with circular exit jets in the present work, the exit cross-sectional area is kept the same as that of circular exit pipe jet so that the mass flow rate remains constant in order to study the effect of varying exit geometry. The thesis deals with the results obtained via experimental as well as computational approaches and establish a comparison between theoretical predictions and actual cases

of flow behaviors of certain shapes of jets. As such, computer aided analysis was chosen as the first and foremost method of study. Software aided calculations as ANSYS would facilitate the research work. The academic version of the software ANSYS was used at the foremost. A tentative experimental analysis was also done in addition to the computational approach. The experimental study was conducted in an 'Air Flow Bench', designed specifically for this purpose. It includes different shapes for the exhaust geometry to assess the flow performance and validate the computational results. The comparison between the two types of work methodology consolidated the idea and the result as well. The experimental method is the oldest but the most reliable approach to judge flow performance. A 'Pitot-static Tube' arrangement was used with the help of a manometer assembly. A general literature survey was also done prior to the computational as well as the experimental approach so that the theoretical knowledge and the different works of researchers and scientists can be brought to light. The initial approach was to bring some sort of uniqueness to this study, because this topic of research is most likely to find its use in different industries.

1.5 <u>Outline of the Thesis</u>

The entire thesis has been segmented into 7 chapters and later rearranged to adjust the different sub-chapters. These chapters help to identify the different segments of the entire work at a glance. The 'Introduction' chapter deals with a general overview on the research methodology and how it can be implemented; followed by the 'Literature Review' chapter. Then a 'Theory' chapter is included to highlight the basic theories on the thesis topic. The next chapter is on the design and construction of the 'Experimental Set-up' and 'Computational set up'. The chapter 'Circular and non-circular jets' discusses various base parameters for the jet. After that, the Effect of twist rate is discussed in the next chapter. Finally, a chapter entitled the 'Conclusion' is mentioned at the end of the thesis.

1.6 <u>Applications</u>

Different geometries are likely to facilitate various applications. As such, the scope for applications for a definite shape is to be ascertained to help in the progress of a particular field. Compared to circular jet, the non-circular ones have been found to be more effective in mixing scenarios with ambient fluid. The shape of air inlet has a lot to do with flow conditioning. Uniform flow is possible in case of a circular air intake, however

in practical; this is absurd for supersonic flights. It is important to note that the air intake system of fighter jets is traditionally non-circular. They are not typically square, mostly rectangular.

The mixing tendency is superior in non-circular jets, in which axis-switching occurs. Extensive research over the years revealed that rectangular, triangular and elliptic jets have higher velocity decay, jet spreading, mass entrainment, and consequently higher mixing capability compared to the circular counterparts.

Rectangular nozzles have particular applications in the aviation sector. As the shear layer from both sides converges quicker, it has a lower potential core length resulting in a reduced noise generation. Also, in industrial purpose it can be used as a discharge duct. For air handling units and cooling ducts, the contribution of rectangular nozzles is noteworthy. In different commercial and institutional buildings, HVAC Duct systems are incorporated which are mostly rectangular in shape.

The fuel injector is yet another sophisticated component of the engine section that optimally sprays the fuel into the combustion chamber. The shape of the injector has something to do with the optimization of the engine.

A proper mixing of the fuel with air is important for efficiency. Mixing capabilities increase with the increase of turbulence. In different engines (such as diesel engines), fuel injector nozzle will affect the performance to a great extent. The dimensions of nozzle, the core length of the jet as well as turbulence intensity influence the emission and performance over time.

Jet impingement cooling has diverse applications. Different shapes which were analyzed can be of use to heat transfer application involving jet impingement. Basically, this procedure is followed to make heat transfer in a convective manner. With the decrement of jet diameter i.e. smaller nozzle which also incorporates higher jet velocities, area averaged heat transfer can be increased.

Mixing of fluids is done in different aspects such as industrial and edible fluids. In food industries, different ingredient mixing and ejection of liquid colloidal are another application of jets. Tank and valve optimization, cleansing etc. are also done using nozzle-based products.

Chapter 2

Literature Review

Jet flow is considered a basic flow configuration, having various applications in different industries. Simple flow mechanisms are easy to use and theoretically they are easier to solve, compared to swirling fluid streams, which are too complicated and difficult to handle from a theoretical point of view. Jet flow and their interactions with the flow field is considerably affected by the exhaust geometry. It is necessary to accomplish smooth mixture of the jet. Therefore, experimental investigation is the best possible option to justify the flow field interactions of jet flows after a computational analysis is done beforehand.

Due to the wide range of application of jets in industries, it is deemed to be an important research topic. Many researchers have done experiments and have consolidated their ideas. In fact, researches and experiments are still going on free jet flow mixing performanc and other characteristics.

A literature review was done to adhere to the possible research criteria and gather tentative knowledge on the same. It helped to highlight various aspects of this research topic.

2.1 Experimental Studies

Shih et al. (1999) [3] incorporated PIV velocity fields to obtain time-averaged flow field to justify the general notations regarding the flow field generalizations and typical flow visualization purpose.

Zheng, X., Jian, X., Wei, J., & Wenzheng, D. (2016) [5] investigated the mixing characteristics for circular round jets both computationally and experimentally. Particle Image Velocimetry (PIV) was used to gather the experimental [5]. The critical characteristics of mixing region are predicted by jet spacing and pressure ratio. Three typical regions (con-verging region, merging region, and combined region) are commonly examined. Along the downstream location, the two jets gradually become a self-similar signal jet. the double jets on both sides lean and bend towards the central symmetrical plane. At the nozzle exit, high velocities lead to entrainment of gas in the shear layers of the jets. The jet interaction (in terms of merge point and pressure) varies

significantly while the jet spacing differs. Also, the effects of jet interaction decrease as pressure ratio increases, and thus the merge point location moves further downstream [5].

Peram and Bommera (2016) [6] concluded that effect of geometrical modification is significant for rectangular and square model compared to circle at both the pressure heads[6]. They experimented at two pressure heads i.e. at 30 *cm* of water and 40 cm of water respectively. Overall pressure drop is more significant in rectangular jet at 30 *cm* of water, compared to the square one. Centerline pressure drop is more noteworthy in case of the square jet at 40 *cm* of water, compared to the circular and the rectangular jets. A passive control method vortex generators have been used to control the incompressible fluid flow jets which also improves the mixing characteristics. Rectangular model showed significant effect on mixing mechanism. Rectangular jet has significant pressure drop compared to square jet. Non-circular jets have been to have the potential to entrain ambient fluid more effectively than comparable circular jets [6].

Gutmark and Grinstein (1999)[7] have indicated the significance of axis rotation of noncircular jets, which make them more efficient mixers than the circular jets. The jet core length was also stressed as a measure of mixing, and the results showed that the isosceles triangular jet is the most efficient mixer over other jets investigated. [7].

An analytical expression for the discharge co-efficient of conical convergent nozzles operating under varying pressure ratios was determined by Hebbar, Sridhara & Paranjpe (1970) [8]. conical convergent nozzles are analyzed operating under varying pressure ratios. The theoretical results based on this approach have been compared with discharge coefficient of conical jet nozzles determined experimentally covering a range of pressure ratio up to 3.25. Conical convergent nozzles have been widely used in subsonic jet engines as a means to convert pressure energy into kinetic energy because of their inherent simplicity in construction. Several features of the behaviour of the discharge coefficient with respect to pressure ratio are exemplary. First, for a given convergence semi-angle, the discharge coefficient increases with the overall pressure ratio, Secondly, it increases with decreasing convergence semi angle. Thirdly, it attains high values in the supercritical range. [8].

Flow structure of a free round turbulent jet in the vicinity of the flow exhaust was experimented by Boguslawski and Popiel (1979) [9]. Measurements of radial and axial

distributions of mean velocity, turbulent intensities and kinetic energy as well as radial distributions of the turbulent shear stress in the initial region of a turbulent air jet issuing from a long circular pipe into still air is analyzed. In the core sub-region the mean centre-line velocity decreases slightly. The turbulence intensity first builds up at locations where the velocity gradient is high (in the mixing sub-region) and further downstream turbulence of high intensity fills the whole cross-section of the jet. The profiles of the transverse intensities (radial and tangential) are very similar in shape and about half the size of the longitudinal ones. [9].

On a different note, the stability of slowly diverging jet flows was studied by Crighton and Gaster (1976) [10]. Coherent axisymmetric structures in a turbulent jet are typically modelled via some linear instability modes of the mean velocity profile, which is usually considered as that of a fictitious laminar inviscid flow. The expansion methods of the usual multiple scales were used in conjunction with a family of profiles consistent with the similar mixing regions [10].

Sforza et al. (1966)[11] and Yevdjevich, V. M. (1966[12] have shown that the flow field of the rectangular jet may be subdivided into three main regions: PC (potential core) region, followed by CD (characteristic decay) region and AD (axisymmetric decay) region. It was also found that the saddle-backed velocity profile on the span wise axis and the direction-dependent spread in the jet cross section. It was concluded that low speed jets that come out of non-axissymetry orifices decay to axissymtry far downstream of the jet exit.

Miller et al. (1995)[13] compared the performance of circular jets with elliptical, rectangular and triangular jets and concluded that the coherent large structure in non-circular jet is quickly masked by small structures unlike in circular jets. It was also concluded that triangular jets are more efficient in mixing and rectangular jets take second position.

Öçer et al (2012) completed an experimental study on turbulence structures and mixing levels in the near fields of jets emanating from circular and non- circular jets (triangular and square nozzles with corner radii). The author concluded that the axis switching phenomenon was not observed for all the jets. The entrainment rate value was found to be the highest for the triangular and the lowest for the round jet. The turbulent kinetic energy within the jet flow structures rise and decay much quicker for triangular jet than

other two types. The triangular jet flow has the shortest core length and higher turbulence level. It was finally concluded that a triangular jet flow possesses better mixing characteristics such as the highest mixing rate, mass entrainment rate, and turbulence level over other two jet types. [14].

duPlessis M.P. (1974) [15] explained a method that enables fast and accurate prediction of square jet center-plane characteristics starting from known velocity profiles at the nozzle exit. Velocity and turbulent shear stress measurements were taken within the first 20 nozzle widths of incompressible turbulent air jets issuing from square apertures.

Islam (1995) [16] experimented the flow characteristics in the near field of a circular splined jet. He conducted an experiment to investigate the flow characteristics in the near field of a circular splined jet. Both mean velocity and longitudinal turbulence quantities were measured based on the nozzle exit diameter and centerline mean velocity at Reynolds Number of 5.6×10^4. The centerline mean velocity decelerated about 1.5% of the exit velocity within the potential core [16]. The presence of the spline caused the mean velocity profiles to diminish. The spread rate and the entrainment of the splined jet decreased in comparison to the other nozzle shapes. The author made use of pitot static tubes and hot wire anemometer in this experimentation [16].

Krothapalli, A.(1981) [17] presented hot-wire measurements in an incompressible rectangular jet, issuing into a quiet environment at ambient conditions. Three distinct regions characterized the jet flow field: a potential core origin, a two-dimensional-type region, and an axisymmetric type region. The onset of the second region appeared to be at a location where the shear layers separated by the short dimension of the nozzle meet; and the third region occurred at a downstream location where the two shear layers from the short edges of the nozzle meet. In the central plane, similarity was found both in the mean velocity and shear stress profiles beyond 30 widths downstream of the nozzle exit; profiles of rms velocity showed similarity in the second, but not the third region.

Marsters, G. F. (1981) [18] examined the mean and turbulence velocities of the jets for which strong peaks are evident. Contour plots of the mean velocity fields were presented. Outputs from two hot-wire anemometers had been subjected to both analog and digital analysis, allowing extensive correlations between the results.

Sfeir, A. A. (1976) [19] measured the mean velocity and temperature profiles of

10

rectangular jets having different aspect ratios and nozzle geometries using hot-wire anemometry. The flow-field, for both velocity and temperature, is found to be divided in three distinct regions, respectively, referred to as, the potential core, the two-dimensional region and the axisymmetric region. The extent of each of these regions is a function of the nozzle aspect ratio. The flow in the two-dimensional region as well as the transition to axis symmetry are strong functions of the nozzle geometry. At large distances from the nozzle exit, both the velocity and temperature fields are found to behave in the same way as in the flow out of a circular nozzle of the same area.

Komori and Ueda (1985) [20] used a somewhat similar technique by adding a convergent nozzle to the rotating pipe. But, in this case, the azimuthal and the axial velocity components were affected differently. From an inviscid analysis, the axial velocity increased in proportion to the contraction ratio, whereas the azimuthal remained related to the square root of the contraction ratio. In reality, the geometry of the contraction section played an important role and therefore different set ups would possibly give different outlet profiles [20].

Billant, Chomaz and Huerre (1998) [21]used a motor driven, rotating honeycomb structure before the contraction nozzle. In this experiment, the Reynolds Number is low and the honeycomb ensures a laminar flow with the solid body rotation. However, when the flow passed through the contraction cone, it became distorted and the axial velocity became pointed at the center zone i.e. the flow did not correspond to the solid body rotation [21].

The instability of the swirling jet was experimented in detail by Loiseleux and Chomaz, (2003) [22]. They found three different flow regimes for swirl numbers and below that vortex breakdown occured. The same experimental setup as that of (Billant, Chomaz and Huerre, 1998) was during this experiment as well. For small swirl numbers, the rotation did not affect the jet column mode and development of the profile remained similar to that of the non-swirling case [22]. As the swirl number increased, the amplitude of the available mode decreased and instead a helical mode was produced as the outcome.

Hossain (2008) [23] experimented the flow characteristics in the near field of a thermally stratified co-axial free jet. He used a pitot static tube with embedded thermocouple for two different Reynolds Number (3.72×10^4 and 4.8×10^4) based on the exit velocity and the diameter of the inner jet [23]. The effect of the area ratio on the developed region

of the co-axial jets was found to be more prominent that that of the developing region [23]. Thermal diffusion from the hot central jet is found to occur more rapidly at lower velocity ratio. With the increase of velocity ratio, the potential core was noted to be transversely shrunk, but longitudinally elongated. Self-preservation state of thermal field was observed to be independent of dynamic condition [23].

Parekh et al., (1996) [24] demonstrated a technique for injecting high frequency and high intensity signals into subsonic and supersonic shear layer for the purpose of jet mixing enhancement. Based on the previous works in low speed flows, a family of piezo-electric excitation devices was formulated for the active control of shear layers [24]. The effects of these devices on high aspect ratio rectangular jets were investigated for subsonic and supersonic jet Mach number up to M= 1.1 [24].

X. Zhang (2000) [28], investigated effect of turbulence produced by rectangle sloping jet in boundary layer. It was concluded that when properly arranged, the rectangular jet is able to produce a stronger vortex for flow control than a circular jet at the same mass flow rate. Experiments on axisymmetric free jet (impinging jet) over a surface in motion were done by Gradeck et al. (2006) [29]. They also compared the experimental and the computational results. Owing to the effect of heat transfer on cooling in hydrodynamic region, the consistency in results could be ascertained.

Portoghese et al. (2008) [30]conducted surveys on the effect of performance injection to fluidized bed supported by gas nozzle liquid at ambient working conditions .

Effect of sidewalls on the rectangular jets was undertaken by Alnahhal and Panidis (2009) [31]. The investigation results indicate that two jet configurations (with and without sidewalls) produce statistically different flow fields. Sidewalls do increase the two-dimensionality of the jet, increasing the longevity of 2D span-wise roller structures formed in the initial stages of entrainment, which are responsible for the convection of longitudinal momentum towards the outer field. [31].

The results from the detailed experimentation of Chong, Joseph and Davies (2009) [32] on the performance and design parameters of open jet also provided justification on the same. Sharif and Banerjee (2009) [33] investigated the confined slot-jet impingement for a moving isothermal hot plate due to convective heat transfer. Interrupted jolt and characteristics of vortex in coaxial turbulence vortex were studied and documented by

Lee et al. (2010) [34]. This study helped in understanding the effects of the turbulence measures on the aspect of the flow entity. Xu et al. (2010) [35]performed experiments on the heat transfer, interrupted vibration and the Nusselt Number impinging jet on turbulence region. Experimental and computational results of impinging jet inside micro-channel from narrow hole for cooling performances were investigated by Sung and Mudawar (2006) [36]. The heat transfer properties were analyzed by using the standard $'k - \varepsilon'$ turbulence model.

Mallinson, Reizes and Hong (2001) [37] experimented on the flow generated by a synthetic jet actuator with a circular orifice. They also compared the computation results. The synthetic jet established itself much more rapidly than the steady jet, primarily because of turbulent dissipation. The oscillatory nature of synthetic jet flow also gave rise to a much greater entrainment of ambient fluid compared with the case of a steady jet [37].

Narayanan, Seyed-Yagoobi and Page (2004) [38] did an experimental study on fluid mechanics and heat transfer in an impinging slot jet flow. Two nozzle-to-surface spacing of 3.5 and 0.5 nozzle exit hydraulic diameters, which correspond to transitional and potential-core jet impingement, respectively were considered. Fluid mechanical data include measurements of mean flow field and variance of normal and cross velocity fluctuations, mean surface pressure, and RMS (Root Mean Square) surface pressure fluctuations along the nozzle minor axis. According to their study, the heat transfer data followed a trend similar to previous studies, exhibiting high heat transfer rates in the impingement region for transitional jet impingement, and a non-monotonic decay in heat transfer coefficient for potential-core jet impingement [38]. For potential-core jet impingement, the stream-wise location of peak RMS pressure fluctuations corresponded to the highly correlated turbulence in the outer region of the wall-bounded flow [38].

Mi, Nathan and Luxton (2000) [71] compared the centre-line mixing characteristics of jets from nozzles with nine different cross-sectional shapes. The breakdown of axis-symmetry of the initial jet configuration generally results in increased mean velocity decay and increased RMS fluctuations, implying increases entrainment of the ambient fluid [71]. Aleyasin, Tachie and Koupriyanov (2017) [74] conducted an experimental study on the statistical properties of free orifice jets. The mixing tendency is superior in non-circular jets, in which axis-switching occurs. Extensive research by Quinn (1992)

[72] over the years revealed that rectangular, triangular [75] and elliptic [73] jets have higher velocity decay, jet spreading, mass entrainment, and consequently higher mixing capability compared to the circular counterparts.

Quinn, W. (1992) [72] analyzed the influence of aspect ratio on turbulent free jet flows issuing from sharp-edged rectangular slots. Various things were examined such as the measured time-average quantities, turbulence kinetic energy, Reynolds shear stress, and some of the triple-velocity products etc. Four slot aspect ratios (2, 5, 10, and 20), with the same exit plane area of 0.00161 $m2$, were used. Near-field mixing in rectangular jet flows increases with increase in the slot aspect ratio. The aspect ratio 20 jet has the shortest potential core length and the highest shear-layer values of the turbulence kinetic energy, the Reynolds shear stress [72].

On the experimental side, Quinn (2005) [75] investigated the near-field of a flow emanating from a sharp-edged equilateral triangular orifice by taking velocity measurements. The investigation indicated that mixing in the equilateral triangular jet is faster than in the round jet (performance parameters are mass entrainment, spread of the jet, peaking of the turbulence intensity and the recovery of the mean static pressure on the jet centerline). The mean stream-wise vorticity field in an equilateral triangular jet is dominated by counter-rotating pairs of vortices. Mixing in an isosceles triangular jet, as measured by the entrainment of ambient fluid, the spread of the jet, the centerline mean stream wise velocity decay is faster than in the round jet but slower than in the equilateral triangular jet.

Jiang, Lin and Yang, (2017) [76] studied the shapes of the combustion chamber, which has a decisive influence on the turbulence characteristics of cylinder and distribution characteristics of concentration field.

The shape of combustion chamber plays a major role in controlling the combustion process and emission characteristics. Banapurmath et al. (2015) [77] conducted experiments on Different combustion chamber shapes keeping the compression ratio same for the existing diesel engine. A new shape came up in this experimentation i.e. toroidal shape which resulted in overall improved performance and reduced emission levels.

2.2 **Computational Studies**

Numerical capabilities increased by several folds during the last decade. Previously, various aspects could not be adhered to due to certain limitations of the numerical solvency. However, the validation of numerical models has been the motivation for attention to the flow field details in the experimental literature.

Patankar, Basu and Alpay (1977) [40] predicted the jet trajectory and the mean velocity flow field distributions for a single circular jet injected perpendicular to the cross flow, where the ratio of the jet velocity to the main stream velocity varied at a range of 2 to 10. The numerical predictions agreed well with available experimental data. They found uniform vertical velocity at the jet exit [40]. The results of a finite-difference solution for the 3D flow field generated by a round turbulent jet (normal to the jet axis) was the outcome of the study. The time-averaged momentum equations were calculated by a "two-equation turbulence model" in which differential equations were solved for the kinetic energy of turbulence and for the rate of its dissipation [40]. The solution procedure employed an elliptic finite-difference scheme with the three velocity components and the pressure as the main dependent variables [40].

Another interesting work was put forward by Patankar, Liu and Sparrow (1977) [41]. The concepts of fully developed flow and heat transfer have been generalized to accommodate ducts whose cross-sectional area varied periodically in the stream-wise direction [41]. The concepts and solution procedure for the fully developed regime were applied to a heat exchanger configuration consisting of successive ranks of isothermal plate segments placed transverse to the main flow direction. The computed laminar flow field was found to be characterized by strong blockage effects and massive recirculation zones [41]. The fully developed Nusselt numbers are much higher than those for conventional laminar duct flows and show a marked dependence on the Reynolds Number [41].

Leylek and Zerkle (1994) [42] conducted large scale computational analyses and also compared the results with experiments to understand coolant jet and crossflow interaction in discrete-jet film cooling [42]. Detailed 3D elliptic Navier–Stokes solutions, with high-order turbulence modeling were used and a new model (enabling simultaneous solution of fully coupled flow in plenum, film-hole, and cross-stream regions) was proposed [42]. The results also explain important aspects of film cooling, such as the

development of complex flow within the film-hole in addition to the well-known counter rotating vortex structure in the cross-stream [42].

Numerical predictions of the influence of jet exit plane conditions on the downstream of flow were put forward by Garg and Gaugler [43] (1997). They performed simulations on three different blade configurations and examined polynomial jet exit profiles for velocity and temperature distributions [43]. Results were also compared with the experimental data for all the blades. It is found that, in some cases, the effect of distribution of coolant velocity and temperature at the exit can be as much as 60% on the heat transfer coefficient at the blade suction surface, and 50% at the pressure surface [43]. Different effects on the pressure and suction surface were observed depending upon the blade as well as the shape of the hole. Forest's model for augmentation of leading edge heat transfer due to free-stream turbulence and Crawford's model for augmentation of eddy viscosity due to film cooling were used.

Wegner, Huai and Sadiki (2004) [44] predicted the turbulent mixing of jet in cross flow using LES (Large Eddy Simulation) model. Their predictions indicate that the inclination of coolant jet influences the characteristics of vortical structures and the secondary motions have an effect on the mixing process [44].

A computational investigation of 3D flow field resulting due to the interaction of a rectangular heated jet issuing into a narrow channel crossflow had been reported by Pathak, Dewan and Dass (2006) [45]. The jet discharge slot spans more than 55% of the crossflow channel bed, leaving a small clearance between the jet edge and sidewalls [45]. The detailed investigation of the mean flow field and flow structure was carried out, which could not be obtained in a similar 2D experimental work. The commercial code FLUENT 6.2.16 (based on the 'Finite Volume Method') was used to predict the mean flow and temperature fields for the jet to crossflow velocity ratio. Two different turbulence models, namely, Reynolds-stress transport model (RSTM) and the standard $'k - \varepsilon'$ model, were used for the computational analysis [45]. However, the performance of RSTM was found to be better than that of the standard $'k - \varepsilon'$ model [45].

2.3 **Analytical Studies**

Needham, Riley and Smith (1988) [46] proposed a typical model for the flow of an inviscid, incompressible fluid jet, emerging from a cylindrical pipe, of circular cross-

section, into a stream of the same fluid [46]. The component of the external flow (normal to the axis of the pipe) was taken to be small compared to the speed of the jet. The results throw some light on the mechanisms that are responsible for the observed deflection of jets into the crossflow direction [46]. They showed that in the case of low velocity ratio, it is possible to use the boundary layer equations and treat the jet as a perturbation. An inviscid 3D vortex sheet model was used to study the turbulence [46].

From the above literature studies, it can be seen that most researchers only dealt with the circular shapes only. Although different industrial uses require other shapes for the definite usage. Studies on using rectangular and elliptical shapes were hardly attended. In this sense, the present work is focused on to study the other shape variants.

Some of the common applications of circular and plane jets occur in drying processes, air curtains for room conditioning, heating and ventilating applications. In these, parameters like the jet spread rate and potential core decay play a strong role in deciding the efficiency of mixing for the process. Shear layer is the region in which most of the interactions and mixing between the ambient and jet fluids take place. Therefore, understanding the fluid dynamic phenomena in the shear layer during the downstream evolution of a jet is important.

2.4 <u>Literature Survey in a Nutshell</u>

After the intense review of different books, journals, articles, conference papers and dissertations on free jets, it helped to come select the objective for the present research.

Free jet characterization for different cross-sectional outlets of a jet was the topic of concentration. Different exhaust geometries are to be investigated during experiment to consolidate the computational results. Some parameters that can be used to observe the characterization of jet are velocity profile, potential core length, jet spreading etc. Different researchers used various methods to calibrate the velocity values. Many used the hot-wire anemometers; some even used the conventional pitot static tube to measure the values. From the velocity profile the potential core length or the different zone's range of a fluid flow can be identified. Based on these parameters the jets can be of different application accordingly. The effect of turbulence and the axial distributions of air velocity and the turbulence intensity are to be obtained through experiments.

Flow in the pipe can either be laminar or turbulent. If no transition occurs in the boundary

layer, before the end of the transition length, the flow in the pipe remains laminar and the velocity profile is then a parabola. If transition does take place, the fully developed flow is turbulent with a logarithmic profile. This is more flattened than the laminar profile but, as in the case of the flat plate boundary layer, the velocity gradient in the neighborhood of the wall is greater.

It is important that the experimental investigation of jet velocity profiles is in good agreement with that of the computational ones. The comparison of these velocity profiles is important contributions of this thesis work.

Chapter 3

Theory

3.1 General

Free jet becomes completely turbulent at a short distance downstream the exit even when the exit velocity is very small [2]. This turbulent motion is governed by the mass conservation and the Navier-Stokes equations. Exact analytical solutions of these equations are yet to be obtained because of their non-linear forms. Hypothesis and empirical assumptions are to be introduced for obtaining a set of equations with time averaged dependent variables. Conventional order of magnitude analysis is applied to the general momentum equations to obtain the equations in a simpler form.

In spite of the voluminous research literature available on turbulent jets issuing from circular and non-circular nozzles, there are still some important aspects which require greater attention. For instance, in plane jets of large aspect ratio, primarily planar spreading occurs in the near field. But at larger distances, the differential rates of shear layer growth in two lateral directions results in 3D features such as the axis switching phenomena [59]. With the assumption of steady incompressible flow and having no boundary layer effects at the pipe exit, the general equations for motion and energy of turbulent jets can be derived in simpler forms in accordance to the flow configuration and nomenclature as follows;

Continuity Equation	$\dfrac{\partial (U_r)}{\partial x} + \dfrac{\partial (V_r)}{\partial x} = 0$
Momentum Conservation Equation	$U\dfrac{\partial U}{\partial x} + V\dfrac{\partial U}{\partial r} = \dfrac{1}{r}\dfrac{\partial}{\partial r}\left(r\dfrac{\tau}{\rho}\right)$

Where, τ is the shear stress, ρ is the fluid density and α is the thermal diffusivity; U and V are the mean velocities in x and r directions respectively and T is the mean temperature [2].

A free jet is a fluid mass that discharges into an infinitely large environment of ambient fluid [59]. Experimental observations on the mean turbulent velocity field indicate that the entire flow structure of a free jet can be divided into different zones along the axial

direction of the jet flow. These distinct zones are related to the centerline velocity decay.

3.1.1 Flow Structure of a Free Jet

The flow structure in a free jet has been studied by many researchers and four distinct zones have been identified from these studies.

ZONE 1 →*The Convergent Zone*: This zone starts just after the nozzle exit. As the turbulence penetrates towards the axis or, the centerline of the jet, there is a wedge shaped region of a constant mean velocity (equal to the outlet velocity). This wedge is called the potential core of the jet, and is surrounded by a mixing layer on top and bottom. Initial zone extends until the potential core disappears [2]. Normally for a free jet flow, the length of the potential core extends up to four times (or, six times) the diameter of the nozzle exit [59].

ZONE 2 →*The Transition Zone*: This zone starts just after the initial zone where the centerline velocity starts to decrease. It mostly depends on Reynolds Number. The higher the Reynolds Number, the smaller the transition zone [2]. The velocity decay can be estimated to be proportional to $x^{-0.5}$; where, x is the axial distance from the nozzle exit. This usually corresponds to a region from $6D$ to $20D$ (D = the diameter of nozzle exit), and it is known as the interaction region (where shear layers from both sides merge) [59].

ZONE 3 →*The Self-similar Zone*: In this region, transverse velocity profiles are similar at different values of x and the centreline velocity decay is approximately proportional to x^{-1}. It is also called the developing zone, where the entrainment of ambient fluid creates a continuous transfer of momentum and energy from the jet to its surroundings. The flow variables are almost self-preserving and generate instability due to intensive shearing of the ambient fluid forming the shear layer [59].

ZONE 4 →*The Termination Zone*: In this region the centerline velocity decays rapidly. Although this zone has been studied by several researchers, the actual mechanisms in this zone are not understood properly.
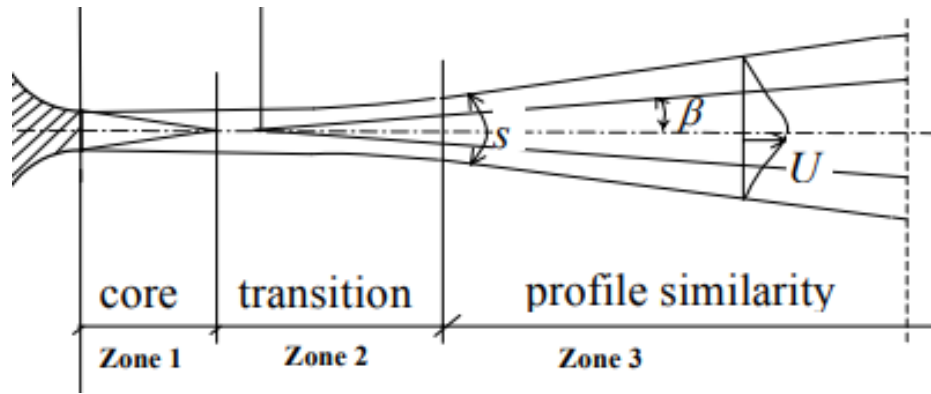
Figure 3.1:Flow Structure of a Free Jet [70]

For an axial jet, the first two zones are strongly influenced by the diffuser, the third zone is the developed jet, and the fourth zone is the zone of jet termination. In the first three zones, room air is entrained into the jet and mixed with supply air. In the fourth zone, the jet collapses inward from the boundaries and the supply air is distributed to the room air as the jet disintegrates [60]. Flow Structure of a Free Jet is shown in Fig 3.1 [70].

3.2 Various Jet flow Parameters

Jet flow properties is a very important factor for this work. To find out the jet flow properties there are several jet flow parameters which was required. Moreover, jet flow properties can also be changed by changing the exit of the shape of pipe. Pipe length can also be modified to observe the jet flow properties such as shear layer, centerline velocity etc. Various pipe length would create different effect on jet flow properties. Shear layer is a layer of flow where a shear or velocity gradient exists. Going by this, boundary layer is also a form of shear layer. The most effective way to characterize the shear layer is to plot the constraint vorticity contour. Inside the shear layer, large velocity differences exist and the vorticity level becomes high. Away from the shear layer, the velocity gradient is small and the vorticity level is low [3]. Therefore, the contour distribution of the vorticity level represents a good measure of the growth of the jet shear layer. As evident from the vorticity contour and the mean velocity plots, the jet spreads outward and entrains ambient fluid into the jet.

Another good measure of the jet spreading is the jet centerline velocity, which is relatively constant inside the potential core of the jet. As the shear layers merge towards the center, the centerline velocity decreases downstream as shown in Fig 3.2.
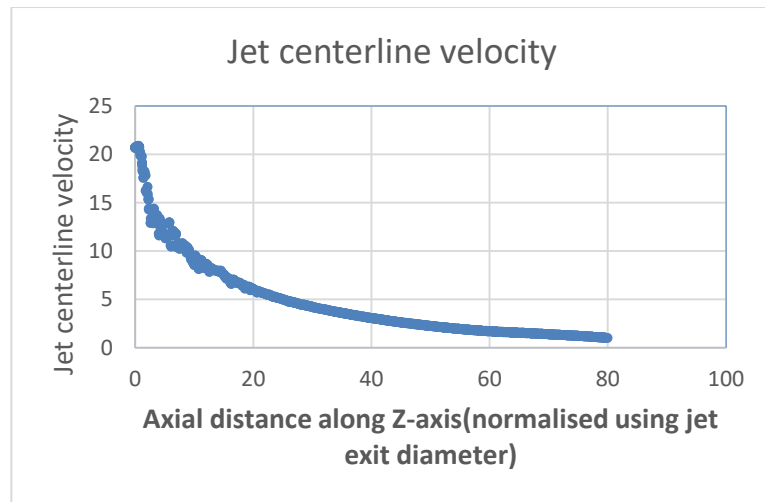
Figure 3.2: Jet Centerline Velocity

Turbulence can be thought of as fluctuations in air flow. A steady flow of air would have low turbulence. An unsteady flow of air would have higher turbulence. A uniform measurement scale is needed. Turbulence intensity is that measurement scale. Turbulence intensity is a scale characterizing turbulence expressed as a percent. An idealized flow of air with absolutely no fluctuations in air speed or direction would have a Turbulence intensity value of 0%. This idealized case never occurs on earth. However, due to how Turbulence intensity is calculated, values greater than 100% are possible. This can happen, for example, the average air speed is small and there are large fluctuations present.

Turbulence intensity is defined in the following equation:

Turbulence intensity $= u'/U$

$u =$ the Root-Mean-Square (RMS), or Standard Deviation, of the turbulent velocity fluctuations at a particular location over a specified period of time, $U =$ the average of the velocity at the same location over same time period
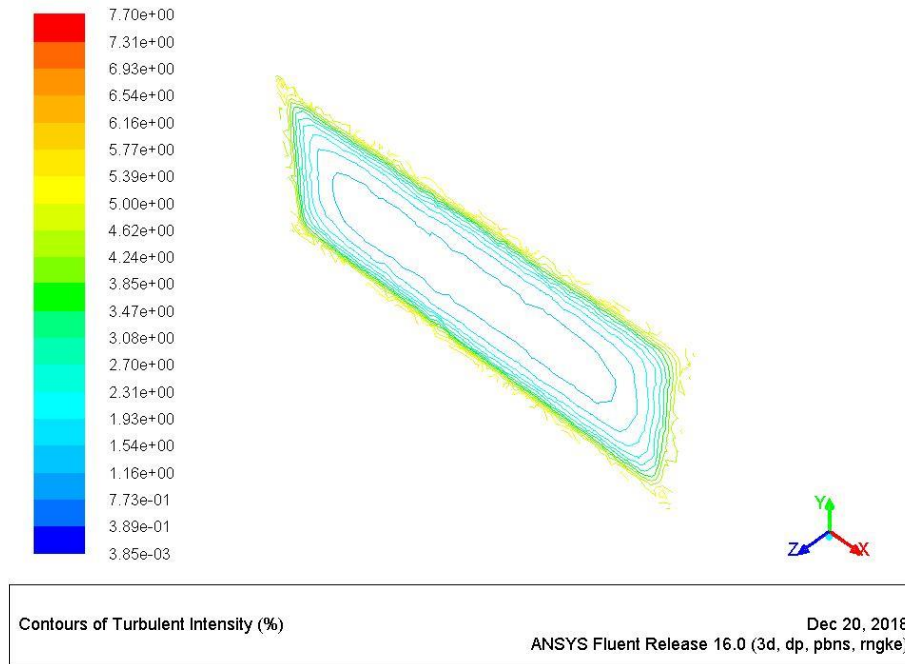
Figure 3.3: Profiles of turbulence intensity

Entrainment is the transport of fluid across an interface between two bodies of fluid by a shear induced turbulent flux [80]. Entrainment is important in turbulent jets, plumes and gravity currents and is a topic of current research. The entrainment hypothesis was first used as a model for flow in plumes by G. I. Taylor (1956) [81] when studying the use of oil drum fires to clear fog from aero-plane runways during World War II. In the present research, entrainment by the jet flow would be observed.

Another commonly used measure to characterize the growth of the jet is the half jet width. The distance measured from the centerline of the jet is precisely the half jet width, where the local mean velocity is equal to half of the local centerline mean velocity [3]. The decay rate of the centerline velocity can then be used to characterize the mixing level of the jet [3].

By imparting some twist rate on the pipe depending on the pipe length, jet flow properties can be changed again. It would create a swirling jet. In a swirling jet, usually a rotating motion is deliberately created upstream of the nozzle. As a result, a circumferential velocity component w is developed in addition to the axial and radial component u and v respectively. The intensity of the swirl is usually characterized by the Swirl number(S). It is a dimensionless quantity. There are several ways of defining it. Usually the ratio of the momentum or mass flux in circumferential and axial direction is used. Often the

nozzle radius or diameter is used for a correct normalization.

The swirling velocity component may have a large influence on the flow. The swirling motion causes a centrifugal force that is directed away from the centerline. As the fluid is forced to move away from the centerline, an area of low pressure arises close to the centerline. The intensity or, strength of the swirl becomes weaker with larger distance downstream of the nozzle.
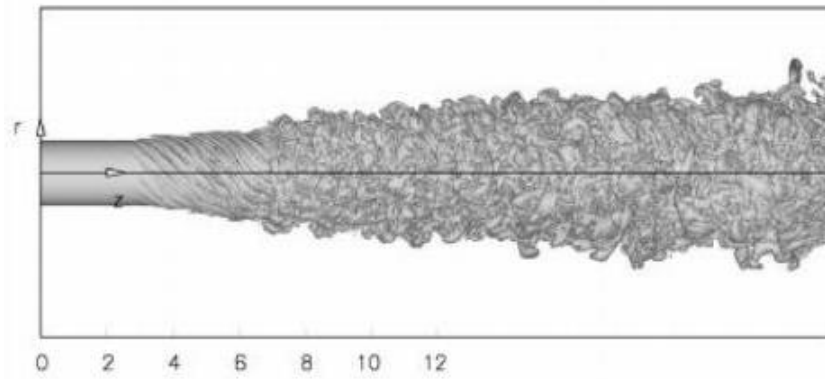

Figure 3.4: Swirling Jet [4]

The flow field of a swirling jet as shown in Fig 3.4 [4] is much more complex than its non-swirling counterpart. Swirling jets impose a radial pressure gradient. They are primarily driven in the near field by the static pressure gradients in both the axial and radial directions. The jet flow is significantly affected by the nozzle or pipe geometry. The transition characteristics of the jets also depend on the nozzle cross sectional shape. The non-circular jets, especially rectangular jets with large aspect ratios undergo the phenomenon of axis switching. During this phenomenon, the major and minor axes switch with axial distance. This is due to the different spread rates for the jet in the two lateral directions. This phenomenon is absent in round jets. Nozzle or pipe geometry has got important role to play in defining the initial velocity profile of the jet. Jet half width shown in Fig 3.5 [68] at any axial location is defined as the distance between the centerline and a traverse plane where the mean velocity becomes half of the centerline velocity. Half width generally increases linearly with X except in regions of axis switching [2]. The slope of the half width line in the axial direction is called spread rate.
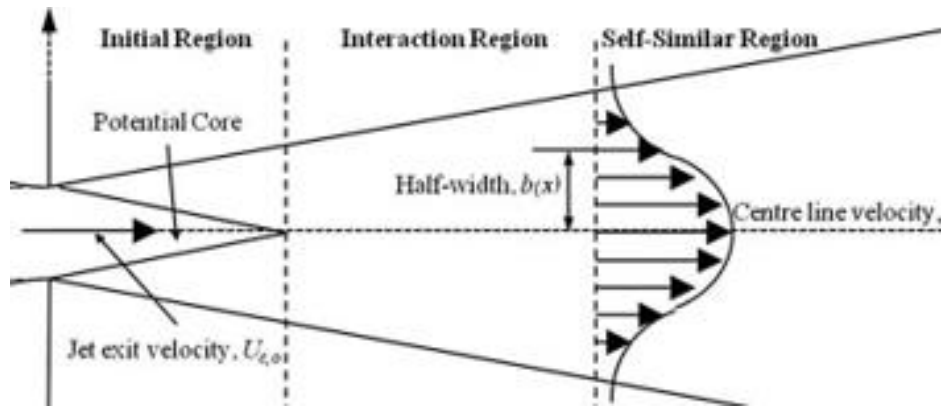
Figure 3.5: Half Width [68]

Virtual origin is the point from which the jet appears to be originating as shown in the above Fig 3.6[67]. It may be different from the geometric origin and may be located inside or outside the nozzle.
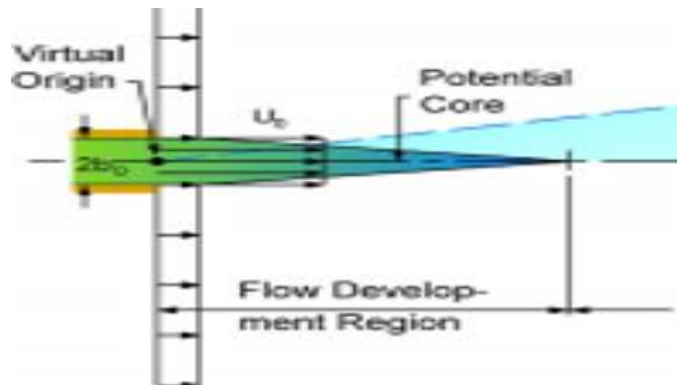

Figure 3.6: Virtual origin [67]

Chapter 4
Experimental and Computational Setup

4.1 Experimental set up

In order to undertake the study of circular and non-circular jets, both experimental and computational investigations have been done. The experimental study was undertaken in a specially designed and fabricated 'Air Flow Bench'. The air flow bench has a centrifugal blower, a settling chamber, flow straightener and the reducer (or, contraction cone). The sketch of the airflow bench showing its different parts is presented in Fig 4.1. The actual photograph of the airflow bench is shown in Fig 4.2. The only measuring device utilized is a pitot-static tube mounted on a 3-axis traversing mechanism. The traversing mechanism can be seen on left side of Fig 4.2. The present study poses a challenge of creation of non-circular cross section jets as the initial jet formed after the flow passes through the converging section is circular in cross section. Therefore, in order to create non-circular jets, a 'jet modifier pipe' is utilized. The jet modifier pipe is a small pipe attached at the convergent end of the experimental set-up through which the jet cross section is gradually changed. An off-white colored 'jet modifier pipe' can be seen in Fig 4.2 mounted in front of the reducer using flange joint. Jet modifier pipes are fabricated using 3D printing. The photographs of different configuration jet modifier pipes are shown in Fig 4.7. In order to keep exit velocity constant, the inlet and exit areas for jet modifier pipe are kept constant. Accordingly, the exit shape of the jet modifier pipe has been calculated and presented in table 4.5.
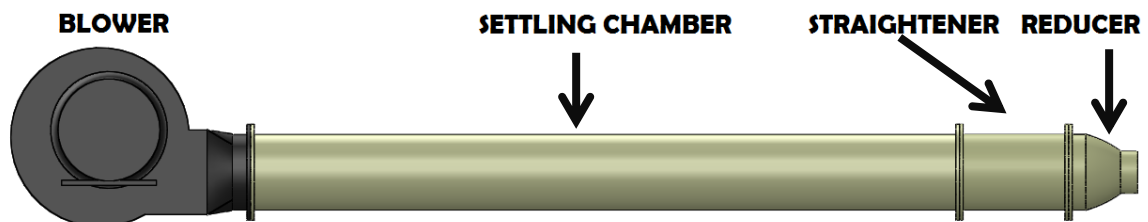

Figure 4.1: Experimental set up assembly

Figure 4.2: Air Flow bench

4.1.1 <u>Centrifugal Blower:</u>

A centrifugal fan or, blower propels air in radial direction, perpendicular to the fan's shaft. Airflow is induced by the centrifugal force generated in a rotating air column, producing static pressure (potential energy), and by the rotational velocity imparted to the air as it leaves the tip of the blades, producing velocity pressure (kinetic energy). In Fig 4.3 centrifugal blower for this set up has been shown.

Figure 4.3: Centrifugal Blower

The specifications of the blower used for the experimental set-up are shown in Table 4.1.

Power	220 *W*
Blower velocity	12 *m/s*
Mass flow rate	9.9 m^3/ *min*
Inner diameter	3.9 *in* or 9.906 *cm*
Outer diameter	12.414 *cm*

<div align="center">

Table 4.1 : Blower Specifications

</div>

The blower is powered by a DC Power Supply Unit of 220 *W*. Connections were given using electrical wires.

4.1.2 Settling Chamber:

The outgoing airflow from the blower is directed to the settling chamber. It connects the blower to the straightener region. The settling chamber provides time for the generated flow to become stable and reduce the turbulence. It also breaks down the large eddies formed. In Fig 4.4 settling chamber used for this set up has been shown.

<div align="center">
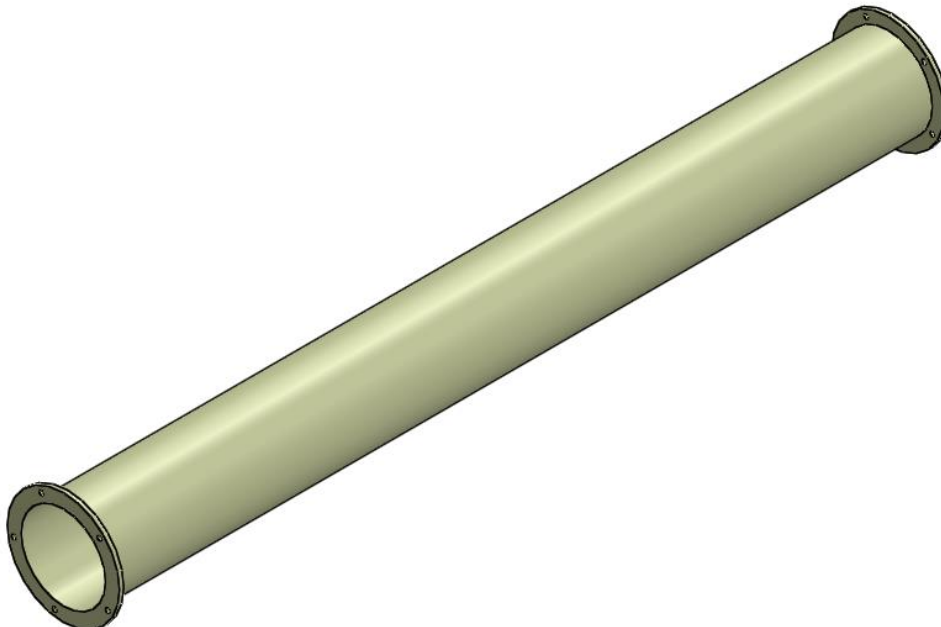
Figure 4.4: Settling Chamber

</div>

The inner and outer pipe diameter of the settling chamber is matched with that of the

blower in order to mitigate flow loss and turbulence. The length of the pipe should be large enough to allow better flow development. The specifications of the chamber used for the experimental set-up are shown in Table 4.2.

Length	97.5 *cm*
Inner Diameter	9.906 *cm*
Outer Diameter	12.414 *cm*

Table 4.2: Settling Chamber Specifications

4.1.3 Flow Straightener:

Followed by the settling chamber, the flow straightener is attached. It consists of honeycomb structure of circular cells. Uniform, circular pipes of 1.5 *cm* diameter act as the cell of the honeycomb structure. Instead of wire meshes (at the two ends), the pipes are welded together, in order to hold them together. The entire setup is tentatively small enough as such just one settling chamber will do the job. The specifications of the straightener and internal pipes used for the experimental set-up are shown in Table 4.3 and 4.4.
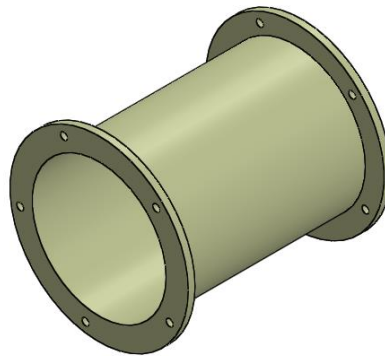
Figure 4.5: Straightener

Length	15 *cm*
Inner Diameter	9.906 *cm*
Outer Diameter	12.414 *cm*

Table 4.3: Straightener Specifications

The purposes of using the straightener section are to straighten the flow and to ensure that the flow is free from large eddies. It also allows straight and smooth flow to the discharge section.

Shape of the Pipes Used	Circle
Number of Pipes	37
Diameter of Each Pipe	1.5 *cm*

Table 4.4: Internal Pipe Specifications

The Fig 4.6 shows a cut section of the straightener segment of the 'Air Flow Bench'.

Figure 4.6: Honey Comb Structure (Inside Straightener)

4.1.4 Reducer:

The flow from the straightener is channeled through a reducer. The entry dimension of the reducer supposedly corresponds to that of the diameter of the settling chamber. The purpose of using the reducer is to connect two ducts of different diameters and to accelerate the flow.
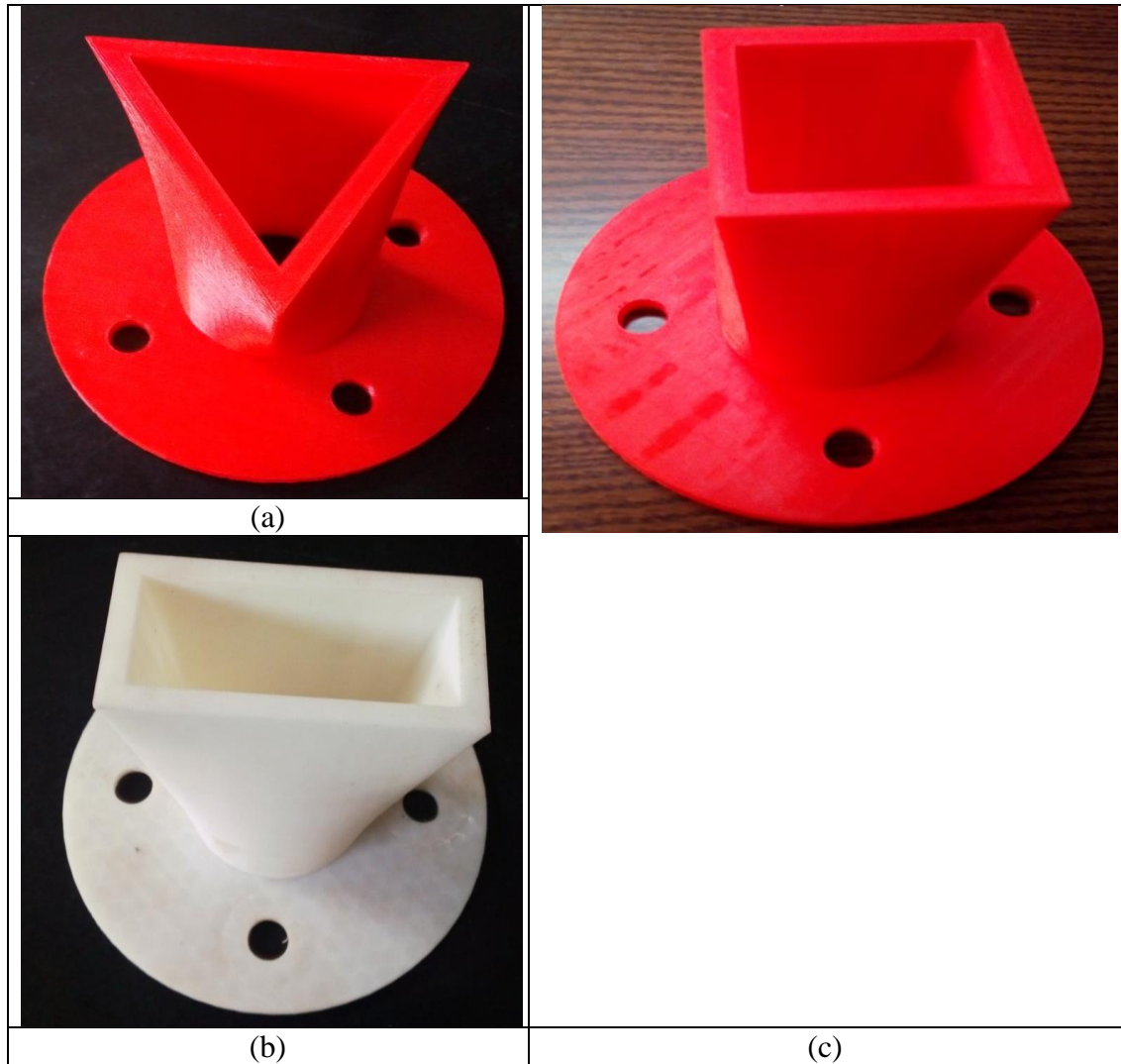
Figure 4.7: jet modifier pipes (a) Triangular (b) Rectangular and (c) Square cross section

Circular Inlet	Triangular exit	Square exit	Rectangular exit
Diameter, D=5.41 *cm*	Height, h=6.06 *cm*	Side, s=4.79 *cm*	Width, w=7.58 *cm*
	Base, b=7.58 *cm*	Area, A=22.94 *cm²*	Height, h=3.03 *cm*
Area, A=22.98 *cm²*	Area, A=22.98 *cm²*		Area, A=22.97 *cm²*

Table 4.5: Exit dimensions of non-circular cross section jet modifier pipes as compared to inlet dimensions

4.2 Co-ordinate System

Throughout the experimental study, the origin is fixed at the center of the jet exit with z-axis aligned along jet axis. Both *x* axis and *y* axis are taken perpendicular to z axis. The coordinate system used for experimental study is shown in Fig 4.8. The pitot-static tube mounted on the traversing mechanism is calibrated for zero position, every time the experimental readings are taken.
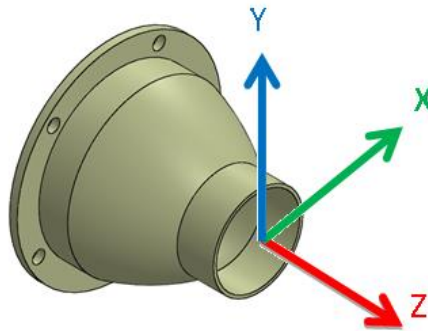
Figure 4.8: Co-ordinate System of the jet exit

4.3 Computational Set-up Prerequisites

The 3-D computational study is undertaken using ANSYS 16.2 Fluent software. Since the flow velocity is limited to less than 0.3 *Mach,* flow can be considered as incompressible. The working fluid utilized is air, which is a Newtonion fluid.

The 3D steady state steady state Reynolds Averaged Navier-Stokes forms the governing equations in numerical studies of the fluid flow. These equations are expressed as follows.

$$\text{Continuity}: \quad 0 = \frac{\partial u}{\partial x} + \frac{\partial v}{\partial y} + \frac{\partial w}{\partial z}$$

$$\text{Momentum}, x: \quad \rho\frac{Du}{Dt} = \rho g_x - \frac{\partial p}{\partial x} + \mu\left(\frac{\partial^2 u}{\partial x^2} + \frac{\partial^2 u}{\partial y^2} + \frac{\partial^2 u}{\partial z^2}\right)$$

$$\text{Momentum}, y: \quad \rho\frac{Dv}{Dt} = \rho g_y - \frac{\partial p}{\partial y} + \mu\left(\frac{\partial^2 v}{\partial x^2} + \frac{\partial^2 v}{\partial y^2} + \frac{\partial^2 v}{\partial z^2}\right)$$

$$\text{Momentum}, z: \quad \rho\frac{Dw}{Dt} = \rho g_z - \frac{\partial p}{\partial z} + \mu\left(\frac{\partial^2 w}{\partial x^2} + \frac{\partial^2 w}{\partial y^2} + \frac{\partial^2 w}{\partial z^2}\right)$$

Since the jet flows are free shear flows, the turbulent model needs to be specified to capture the effects of turbulence. Accordingly, the standard two equation K-epsilon (k-ε) turbulence model is used to capture the turbulence effects in the computational analysis. The equations are as follows [57].

For turbulent kinetic energy k

$$\frac{\partial(\rho k)}{\partial t} + \frac{\partial(\rho k u_i)}{\partial x_i} = \frac{\partial}{\partial x_j}\left[\frac{\mu_t}{\sigma_k}\frac{\partial k}{\partial x_j}\right] + 2\mu_t E_{ij}E_{ij} - \rho\epsilon$$

For dissipation

$$\frac{\partial(\rho\epsilon)}{\partial t} + \frac{\partial(\rho\epsilon u_i)}{\partial x_i} = \frac{\partial}{\partial x_j}\left[\frac{\mu_t}{\sigma_\epsilon}\frac{\partial\epsilon}{\partial x_j}\right] + C_{1\epsilon}\frac{\epsilon}{k}2\mu_t E_{ij}E_{ij} - C_{2\epsilon}\rho\frac{\epsilon^2}{k}$$

Prior to undertaking the computational analysis, it is customary and mandatory to validate the computational set up with experimental results. Hence, the experimental result published by Y. Tsuchiya and C, Horikoshi has been considered [1] as benchmark data for validation of the computational model before applying it to the present research.

4.4 Validation of the Computational process

Y. Tsuchiya and C. Horikoshi had undertaken experimental study of free jets issuing from a rectangular exit. Velocity measurements were undertaken using the total-head probe at different distances from jet exit in both horizontal and vertical axis. This paper is considered as benchmark case to validate the computational studies. Accordingly, a computational model was created and solved using the Ansys Fluent CFD software.
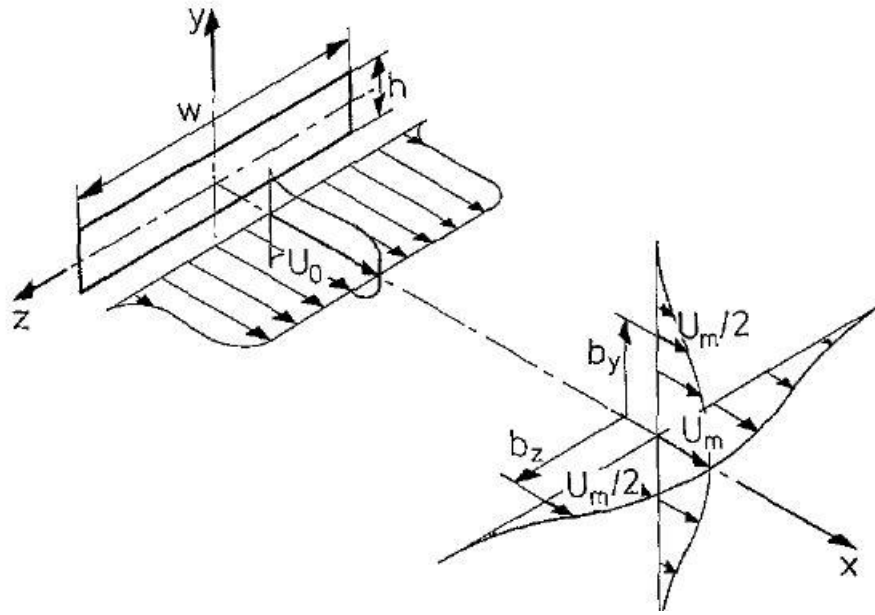
Figure 4.9: Coordinate System by Y. Tsuchiya and C. Horikoshi [1]

The velocity plots (both experimental and computational) along z and y axis at x/h=13 (h=10.10 *mm*) distance along the jet axis are compared in Fig 4.10. The velocity plots in Fig 4.10 indicate that the computational studies closely match with experimental results. The maximum percentage of error (with respect to the experimental values) was found to be within 2 *percent* (for velocity plot along y axis) and 5 *percent* (for velocity plot along z axis) which can be considered within acceptable range. The numerical and grid generation schemes used for validation of the benchmark case are utilized for present study after optimizing the number of grids cells for accurate results and faster computational efforts.
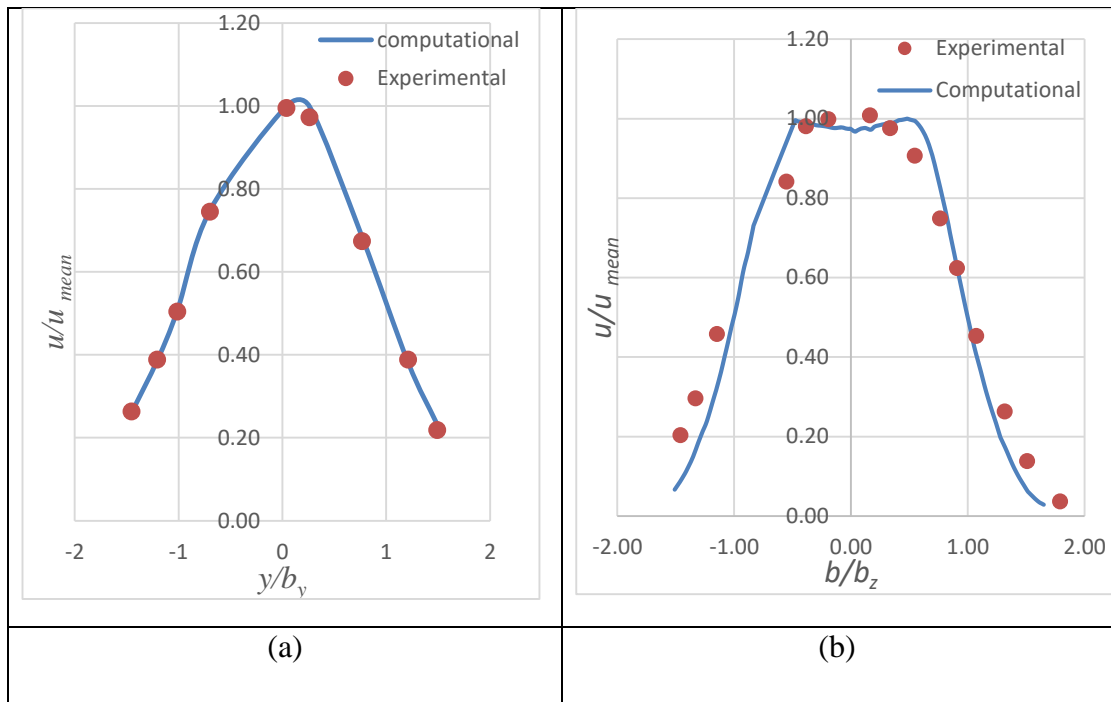
Figure 4.10: Comparison of computational and experimental solutions along (a) Y-axis (b) Z- axis at *x/h*=13 (*h*=10.10*mm*) from nozzle exit

4.5 Grid Independence check

The numerical solution is sensitive to mesh size and type. In order to ensure the results are invariant of mesh size, grid independence study is undertaken for a non-circular jet (Square cross section). The domain is discretized using three different mesh sizes viz. 0.2 *million*, 1 *million* and 2 *million* cells. The velocity plots along *X* and *Y* axis at three locations away from jet exit (1.5*D*, 3*D* and 6*D*) and at jet exit are compared and shown in Fig 4.11.
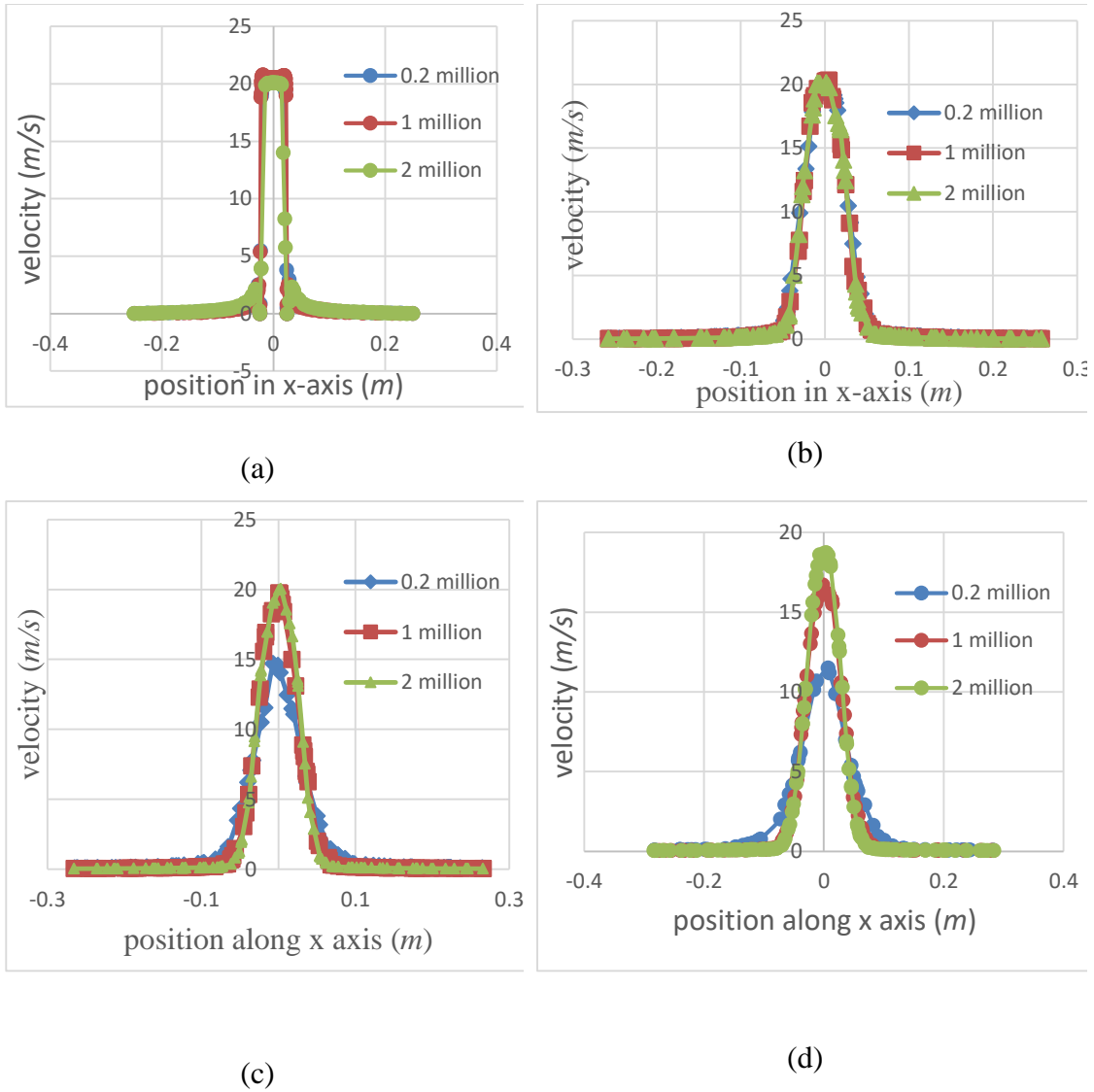
Figure 4.11: Comparison of velocity distribution along *X*-axis for different grid sizes at (a) *Z=0* (b) *Z=1.5D* (c) *Z=3D* and (d) *Z=6D* from jet exit

In order to choose the optimum grid size, the maximum variation between velocity distribution curves for grid sizes 0.2 *million* and 2 *million* is compared with 1 *million* grid size and presented in table 4.6. From the table, it is evident that as the grid size increases, the maximum percentage of deviation in velocity reduces. At the same time, as the grid size increases the time required for each computational run also increases. The time required to complete a computational study /run with respect to grid size is shown in Fig 4.12. From the table of percentage variation of velocity distribution and time required for each set of calculations, it is decided to use the 1 *million* grid size for entire sets of computations using the same grid clustering and computational schemes as

used for validation of bench mark case.

Percentage of variation with respect to 1million cells			
	0.2 *million*	1 *million*	2 *million*
0*D*	1	-	.1
1.5*D*	2.6	-	.3
3*D*	15	-	4.5
6*D*	25	-	12.5

Table 4.6: Percentage of error with respect to 1million mesh cells
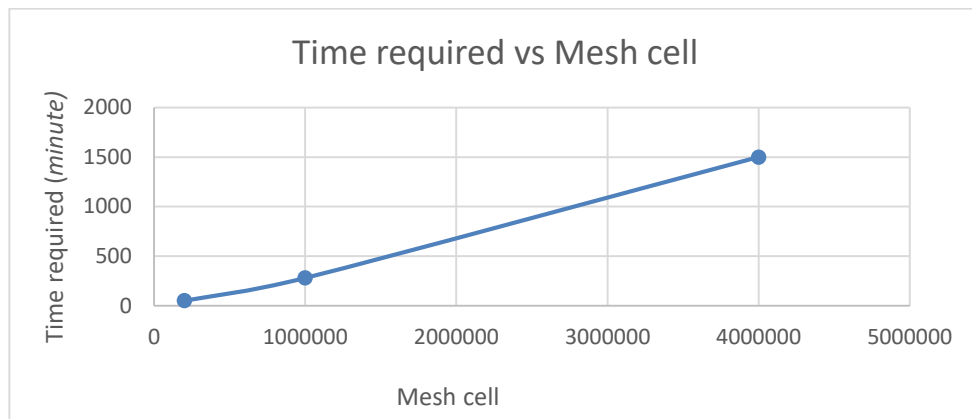
Figure 4.12: Time required vs Mesh cell

4.6 Computational setup

4.6.1 Domain:

The geometry of domain along with boundary conditions for the current study is shown in Fig 4.13.
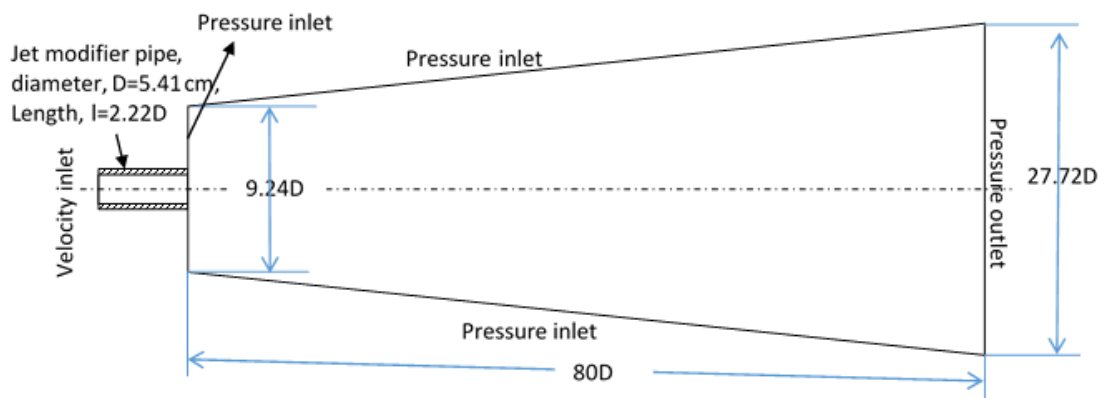
Figure 4.13: Schematic diagram of domain

Since the jet flow is the free shear flow, the free shear is expected to be present at the jet boundaries as well as inside the jet itself. In order to capture the flow features within this zone, a 'body of influence' technique is utilized while discretizing the domain. The body of influence is accordingly defined within fluid domain and is shown in Fig 4.14.
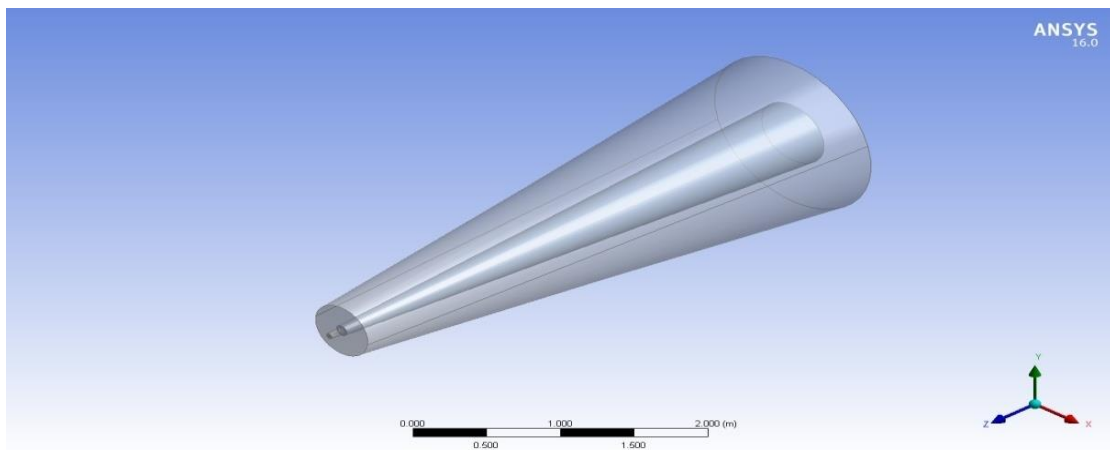
Figure 4.14: Body of influence defined within the fluid domain

4.6.2 Numerical Modelling and Boundary Conditions

The k-ε turbulence model (realizable) is used to capture the turbulence features of the jet flow. The jet inlet velocity is specified at 20 *m/s* for the jet modifier tube and turbulent viscosity ratio as 10. One atm pressure was taken as boundary conditions at the pressure inlet and pressure outlet. The domain meshing was undertaken using meshing software of Ansys. A total of 1 million elements were created. The mesh distribution is shown in Fig 4.15 which indicates the good clustering in the central zone of the domain where viscous interactions are centered.
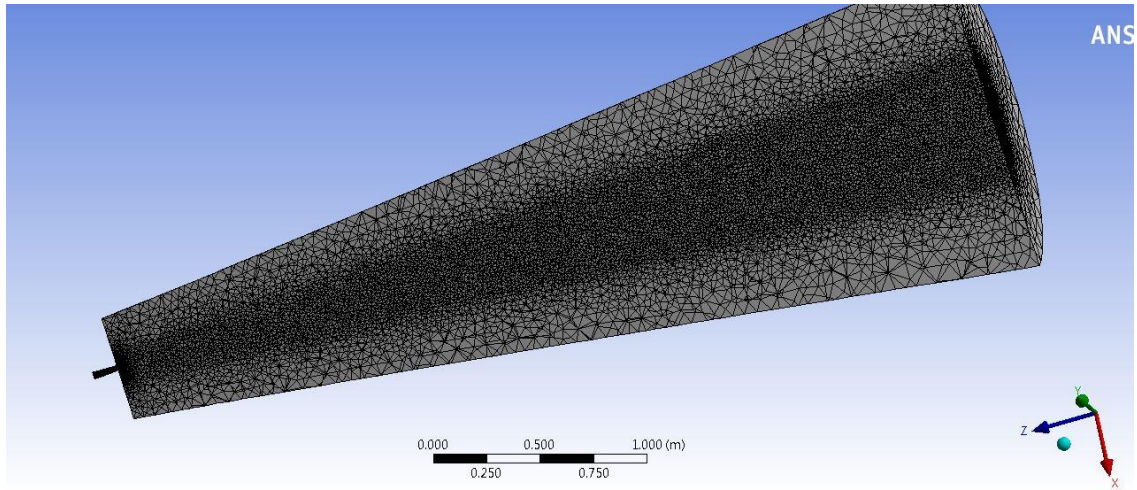
Figure 4.15: Mesh distribution

Chapter 5

Results and Discussion: Circular and Non-circular Jets

The computational and the experimental results for both circular and non-circular jets are presented in this chapter. The parametric study considered is variation of the jet exit shapes (i.e. circular, triangular, square and rectangular cross section shapes). The effect of exit shapes on the jet characteristics for experimental and computational data is analyzed in terms of (a) variation of velocity magnitude and (b) jet spread (indicated by velocity distribution along horizontal axis). In addition, the computational analysis is extended for (c) Variation of axial velocity and (d) turbulence intensity along jet axis.

5.1 Experimental Results: Circular and Non-circular jets

The plots at Fig 5.1 (a) circular, (b) square, (c) triangular, (d) rectangular present the experimental observations of velocity variation at different Z locations (i.e. $1.5D$, $3D$ and $6D$ from jet exit) along x-axis of the jet.
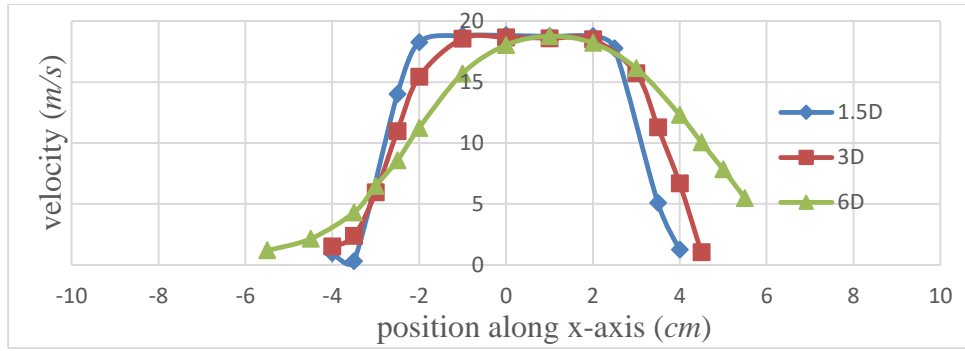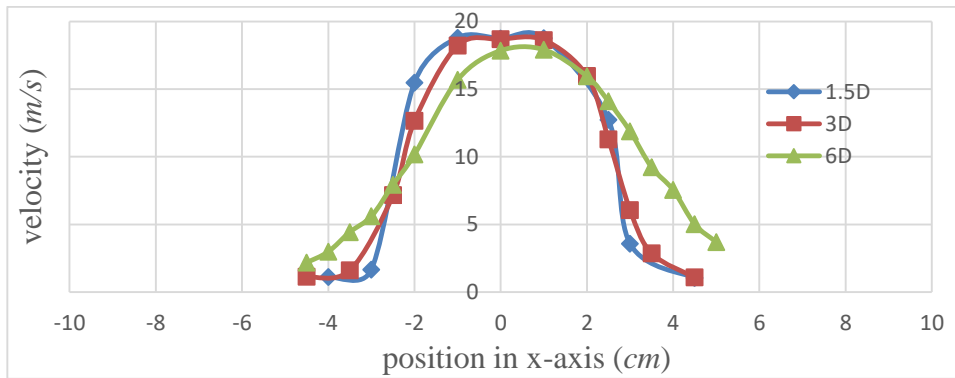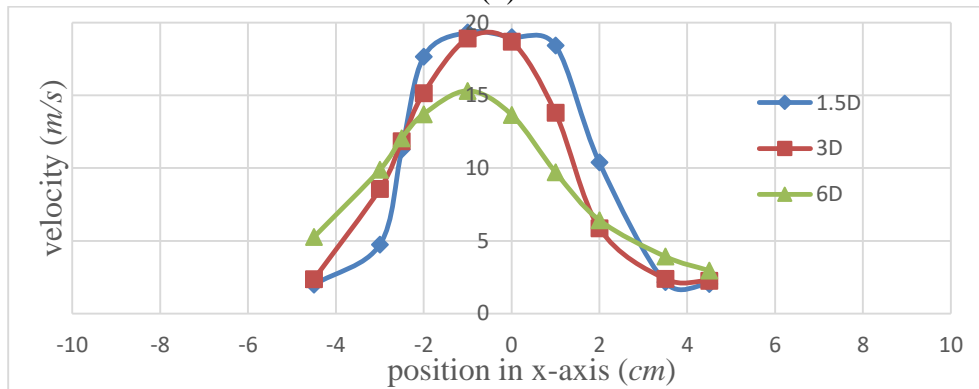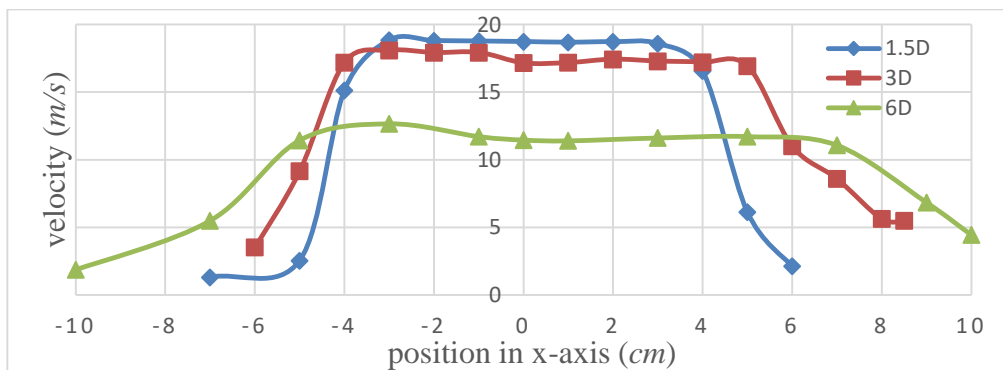
Figure 5.1: Experimental Velocity Profile (a) circular, (b) square, (c) triangular, (d) rectangular

The velocity plots indicate the following:

(a)   velocity reduces along *z*-axis and the jet spread increases for all shapes with further downstream of the pipe exit.

(b)   The jet spread calculated in terms of width of the 'jet exit cross section' indicate that the rectangular cross section gives maximum jet spread (*164%*) while triangular cross section gives minimum jet spread (*78%*) at *6D* distance.

5.2 Comparison of Computational and Experimental Results

The velocity plots at different axial distances (1.5*D*, 3*D* and 6*D* from jet exit) for experimental and computational studies are presented in Figures 5.2, 5.3, 5.4 and 5.5 for circular, square, triangular and rectangular jet exit shapes, respectively.
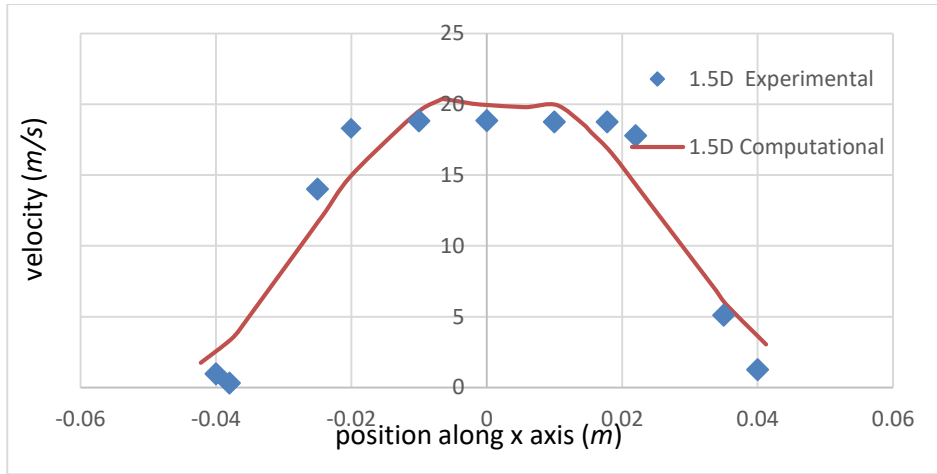
(a)
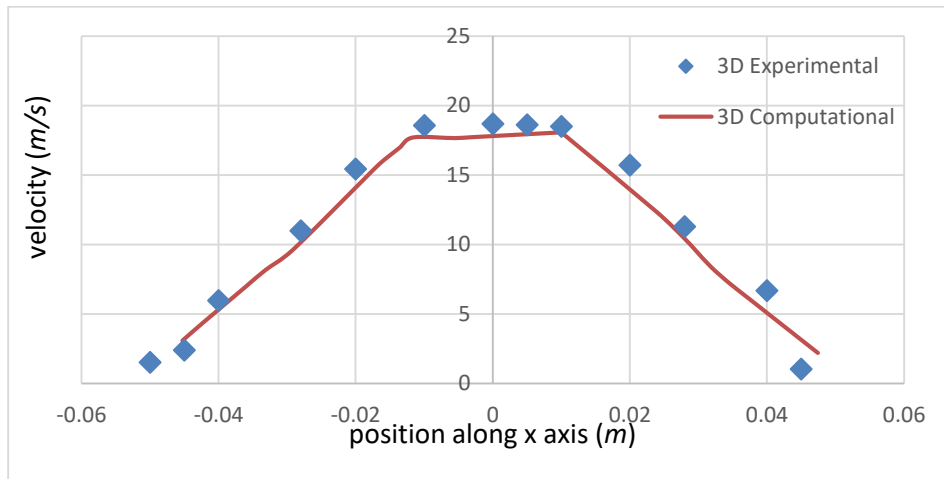
(b)
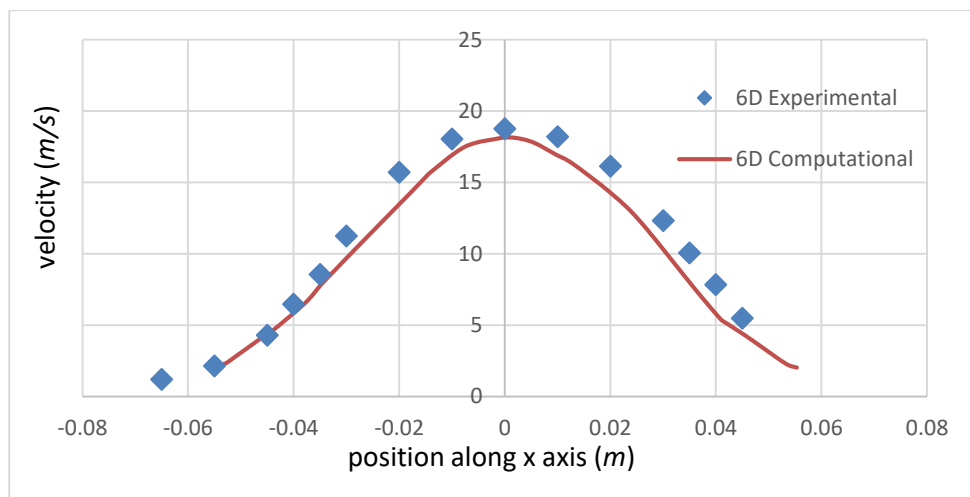
(c)

Figure 5.2: Comparison of Experimental and Computational Result for circular cross-section shape at (a)1.5*D* **(b) 3** *D* **(c) 6** *D* **behind nozzle**

Observing all these following graphs we can conclude that the computational data almost matched with the experimental data for the circular shaped pipe.
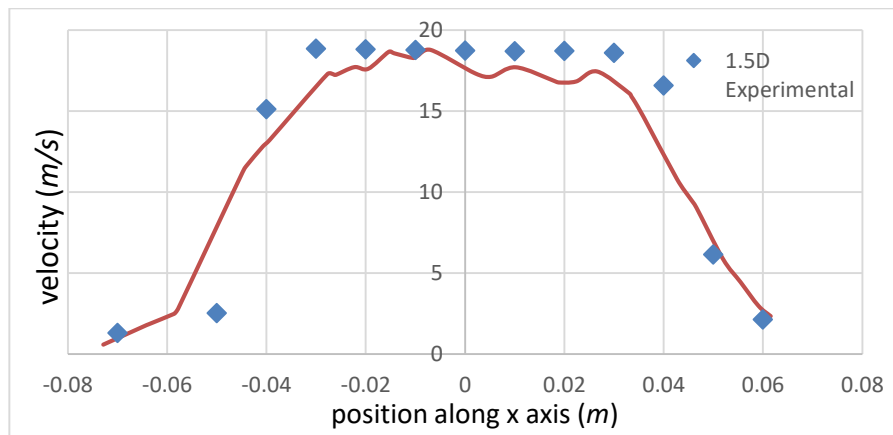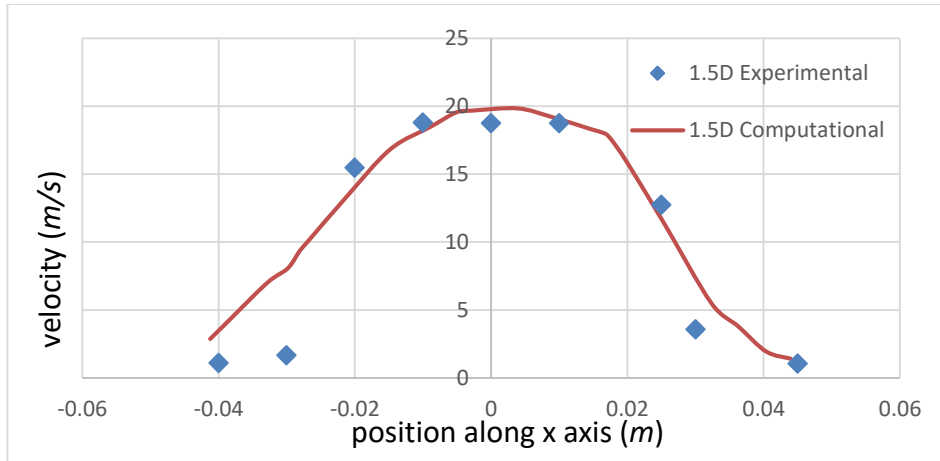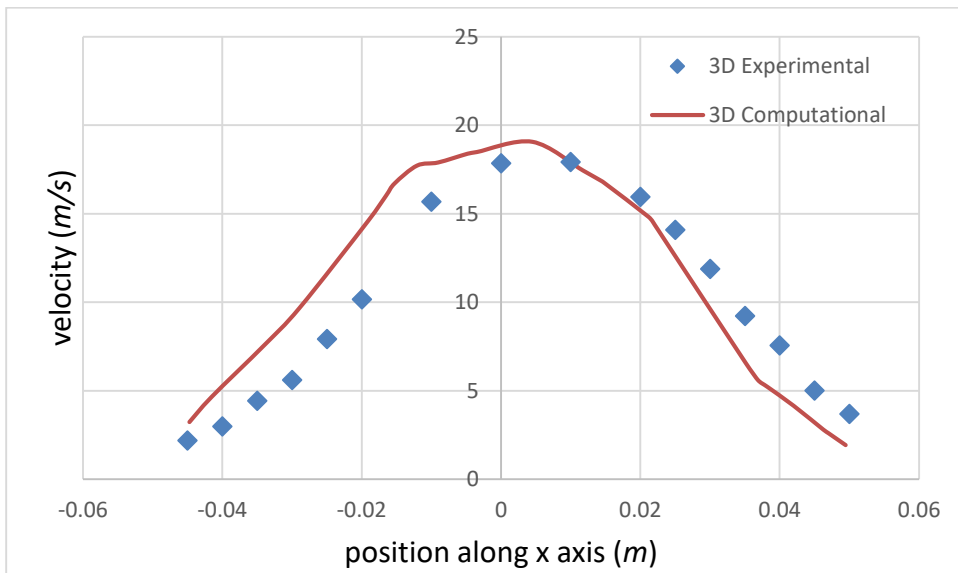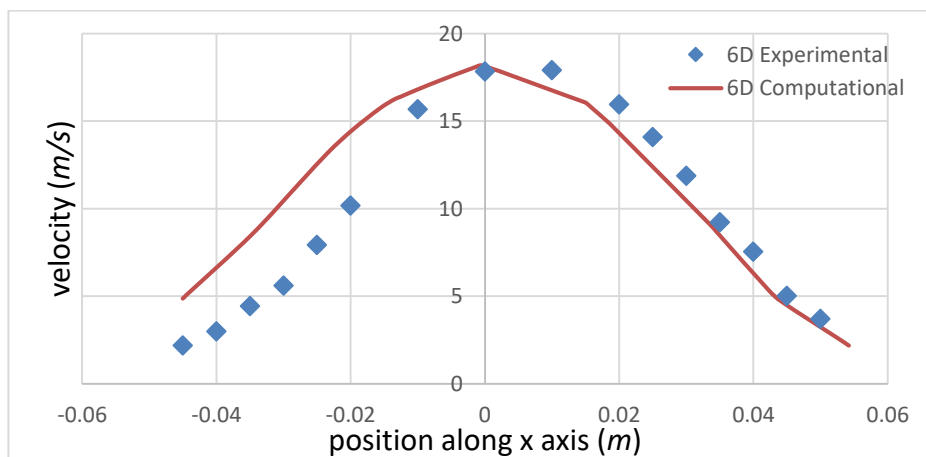

(a)
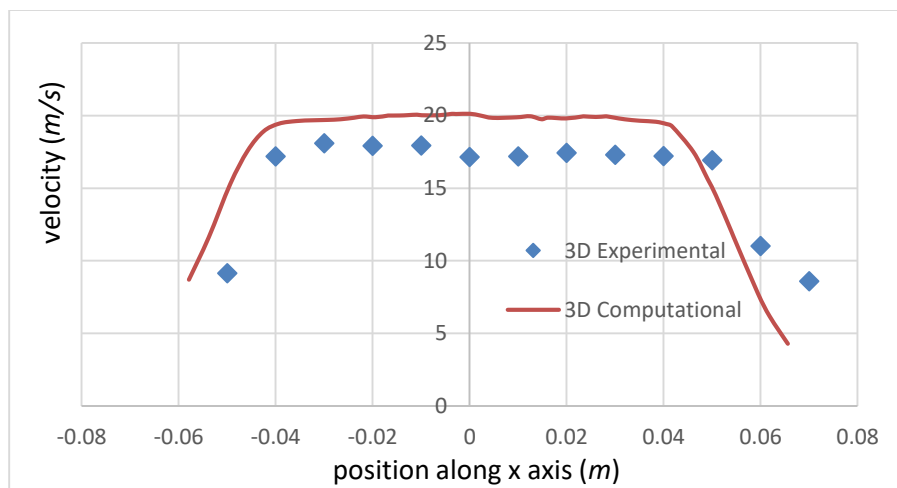
(b)
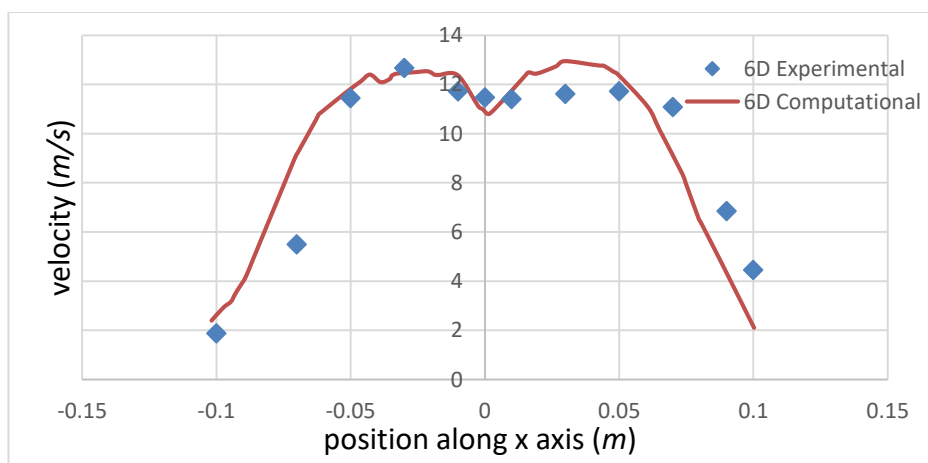
(c)

Figure 5.3: Comparison of Experimental and Computational Result for rectangular cross-section shape at (a)1.5D (b) 3 D (c) 6 D behind nozzle
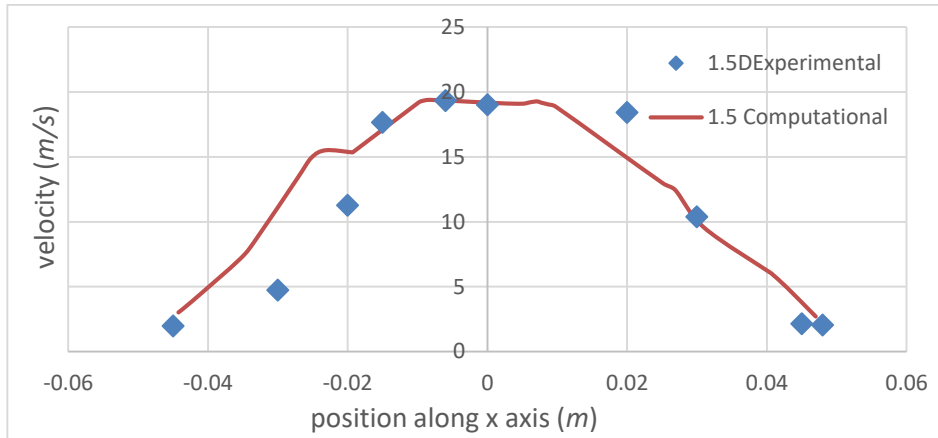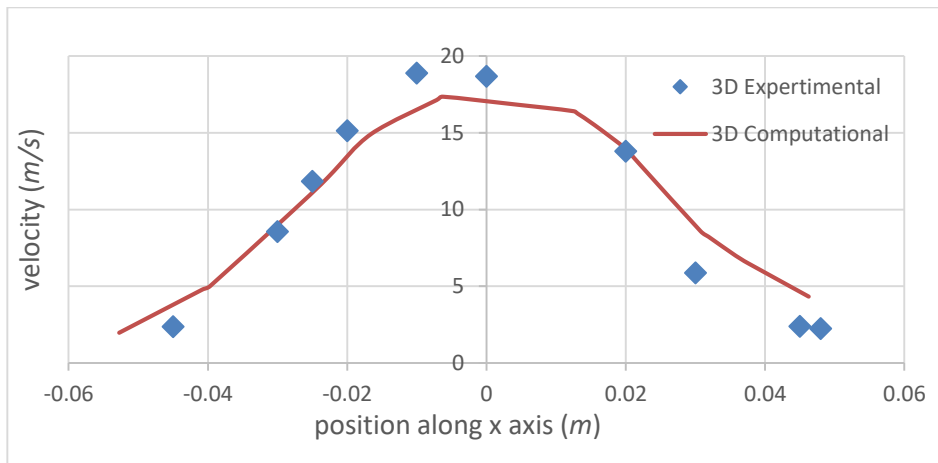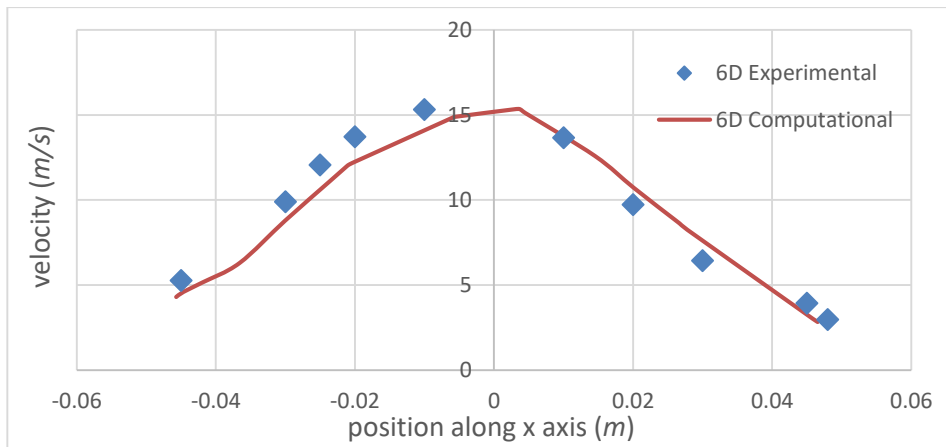
(a)

(b)

(c)

Figure 5.4: Comparison of Experimental and Computational Result for square cross-section shape at (a)1.5*D* (b) 3 *D* (c) 6 *D* behind nozzle

(a)

(b)

(c)

Figure 5.5: Comparison of Experimental and Computational Result for triangular cross-section shape at (a) 1.5*D* (b) 3*D* (c) 6*D* behind nozzle

From the above velocity plots, we can observe that:

(a)   The experimental and computational velocity plots show similar trends of velocity distribution. However, in some cases, the experimental curve appears to be shifted either to right or left of the axis. This is attributed to rudimentary traversing mechanism used to obtain experimental data.

(b)   In the vicinity of axial positions, the velocity plots (experimental and computational) match within the variation of 4-6%. However, in some cases, the variation is 30-40% (extreme cases). All other cases show that both experimental and computational pots are very close to each other. There were some alignment problems in the traverse mechanism system which causes some error in the experimental data. Maximum variations with respect to the computational plots are approximately 15% (3*D*) for rectangular jet, 28% (6*D*) for square jet and 26% (1.5*D*) for triangular jet respectively.

(c)   For the rectangular cross section jet, a saddle shape velocity profile can be seen (i.e. two peaks on both sides of the axis) at 6D location.

5.3 Comparison of local velocity along jet axis

Fig 5.6 presents variation of axial velocity along jet axis for both circular and non-circular jets. All the jets possess potential core, where the local velocity on the axis of the jet is same as the jet exit velocity ($V_{jet\ exit}$). The length of the potential core is the one of the performance parameters indicating jet distortion due to shear/mixing. It implies that lower the core length, better is mixing performance of jet.
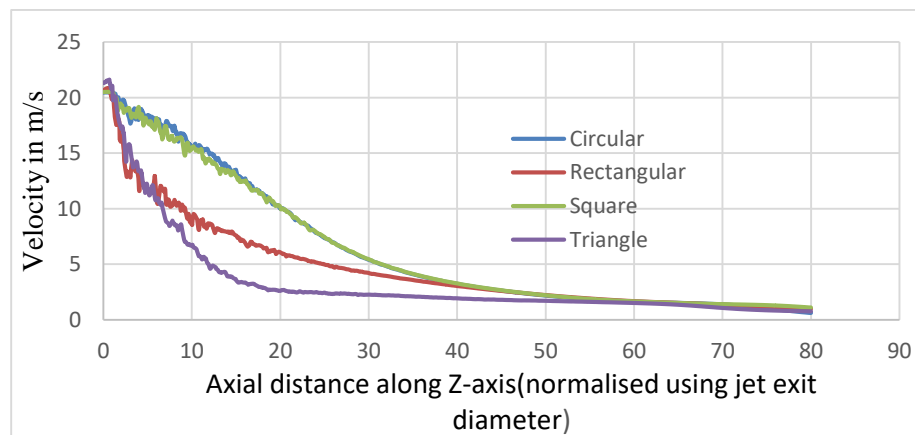

Figure 5.6: Comparison of Jet axial velocity along jet axis for circular and non-circular jets

47

The length of potential core normalized with circular jet exit diameter is calculated for two different cases i.e. (a) 2% variation and (b) 5% variation of local axial velocity from jet exit velocity. The potential core lengths observed from the computational results presented in Table 5.1.

Shape of jet cross section	2% of $V_{jet\ exit}$	5% of $V_{jet\ exit}$
Circular	1.68D	2.43D
Square	1.22D	1.92D
Triangular	1D	1.15D
Rectangular	0.84D	1.14D

Table 5.1: Potential core length for different circular and non-circular jets

From the Fig 5.6 and Table 5.1, following points emerge:

(a)   The axial velocity degradation for triangular jet is maximum while for circular jet is minimum.

(b)   The square jet plot closely matches with circular jet. The rectangular and triangular jet axial velocity plot along jet axis patterns are similar till 5D after which the triangular jet velocity reduces faster.

(c)   The potential core length for circular jet is maximum, while non-circular jets show lower core length than circular jet. The rectangular jet core length is minimum amongst four shapes.

5.4 <u>Comparison of Turbulence Intensity along jet axis</u>

Turbulence intensity of the jets is one of the measures for its mixing characteristics. Therefore, the turbulence intensity plot for all four shapes of jet exit along jet axis is shown in Fig 5.7.
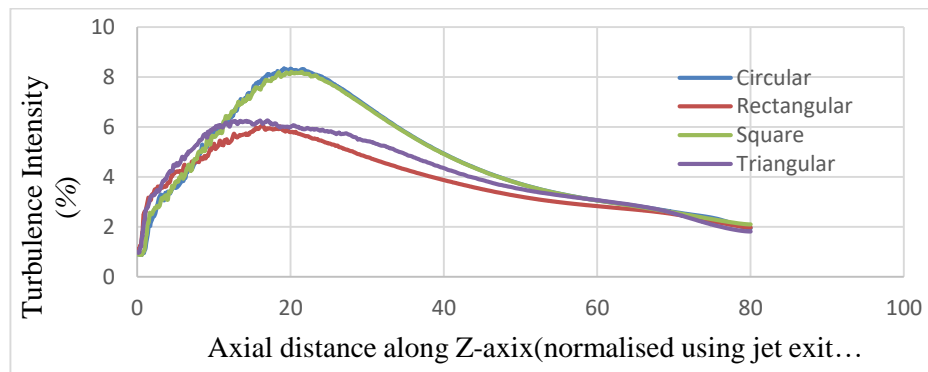

**Figure 5.7: Comparison of Turbulence Intensity along jet axis for circular and non-circular jets**

48

The turbulent intensity chart indicates following:

(a) The turbulent intensity along the jet axis is maximum for circular and square jets at $20D$ from jet exit. However, for triangular and rectangular jets the peak turbulence intensity along jet axis is at $12D$ and $16D$, respectively. This signals that the core length for circular and square jets is longer than other shapes, which is in consonance with core length observation.

(b) The closer the maximum turbulence intensity along jet axis indicate efficient mixing immediately after jet exit (especially for triangular and rectangular jets).

5.5 <u>Comparison of Non-circular cross-sectional shape jets</u>

From the previous analyses, it can be seen that the potential core for circular jet is the largest while for other shapes, its length is smaller. The maximum turbulence intensity along the jet axis is also seen to decrease for non-circular jets as compared to circular jet. The location of maximum turbulence intensity is closer for non-circular jets (exception being square jet) than the circular jets. This indicates that the maximum mixing takes place in closer vicinity for non-circular jets. Hence it can be construed that the non-circular jets are superior in performance than the circular jets when it comes to jet spread, mixing and turbulence. Therefore, it is imperative to look into better performing non-circular cross section jet among the chosen three non-circular jets.
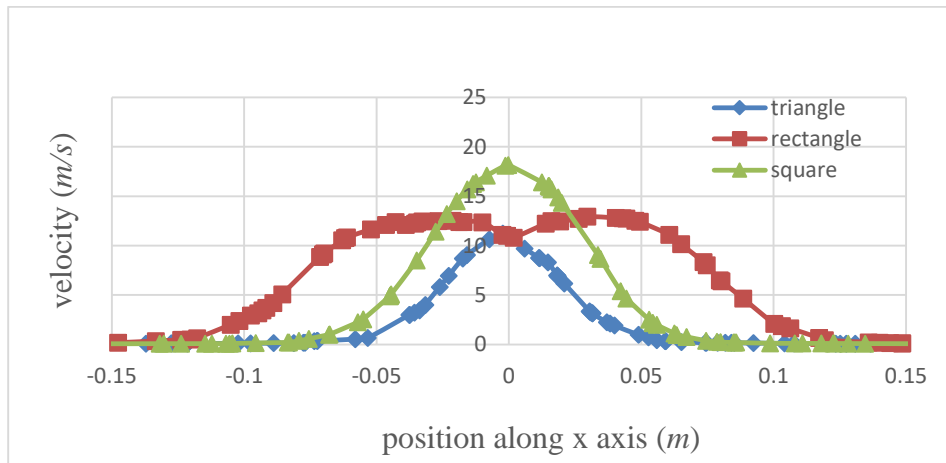
The velocity along x-axis for non-circular jets at different axial locations are compared and shown in Fig 5.8.
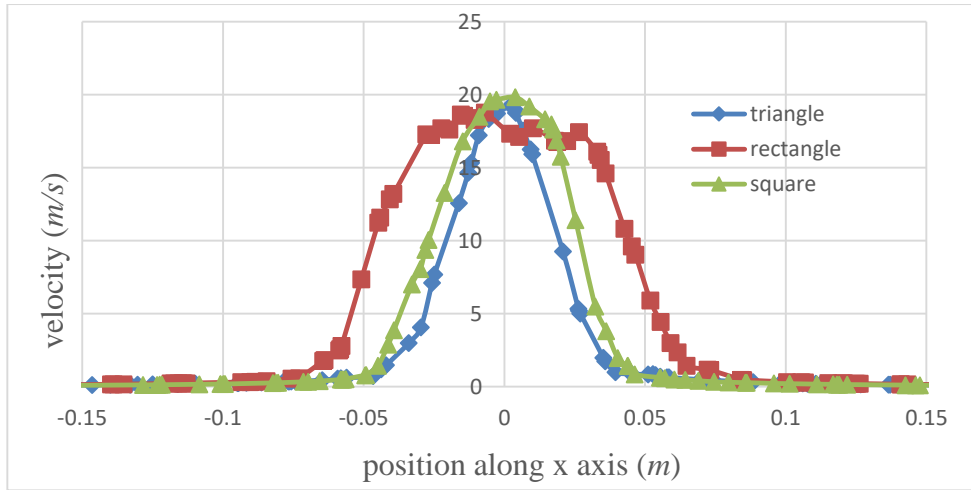
(a)
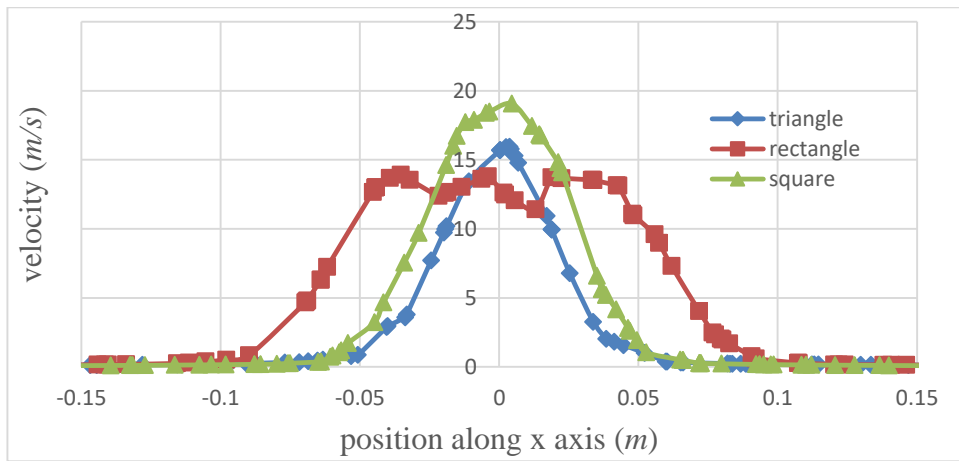
(b)

(c)

Figure 5.8: Comparison of velocity for different non-circular jets at (a) z=1.5*D*, (b)z=3*D*, (c) z=6*D*

From the plots above, following points can be summarized:

(a) The peak velocity for all three shapes is nearly same at $Z=1.5D$. The peak velocity at other Z locations reduce in magnitude for all shapes. The peak velocity for triangular and rectangular shapes reduces almost 38.8% and 30.5% respectively at $6D$ downstream of the pipe exit.

(b) Rectangular jet showcases saddle shape profile clearly at $6D$, while it is initiated at $1.5D$ distance from jet exit. This saddle shape profile makes the jet spread faster.

Chapter 6
Effect Of Peripheral Twist on Non-circular jet

The computational and experimental results as presented in previous chapter indicates that the non-circular jets are more efficient than circular jets in terms of mixing, lower potential core length etc. In order to enhance their performance further, swirl could be introduced. The conventional method of introduction of swirl is use of central vanes. The central vanes in the flow could reduce the energy of the jet due to friction or flow separation over the vanes. Therefore, a novel concept of introduction of peripheral twist to jets is conceptualized, which would not affect the flow energy as no obstructing parts will be present inside the jet. The peripheral twist is introduced in the present study by providing twist to 'jet modifier pipe'. The effect of twist on the non-circular jets is studied by varying the parameters like 'twist rate' (i.e. $40°/m$, $80°/m$, $120°/m$ and $160°/m$) and 'length of the jet modifier pipe' (6cm, 12 cm and 18cm).

6.1 Effect of twist rate: Comparison of tangential velocity

One of the main criteria to measure the swirl incorporated by the peripheral twist is tangential velocity. For different cross-sectional shapes, tangential velocity has been measured at different locations.
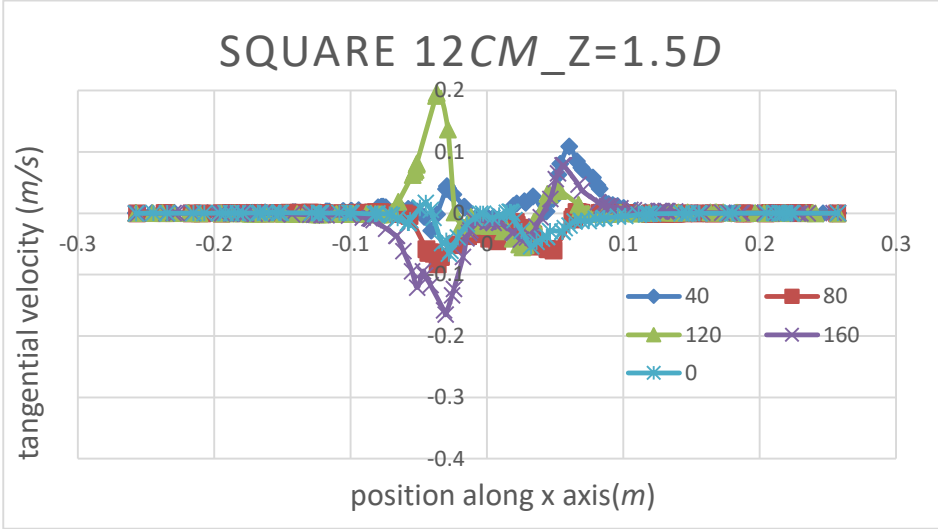
6.1.1 Comparison of tangential velocity: Square Cross section

For square cross-sectional shape, tangential velocity for different location has been compared. Different twist rates have been taken into consideration for comparison of tangential velocity without any twist rate. 4 twist rates i.e. $40°/m$, $80°/m$, $120°/m$ and $160°/m$ have been observed. Moreover, different pipe lengths have also been considered for the same case. Depending upon the pipe lengths, different twist angles have been derived for different pipes to compare the effect keeping the twist rates similar.
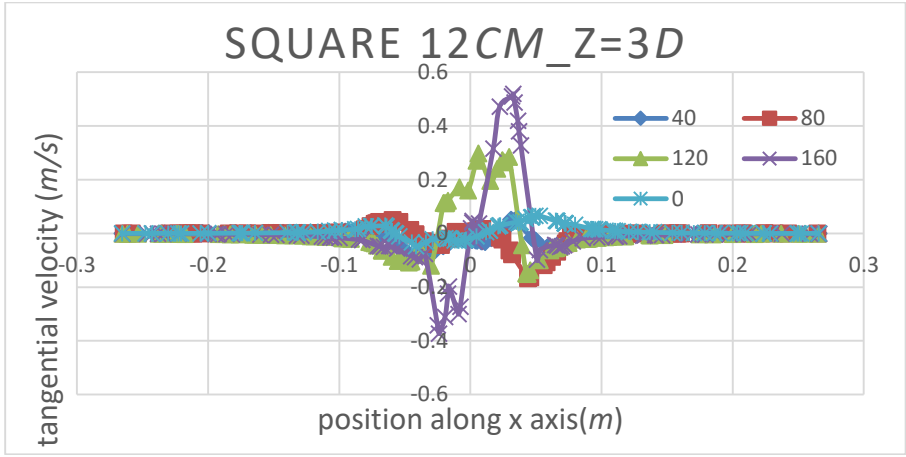
6.1.1.1   Comparison of tangential velocity: pipe length 12 cm: Square Cross section: Z= 1.5D, 3D, 6D

Tangential velocity along x axis has been compared in Fig 6.1 at (a) z=1.5D, (b)z=3D, (c) z=6D for square cross section. Here 12 cm pipe length has been taken into consideration. For this pipe, 4 different twist angles i.e. 4.8, 9.6, 14.4, 19.2 (in *degree*)
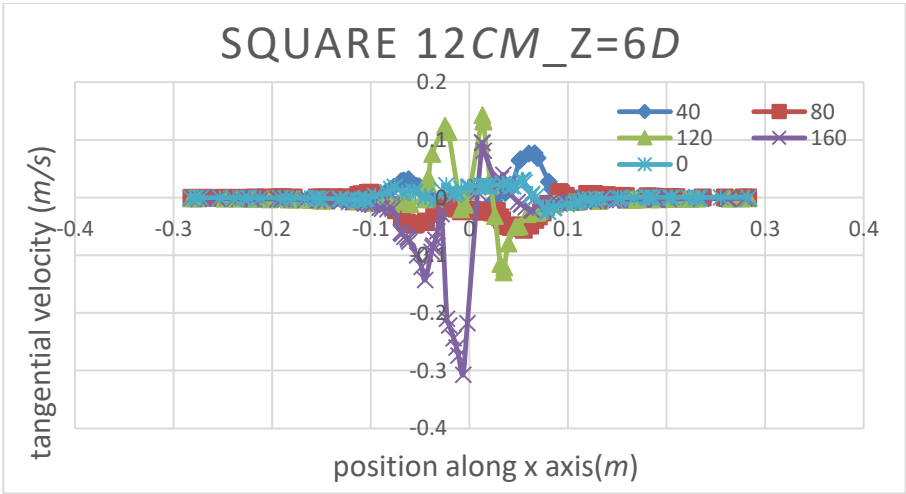
have been derived from the twist rates i.e. $40°/m$, $80°/m$, $120°/m$ and $160°/m$, respectively.
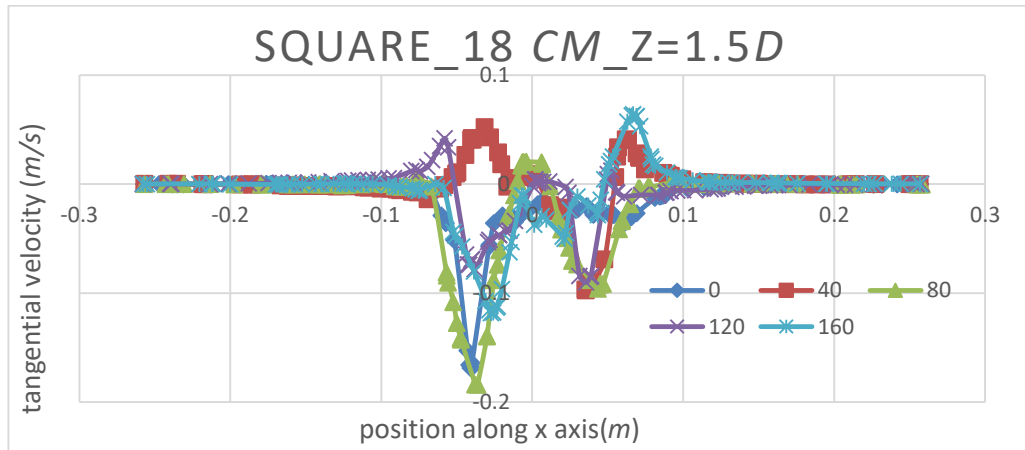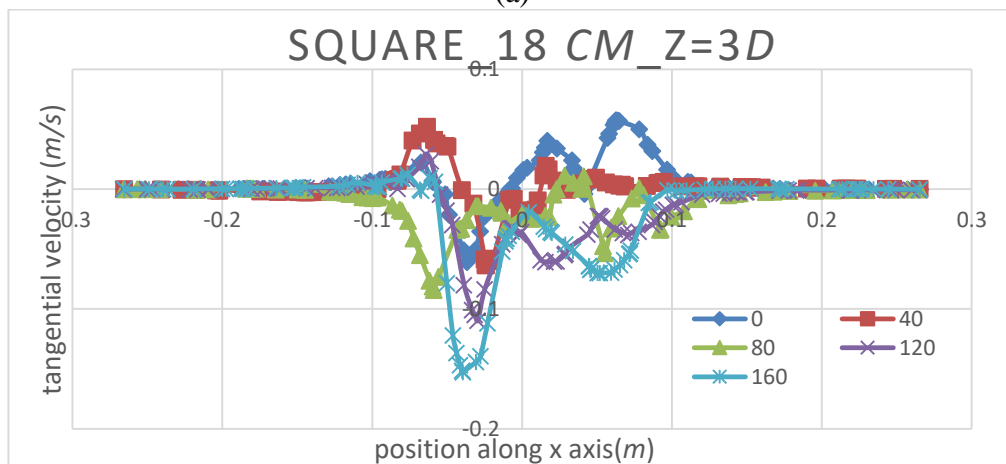

(a)

(b)

(c)

Figure 6.1: Comparison of tangential velocity at (a) *z=1.5D*, (b) *z=3D*, (c) *z=6D* for square cross-section shape for 12 *cm* pipe

6.1.1.2 Comparison of tangential velocity: pipe length 18cm: Square Cross section: *Z= 1.5 D, 3D, 6D*
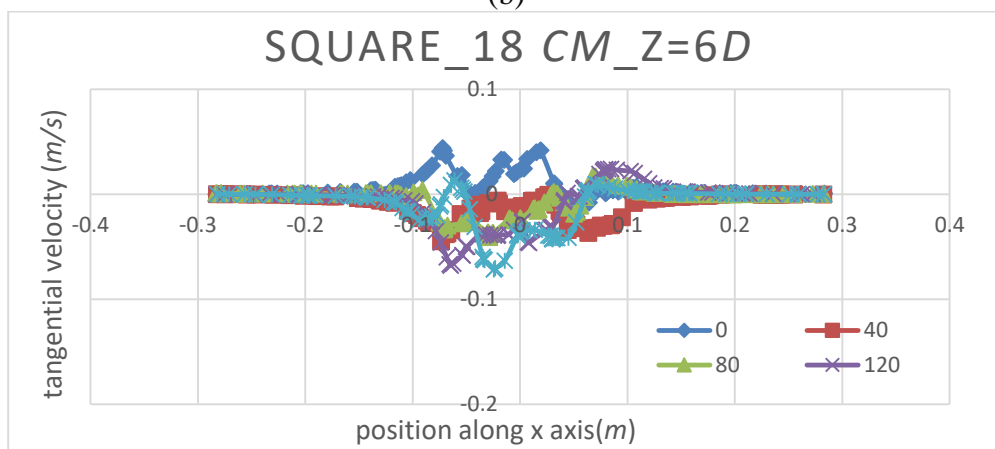
Tangential velocity along *x* axis has been compared for square cross section of 18 cm pipe in Fig 6.2 at (a) *z=1.5D*, (b) *z=3D*, (c) *z=6D*.
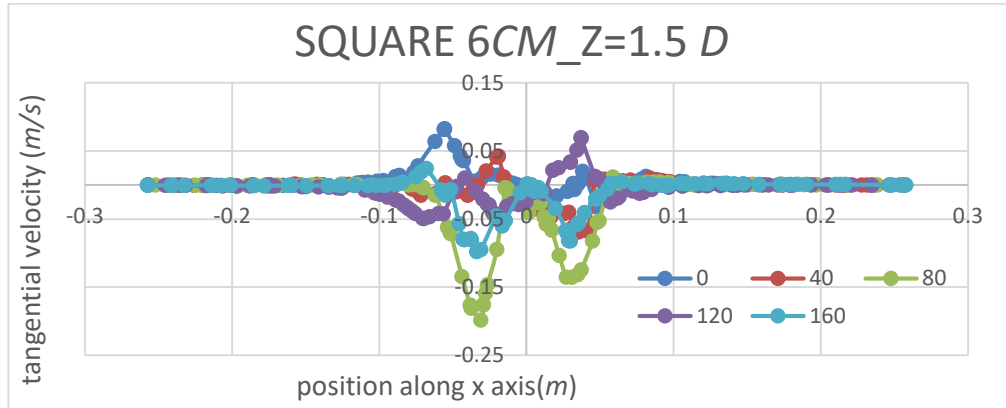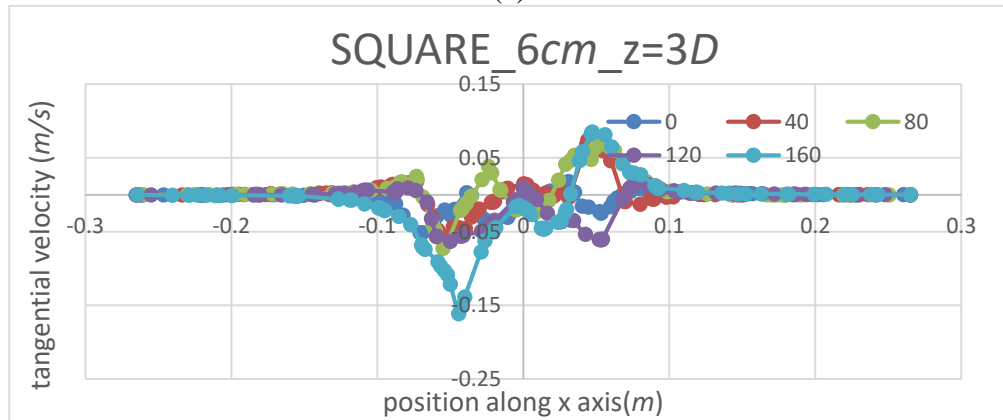

(a)

(b)

(c)

Figure 6.2: Comparison of tangential velocity at (a) *z=1.5D*, (b) *z=3D*, (c) *z=6D* for square cross-section shape for 18 *cm* pipe

6.1.1.3 Comparison of tangential velocity: pipe length 6 *cm*: Square Cross section: *Z*= 1.5 *D*, 3*D*,6*D*
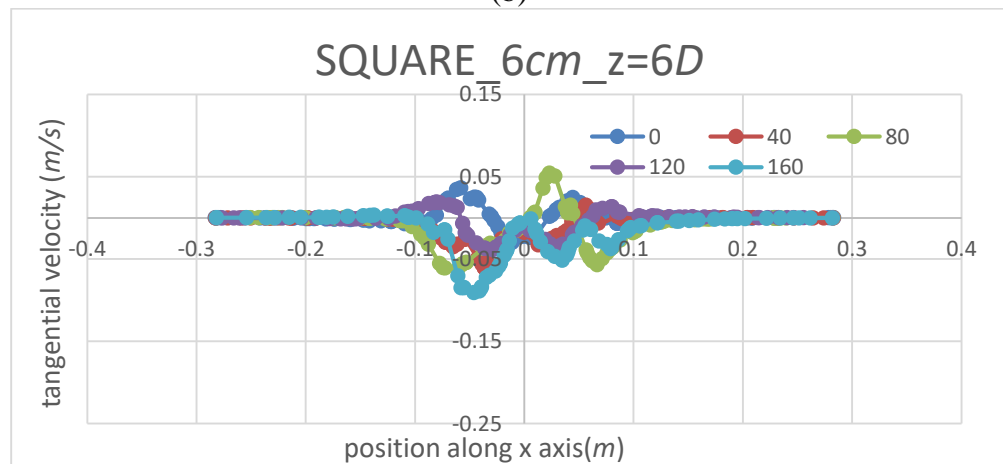
Tangential velocity along *x* axis has been compared in Fig 6.3 at (a) *z=1.5D*, (b) *z=3D*, (c) *z=6D* for square cross section of 6 cm pipe.
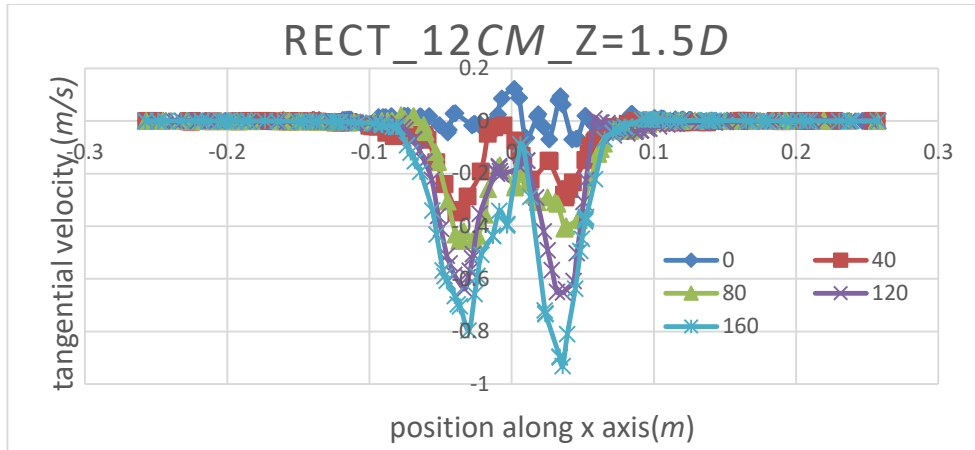

(a)

(b)

(c)

Figure 6.3: Comparison of tangential velocity at (a) *z=1.5D*, (b) *z=3D*, (c) *z=6D* for square cross-section shape for 6 *cm* pipe

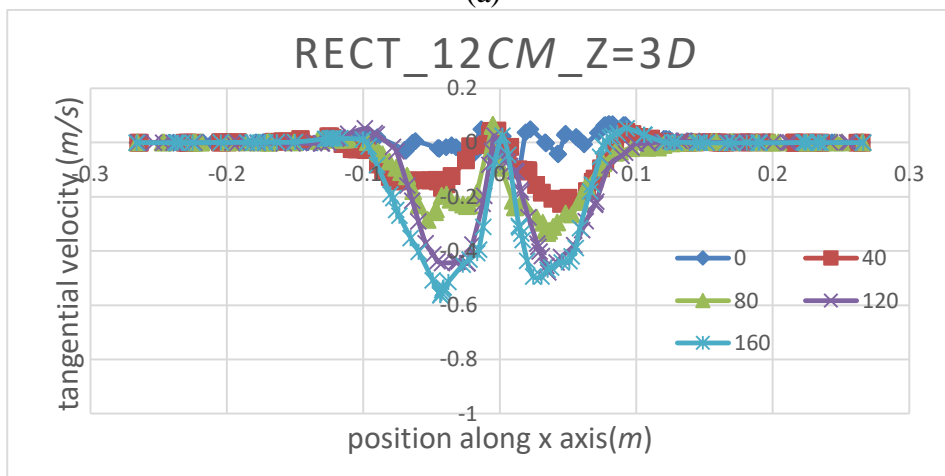### 6.1.2 Comparison of tangential velocity: Rectangular Cross section

For the rectangular cross section, different twist rates have been taken into consideration for comparison of tangential velocity without any twist rate. 4 twist rates i.e. $40°/m$, $80°/m$, $120°/m$ and $160°/m$ and different pipe lengths have been considered here also like the square cross section.

6.1.2.1 Comparison of tangential velocity: pipe length 12 *cm*: Rectangular Cross section: *Z*= 1.5 *D*, 3*D*, 6*D*

Tangential velocity along *x* axis has been compared in the Fig 6.4 at (a) *z*=1.5*D*, (b) *z*=3*D*, (c) *z*=6*D* for rectangular cross section for 12 *cm* pipe length. Twist rates and twist angles have been considered likewise the 12 *cm* pipe for square cross section.
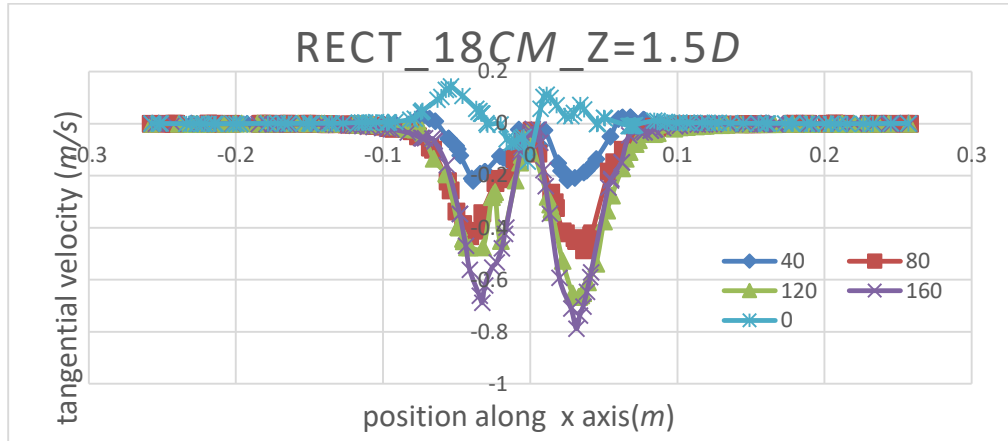
(a)

(b)
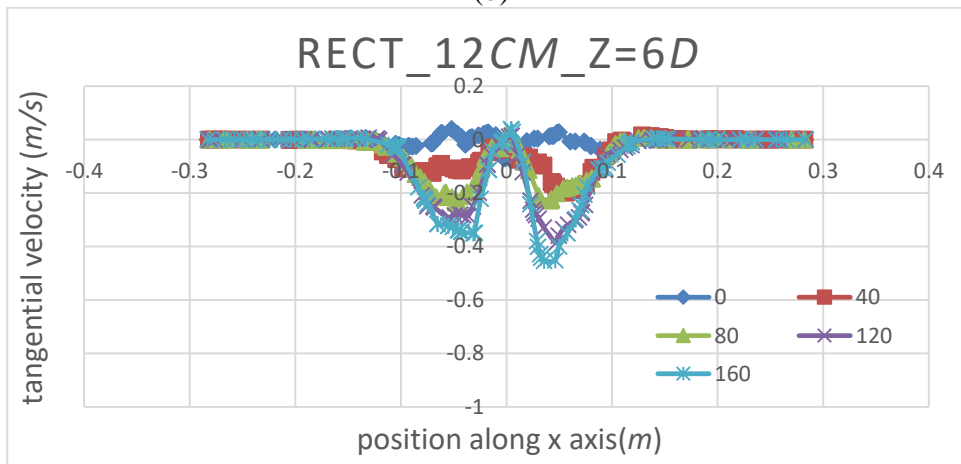
(c)

Figure 6.4: Comparison of tangential velocity at (a) *z=1.5D*, (b) *z=3D*, (c) *z=6D* for rectangular cross-section shape for 12 *cm* pipe

6.1.2.2 Comparison of tangential velocity: pipe length 18 *cm*: Rectangular Cross section: *Z*= 1.5 *D*, 3*D*, 6*D*

Tangential velocity along *x* axis has been compared for rectangular cross section in Fig 6.5 at (a) *z*=1.5*D*, (b) *z*=3*D*, (c) *z*=6*D* for 18 *cm* pipe length

(a)

(b)

(c)

Figure 6.5: Comparison of tangential velocity at (a) *z*=1.5*D*, (b) *z*=3*D*, (c) *z*=6*D* for rectangular cross-section shape for 18 *cm* pipe

6.1.2.3 Comparison of tangential velocity: pipe length 6 cm: Rectangular Cross section: *Z= 1.5 D, 3D, 6D*

Tangential velocity along *x* axis has been compared for rectangular cross section in Fig 6.6 at (a) *z=1.5D*, (b) *z=3D*, (c) *z=6D* for 6 *cm* pipe length.
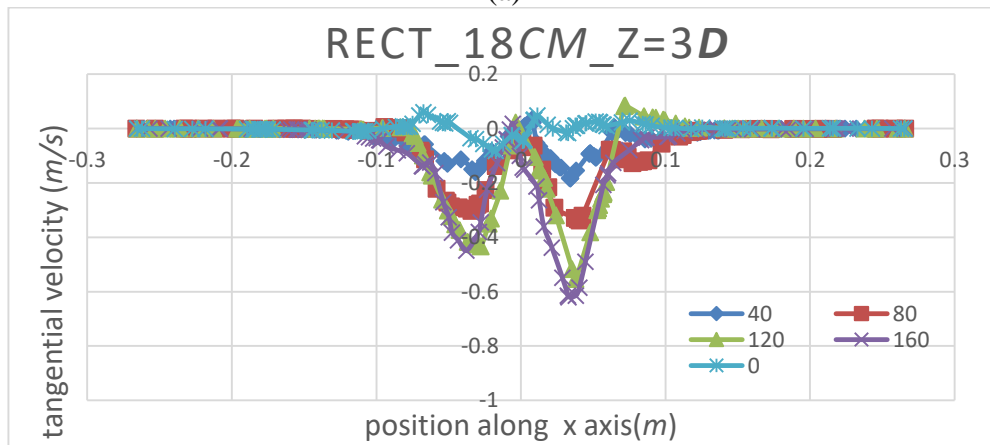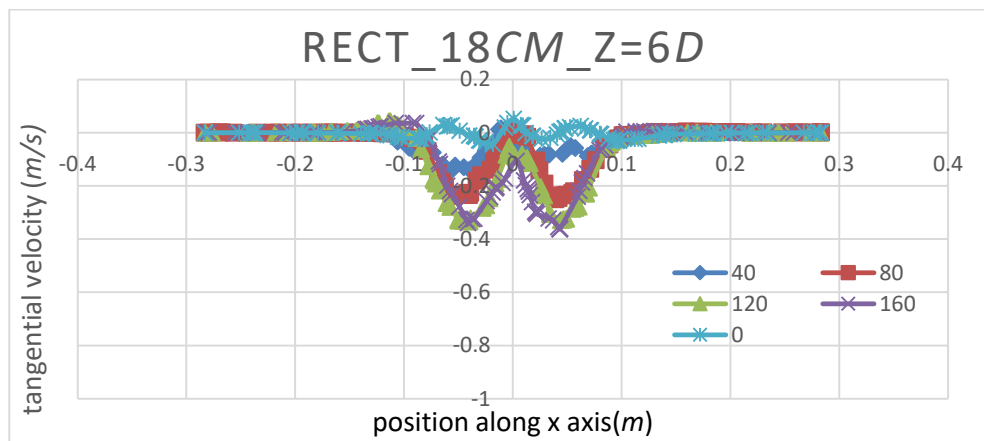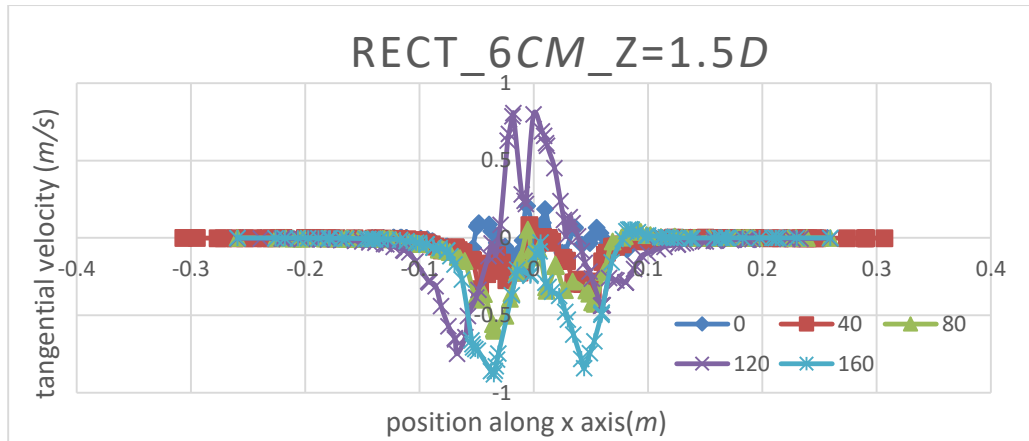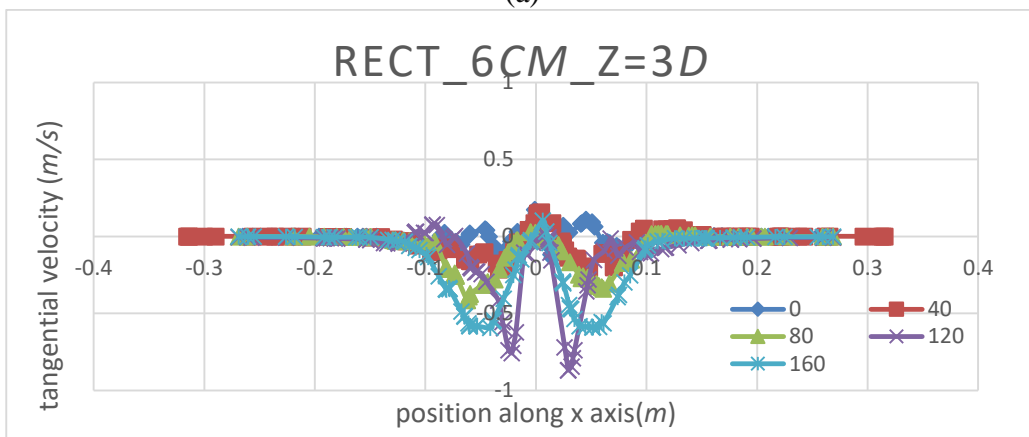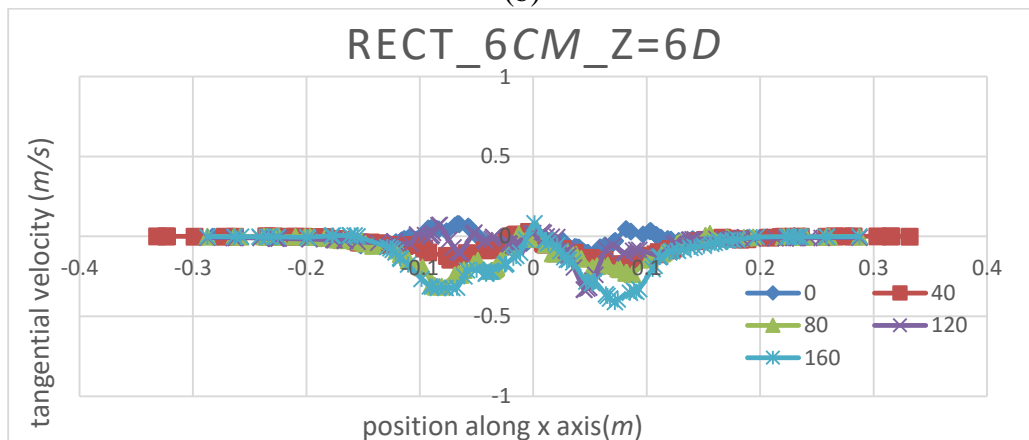

(a)

(b)

(c)

Figure 6.6: Comparison of tangential velocity at (a) *z=1.5D*, (b) *z=3D*, (c) *z=6D* for rectangular cross-section shape for 6 *cm* pipe

6.1.3 <u>Comparison of tangential velocity: Triangular Cross section</u>

For the triangular cross section also, different twist rates have been taken into consideration for comparison of tangential velocity without any twist rate. 4 twist rates i.e. $40°/m$, $80°/m$, $120°/m$ and $160°/m$ and different pipe lengths have been considered here also like the square and rectangular cross section. In the similar way, for the triangular cross-sectional shape also, for different pipe lengths, tangential velocity is observed along x axis with different twist rates.

6.1.3.1 <u>*Comparison of tangential velocity: pipe length 12 cm: Triangular Cross section: Z= 1.5 D, 3D, 6D*</u>

Tangential velocity along x axis has been compared in the Fig 6.7 at (a) z=1.5D, (b) z=3D, (c) z=6D for triangular cross section for 12 cm pipe length. Twist rates and twist angles have been considered likewise the 12 cm pipe for square cross section.

(a)
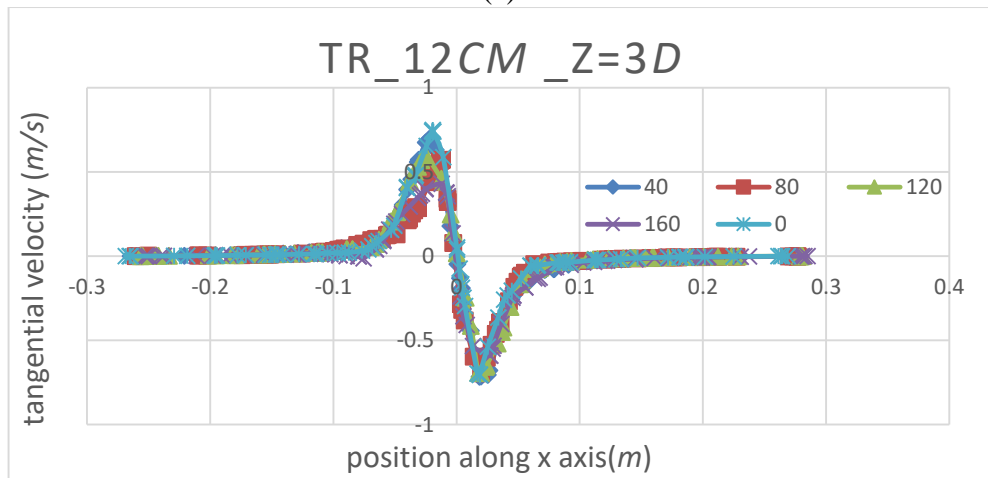
(b)
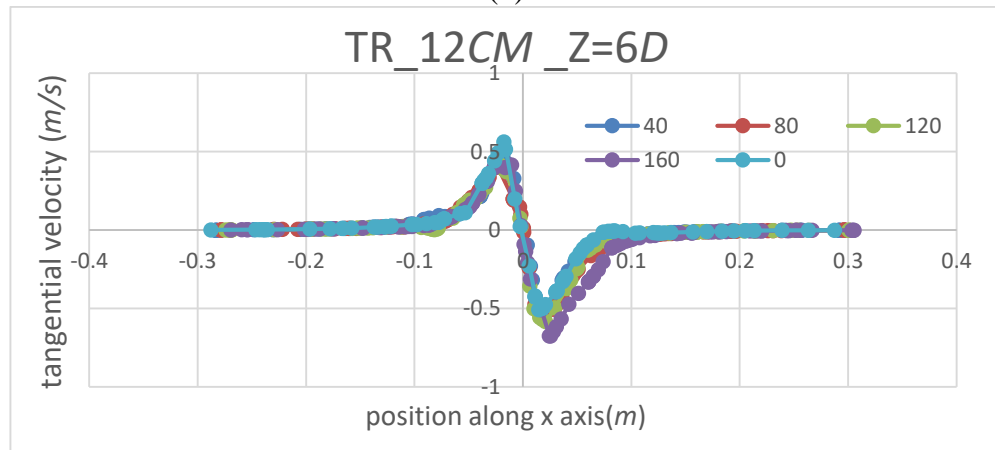
(c)

Figure 6.7: Comparison of tangential velocity at (a) *z=1.5D***, (b)** *z=3D***, (c)** *z=6D* **for triangular cross-section shape for 12** *cm* **pipe**

(a)

(b)
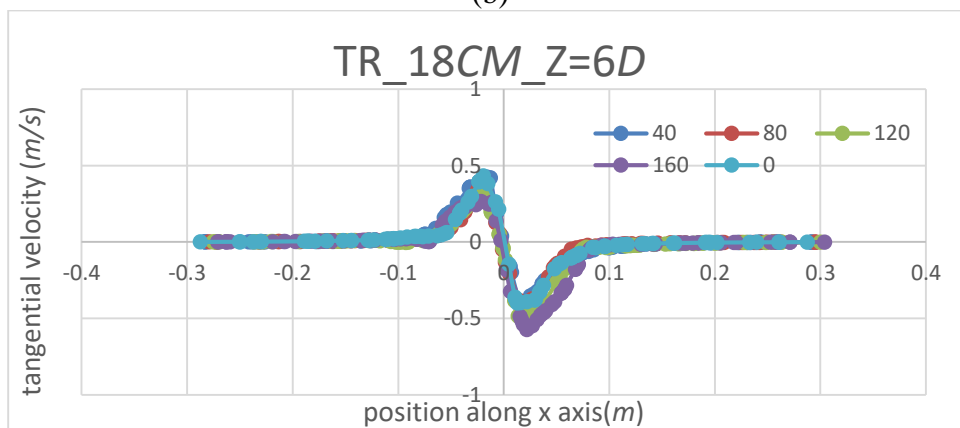
(c)

Figure 6.8: Comparison of tangential velocity at (a) *z=1.5D*, **(b)** *z=3D*, **(c)** *z=6D* **for triangular cross-section shape for 18** *cm* **pipe**
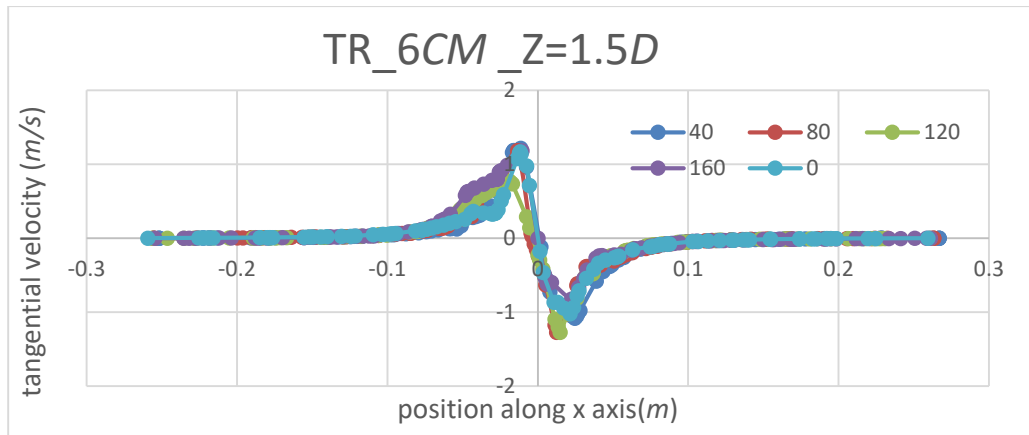
(a)
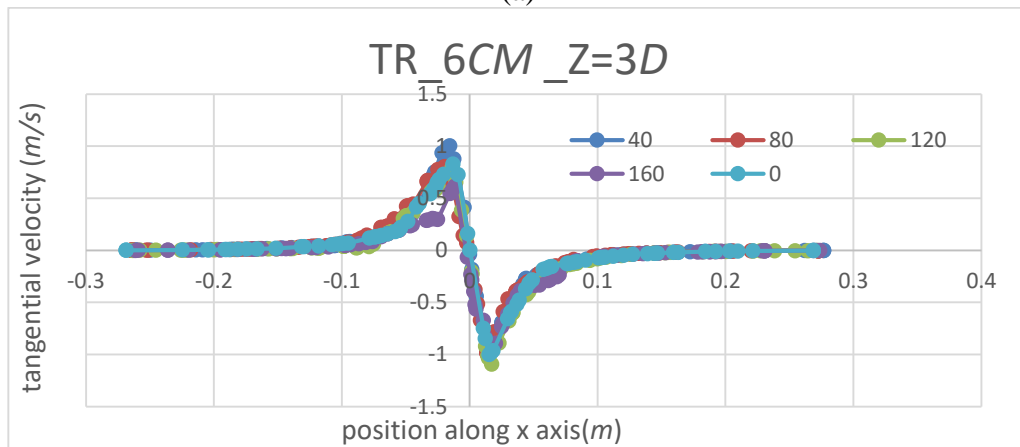
(b)
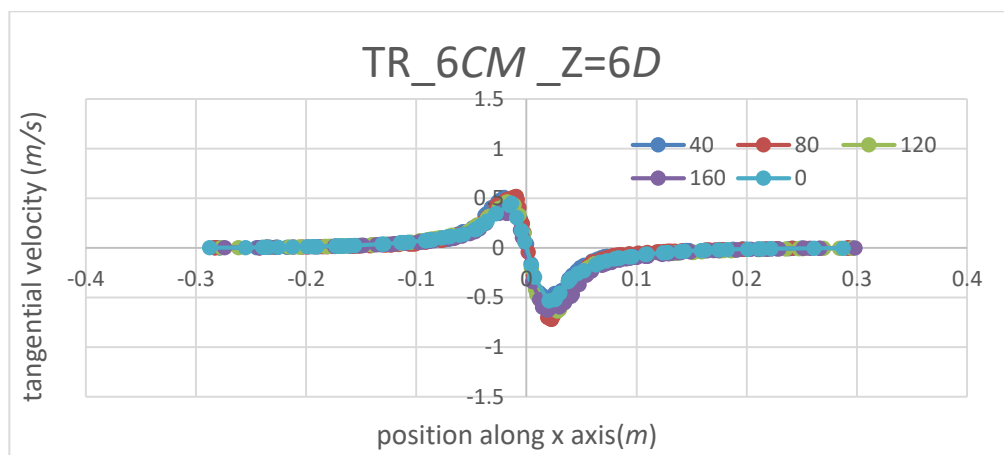
(c)

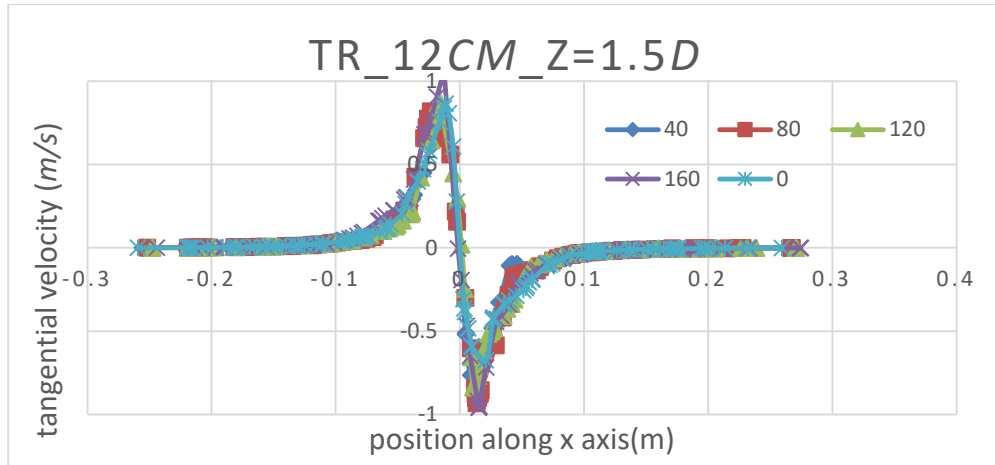**Figure 6.9: Comparison of tangential velocity at (a) *z=1.5D*, (b) *z=3D*, (c) *z=6D* for triangular cross-section shape for 6 *cm* pipe**
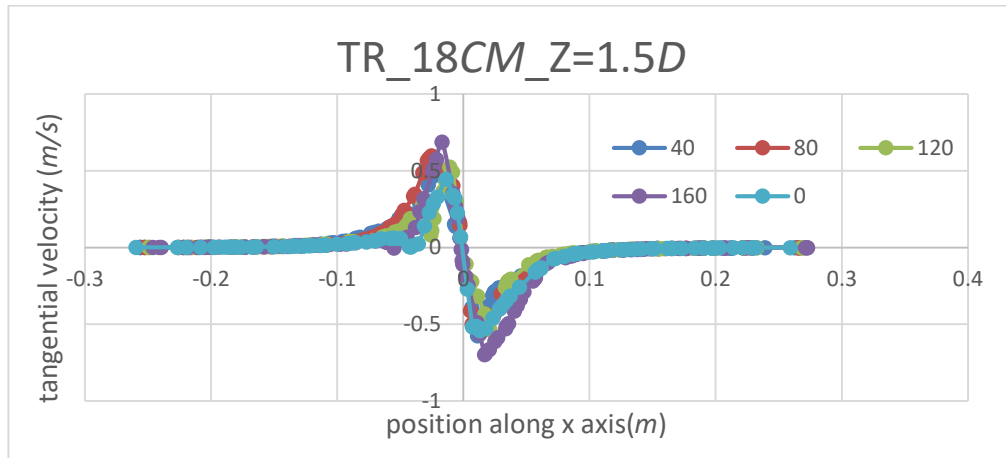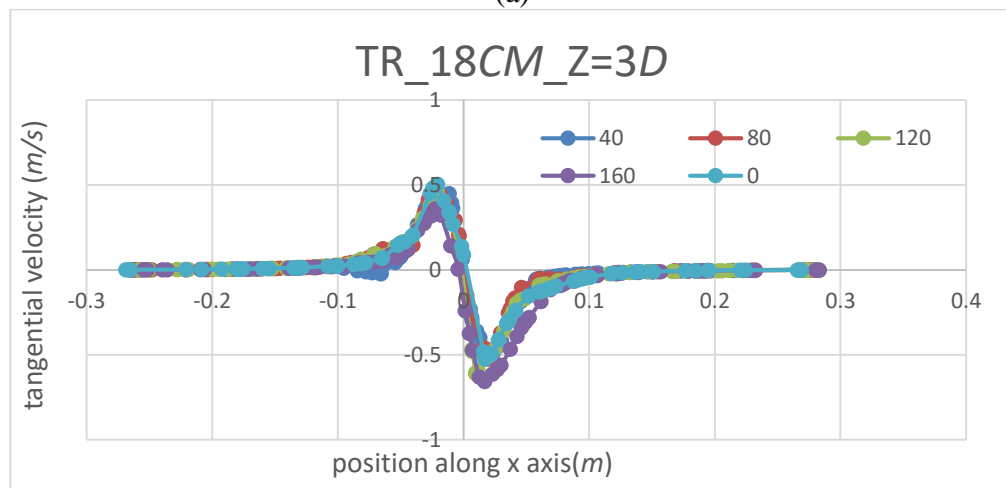
The above tangential velocity plots indicate following:

(a) For rectangular cross-section pipe, it is seen that if twist rate is increased tangential velocity increases with increasing twist rate along x axis. The curve for 40 *degree/meter* twist rate is a bit different to the tangential velocity of zero twist rate. However, tangential velocity increases much for 120 and 160 *degree/meter* twist rate in comparison to 0 and 40 *degree/meter* twist rates which is a clear indication of swirl indicating more mixing for the higher twist rates.

(b) For Square cross-section pipe also, if twist rate is increased tangential velocity increases with increasing twist rate along x axis. But for the triangular cross-section pipe tangential velocity changes very little with increasing twist rate.

6.2 Pipe Length effect

For all the non-circular cross-sectional shapes with 160 degree per meter twist rate, tangential velocity along x direction at different locations (1.5D, 3D, 6D) has been plot in fig. 6.10 (Rectangular), 6.11 (Square) and 6.12 (Triangular) together to find out the overall effect on tangential velocity.

6.2.1 Comparison of tangential velocity: Rectangular Cross section
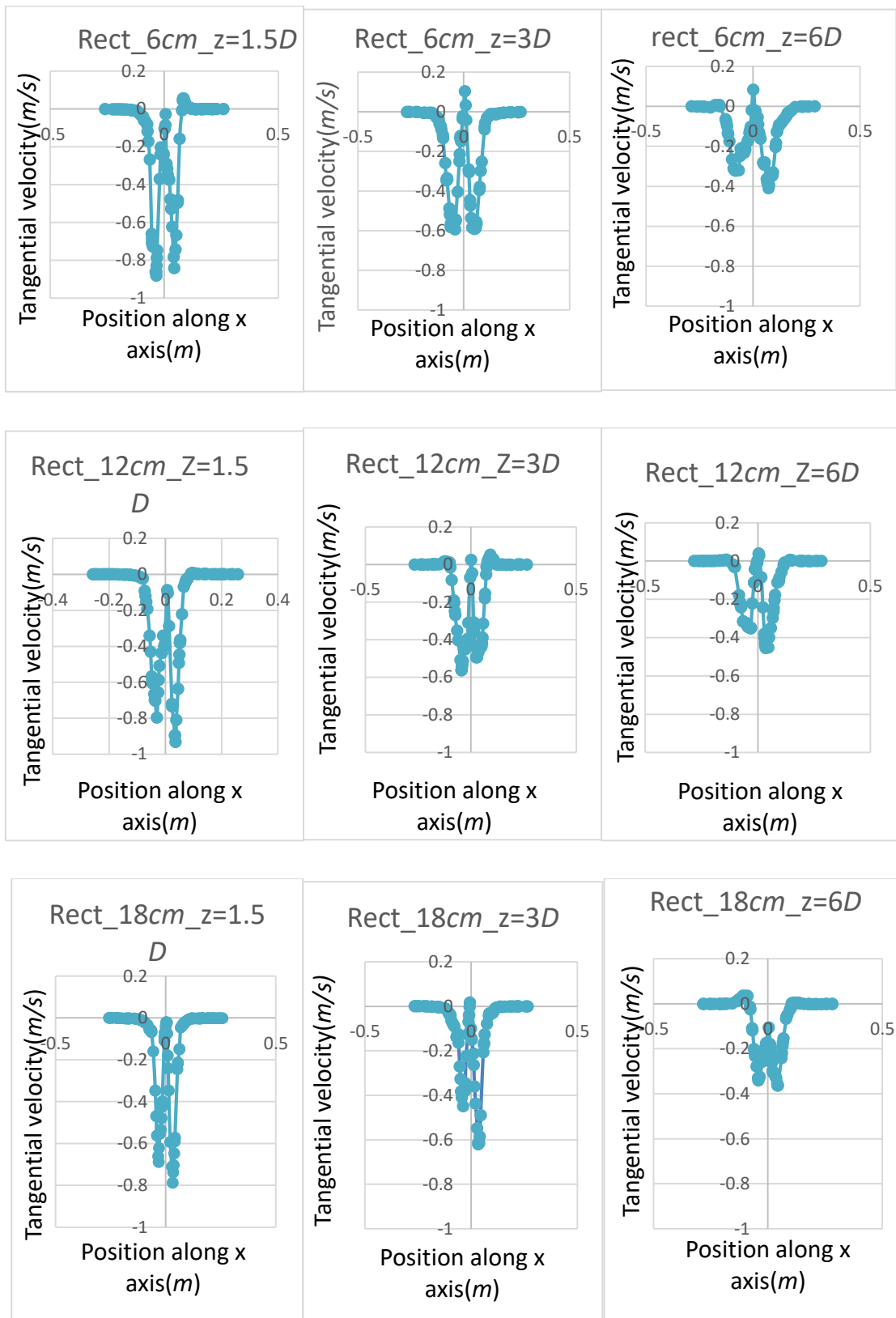
Figure 6.10: Comparison of tangential velocity for rectangular cross-section shape (Pipe length Effect)

6.2.2 Comparison of tangential velocity: Square Cross section
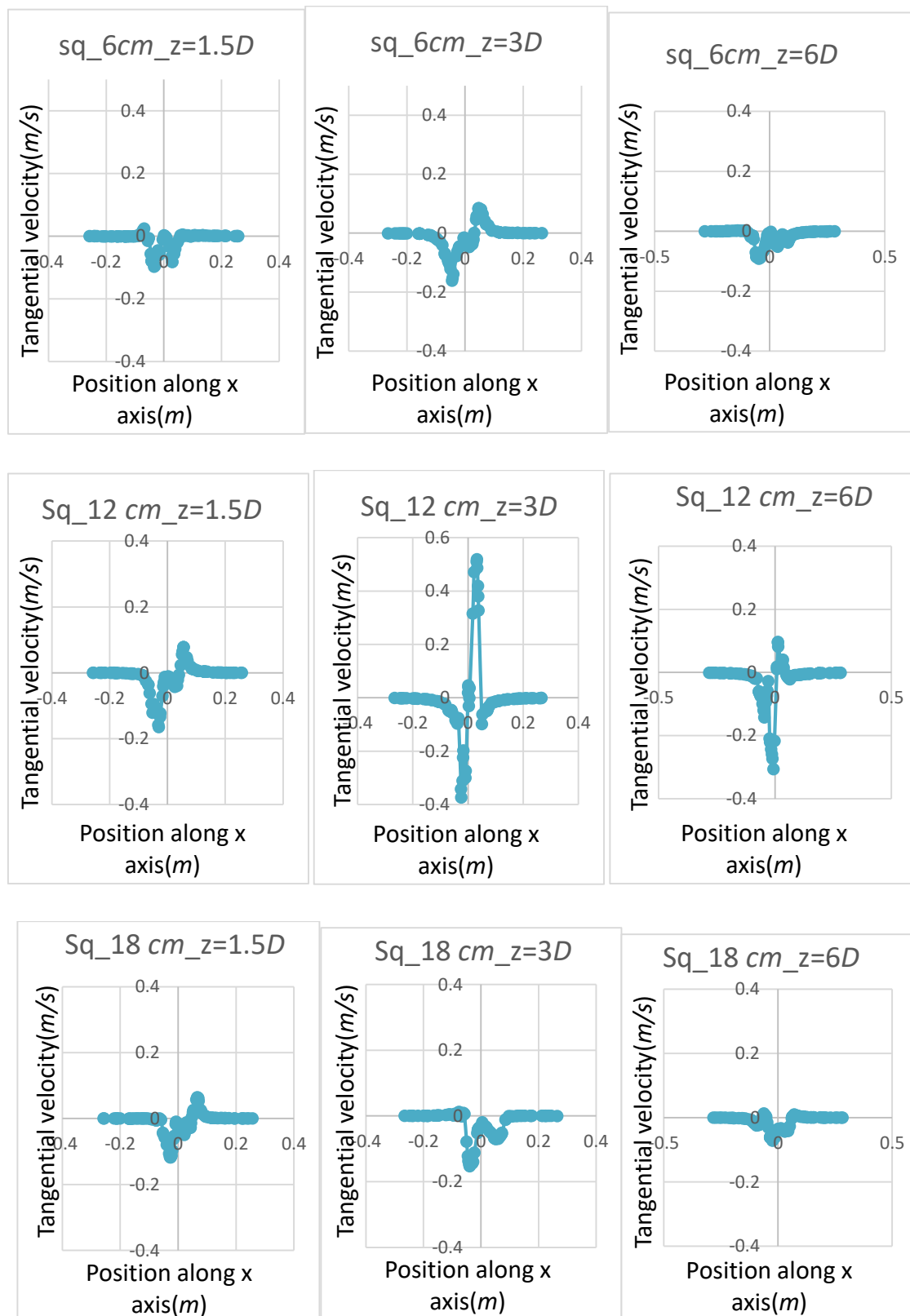
Figure 6.11: Comparison of tangential velocity at for square cross-section shape (Pipe length Effect)

6.2.3 Comparison of tangential velocity: Triangular Cross section
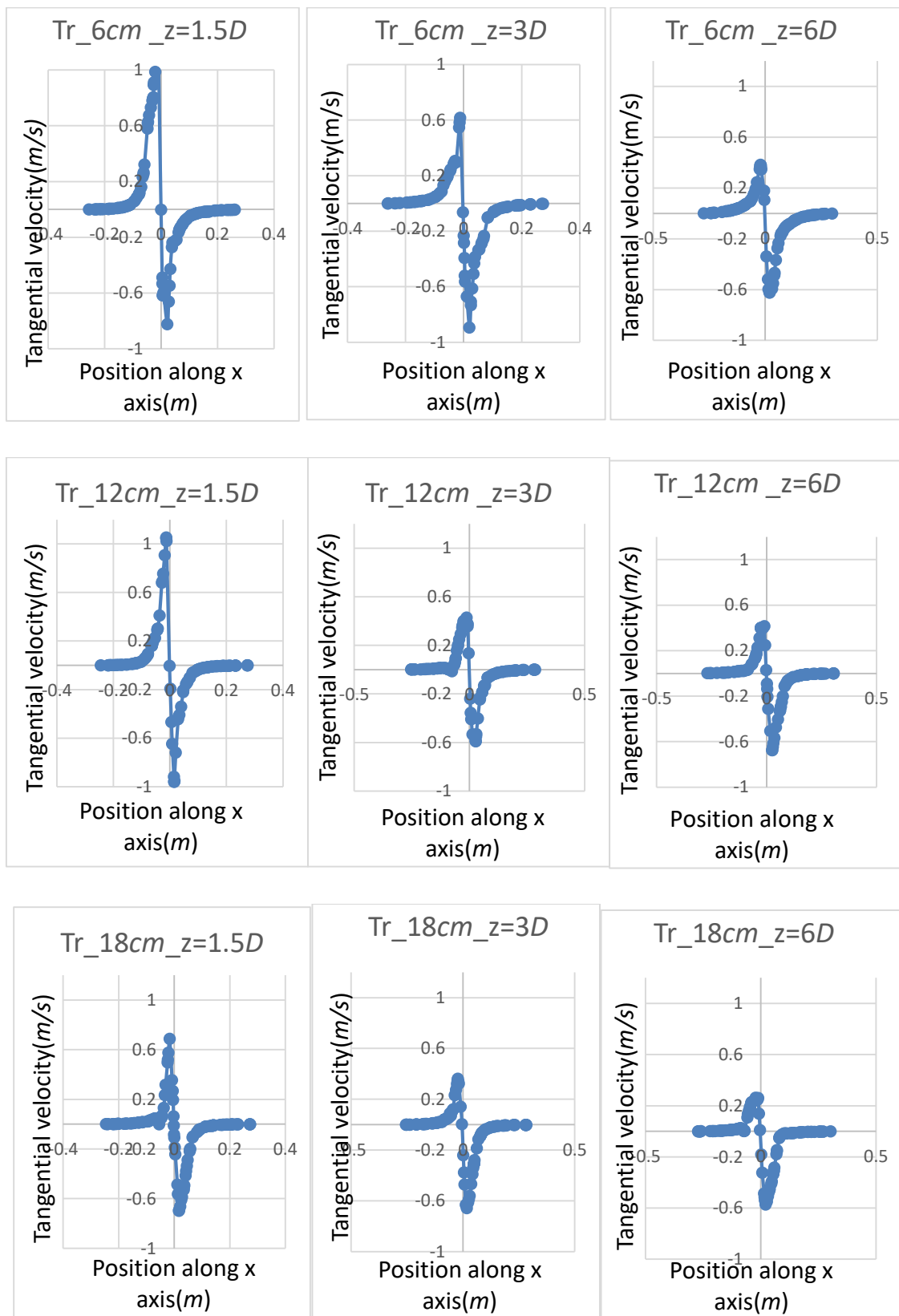
Figure 6.12: Comparison of tangential velocity for triangular cross-section shape (Pipe length Effect)

From the Fig 6.10, 6.11, 6.12, respectively, the following points have been found:

(a) For all the shapes, there is a definite effect of pipe length on tangential velocity at different locations. With increasing pipe length, at the same location, tangential velocity is decreasing in almost all the cases. This is same for all the non-circular cross-sectional shape

(b) 6 *cm* pipe with the same twist rate is creating better turbulence and mixing than 12 *cm* and 18 *cm* pipes for all the non-circular jets.

6.3 **Entrainment**

Mass flow rate has been checked for cross-sectional shapes. A region has been created though which jet air go through. For all the circular and non-circular jets, mass flow has been observed from the computational result. It has been shown in Fig. 6.13. After observing the mass flow at that region, it has been found out that non-circular jets are giving better entrainment than the circular jet and rectangular jet is having the most entrainment.
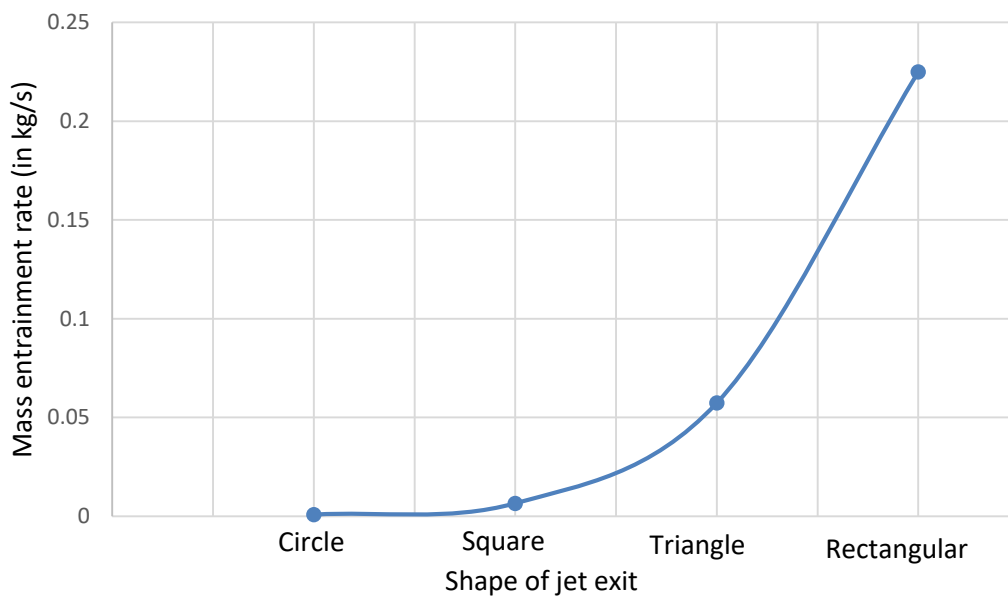
Figure 6.13: Entrainment for different circular and non-circular jets

6.4 **General comparison of twist rate**

Tangential velocity along x direction at different locations (z=1.5 D, z=3 D, z=6 D) has been compared in a single graph shown in Fig 6.14 for Square Cross-sectional pipe. Here two different twist rates (80 and 160 *degree per meter*) is considered.
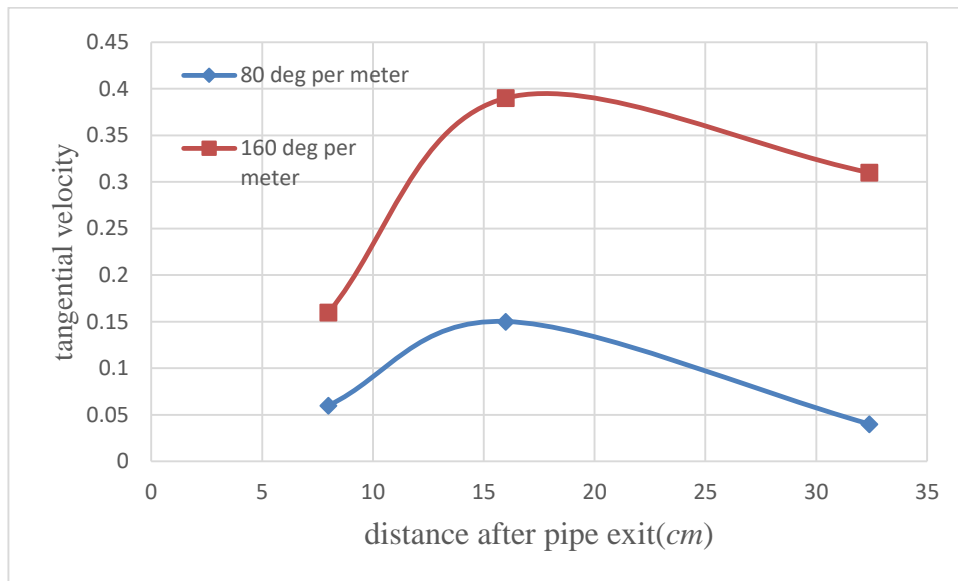
Figure 6.14: Comparison of twist rate: square Cross section

It is seen that if twist rate is increased, tangential velocity along x axis direction increases. In all the locations (*z*=1.5 D, *z*=3 D, *z*=6 D), tangential velocity for the 160 *degree per meter* twist rate is much higher than the tangential velocity of 80 *degree per meter* twist rates which indicates more turbulence and mixing with increasing twist rate.

6.5 **Saddle shape profile**

For the rectangular cross-sectional shape, velocity at different location (1.5D, 3D, 6D) has been compared between the pipe of 14.4 *degree per meter* twist rate and pipe without any twist rate at different locations which is shown in Fig 6.15 (a)*z*=1.5D (b)*z*=3D (c)*z*=6D.
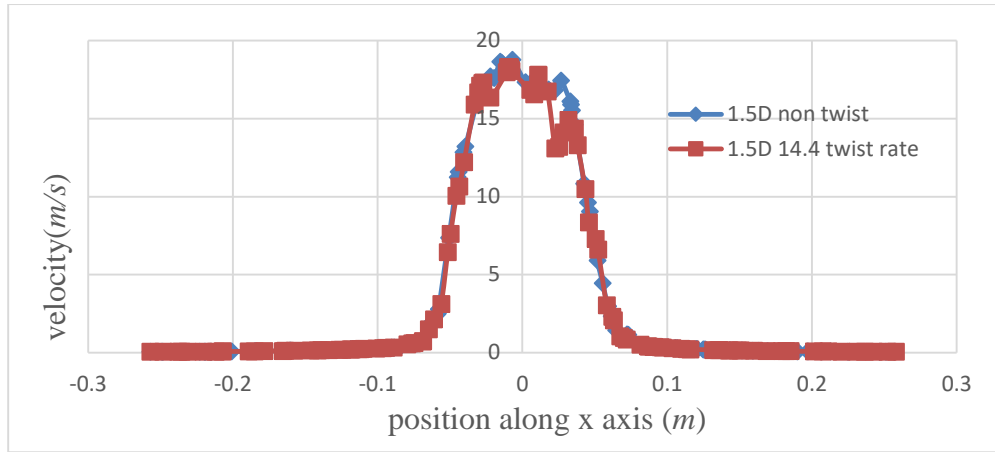
(a)
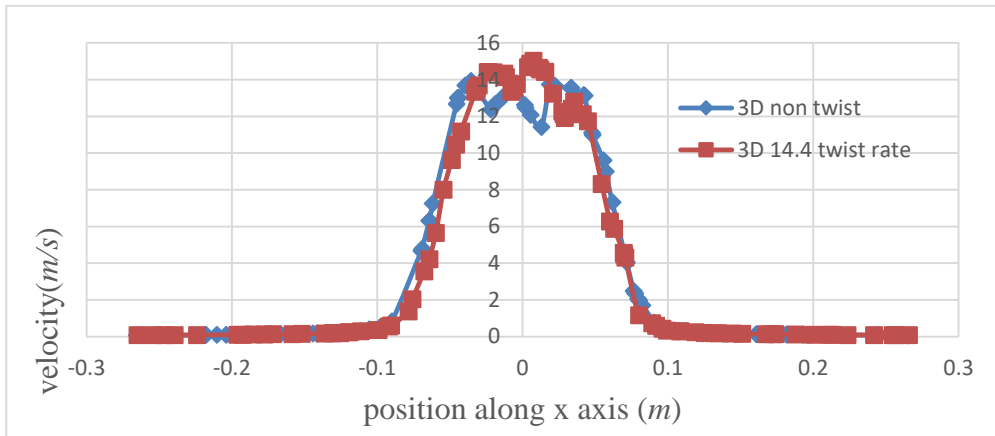
(b)
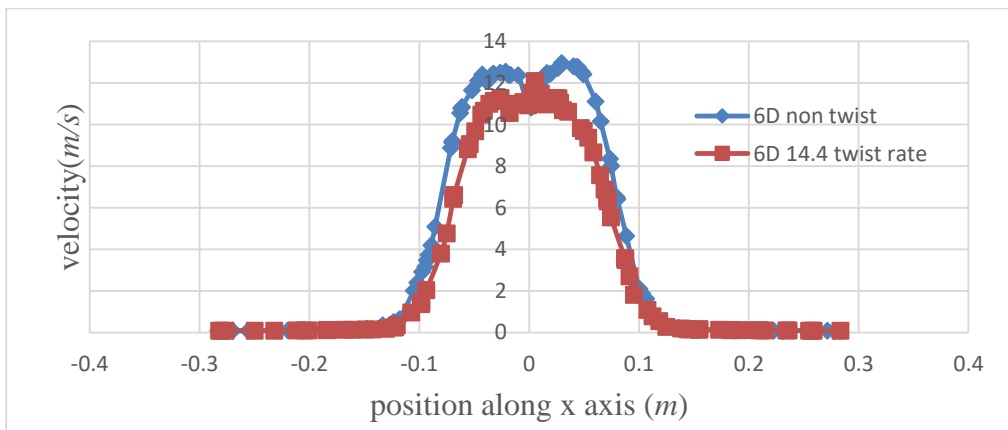
(c)

Figure 6.15: Saddle shape Profile at (a)z=1.5*D* (b)z=3*D* (c)z=6*D*

It is observed that saddle shape profile occurs for both the case. However, at 6*D* location,

for the pipe of 14.4 *degree per meter* twist rate, saddle shape profile almost disappears

while for the pipe without twist rate it still appears. This indicates better mixing for the pipe of 14.4 *degree per meter* twist rate than pipe without any twist rate [1].

6.6 Flow visualization:Comparison between Rectangular, Square and trianglular Cross section

Velocity contour plots and streamline plots for all the shapes have been observed for proper flow visualization in Fig 6.16 for rectangular cross-section shape (a) Velocity plot, (b)Streamline plot, Fig 6.17 for square cross-section shape (a) Velocity plot, (b)Streamline plot, Fig 6.18 for triangular cross-section shape (a) Velocity plot, (b)Streamline plot . Three different locations after nozzle exit has been chosen for observing the effects ($1.5D$, $3D$, $6D$). Streamline for all the non-circular shapes have been observed from the plane at the pipe exit.
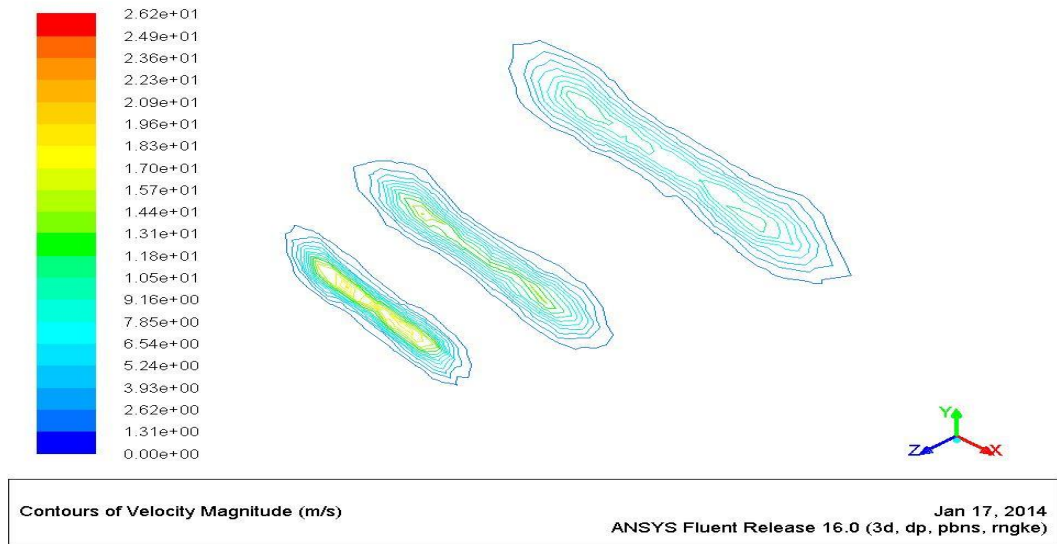
(a)
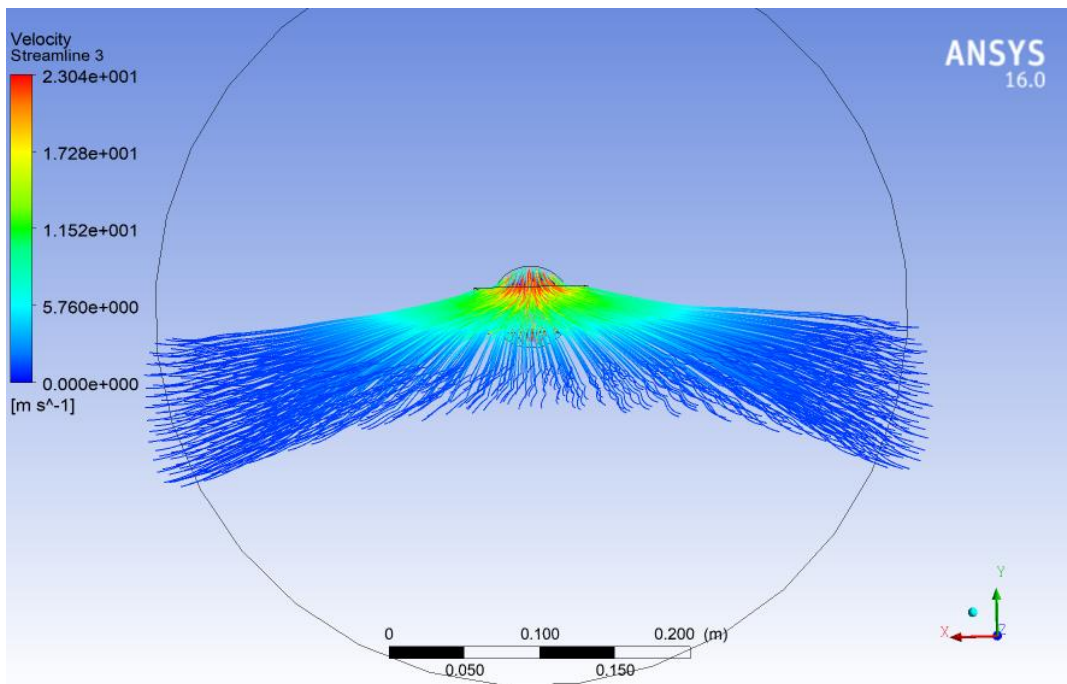
(b)

Figure 6.16: (a) Velocity Contour plot of velocity magnitude (b)Streamline plot for rectangular cross section
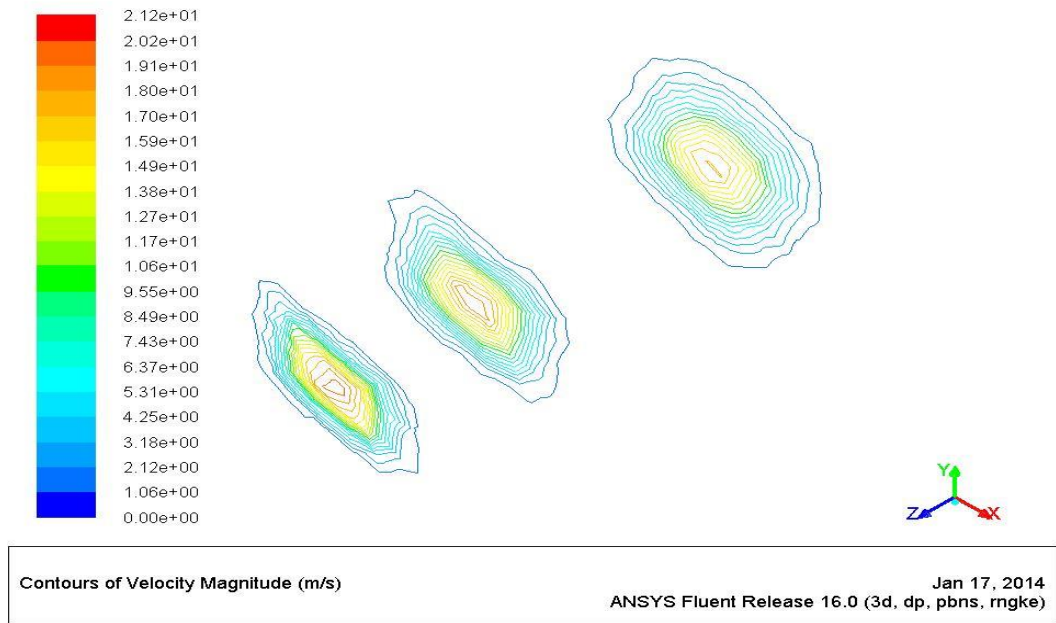
(a)
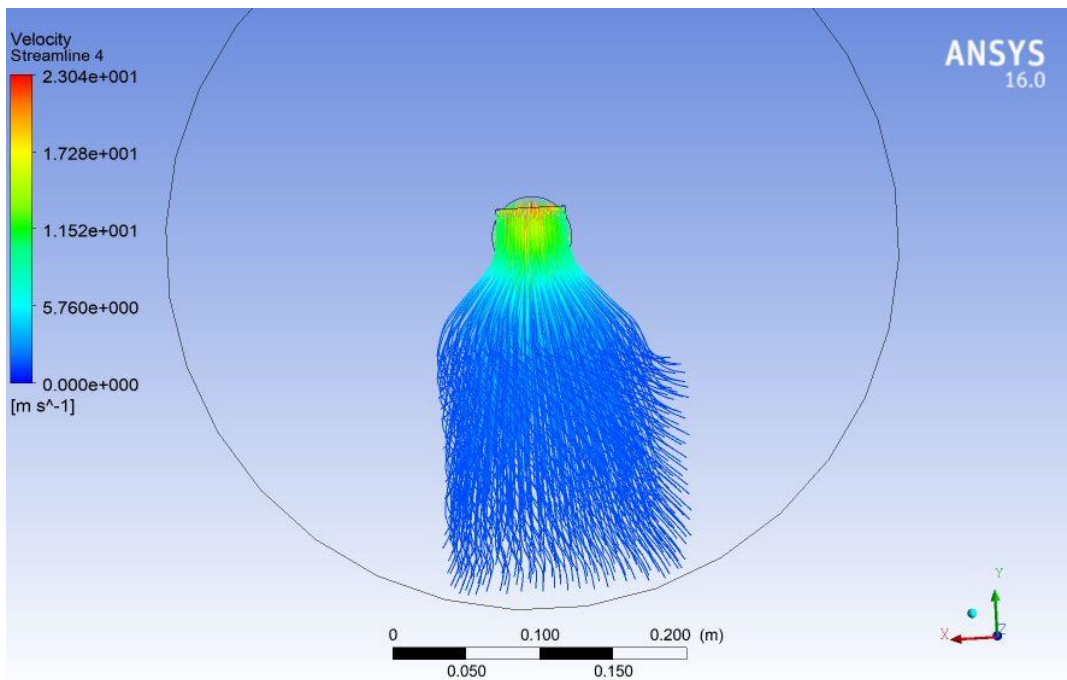
(b)

Figure 6.17: (a) Velocity Contour plot of velocity magnitude (b)Streamline plot for square cross section
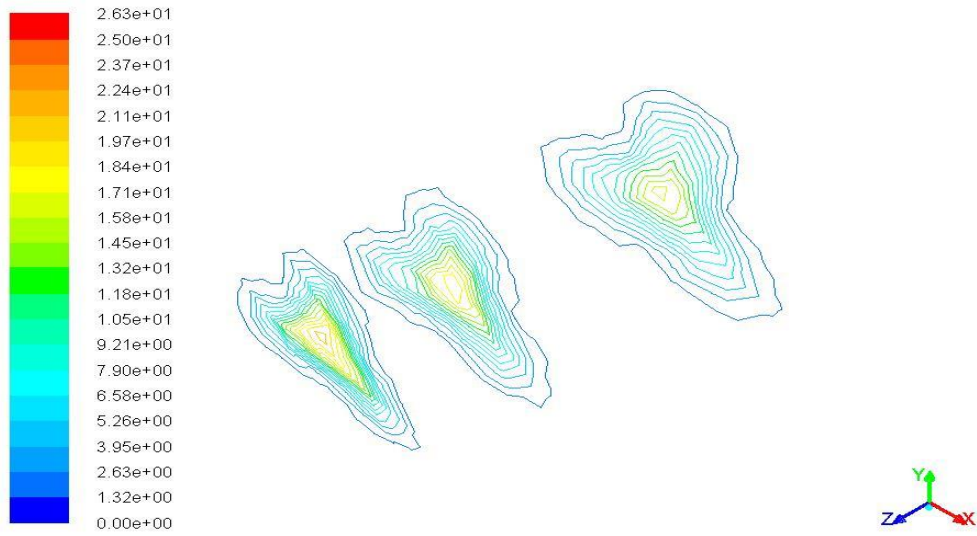
(a)
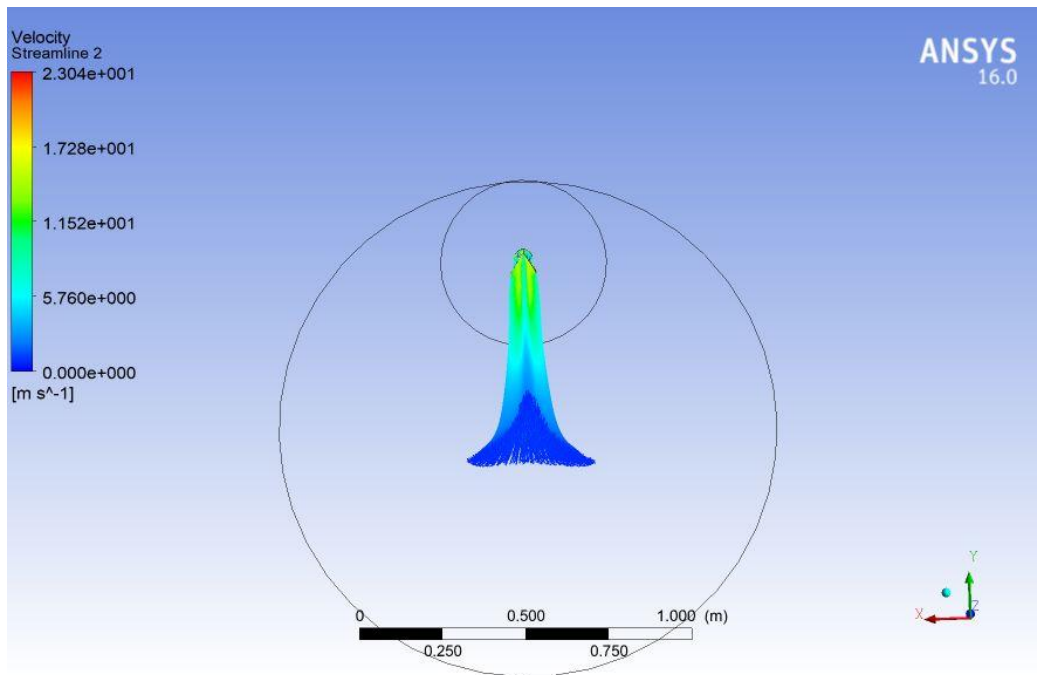
(b)

Figure 6.18: (a) Velocity Contour plot of velocity magnitude (b)Streamline plot for triangular cross section

From the above plots the following points have been found:

(a) From the velocity contour plot it has been seen that for the rectangular cross section, after the pipe exit flow is creating two different circular shape creating rotational motion. It ultimately creates saddle shape velocity profile which helps to create more turbulence and mixing. This same incident is evident from the streamline plot. From the plot, it is seen that the streamline plot is symmetric with respect to x axis and the equation of this pattern on the upper side of the axis is

$-9.2e+03*x^4+3.7e+03*x^3-4.7e+02*x^2+19*x+0.65.$

(b) From the velocity magnitude and streamline plots, for the square cross section, it has been seen that jet flow goes away from pipe exit creating a large square shape. From the plot, it is seen that the streamline plot is symmetric with respect to x axis and the equation of this pattern on the upper side of the axis is $-1.1e+05*x^4+2.3e+04*x^3-1.6e+03*x^2+43*x+0.69.$

(c) From the velocity contour plot for the triangular cross section, it has been seen that flow goes away from the pipe exit creating a triangular shape which is also observed from the streamline plot. From the plot, it is seen that the streamline plot is symmetric with respect to vertical y axis and the equation of this pattern on the right side of the y axis is $-26*x^3-4.5*x^2+3.4*x+0.32.$

Chapter 7
Conclusion

7.1 Conclusion

The analysis was done on free jet flows and the basic idea was to allow the air to flow out of a pipe having different cross-sectional geometries. With a centrifugal blower assembled at the inlet of the 'Air Flow Bench', the pipe was incorporated at the very outlet where the fluid gained a certain amount of velocity. The 'Developing Zone' was emphasized mainly in this research. The parameters that were taken into consideration were Velocity Profiles, Potential Core length, turbulence intensity, tangential velocity etc. The velocity profiles along the radial direction for different axial location were compared among different pipes. The spreading of the jet was also observed along with the velocity profiles.

The pipes had outlets of varying shapes such as circular, square and rectangular, triangular with and without twist rates and these resulted in corresponding case scenarios.

Firstly, the circular, square and rectangular, triangular pipes were observed without any twist rates. The axial velocity degradation for triangular jet is maximum while for circular jet is minimum along the jet axis. The potential core length for circular jet is maximum, while non-circular jets show lower core length than circular jet. The rectangular jet core length is minimum amongst four shapes. This also means that the shear layers from the edges converged quicker in case of rectangular pipe.

Rectangular jet showcases saddle shape profile clearly at $6D$, while it is initiated at $1.5D$ distance from jet exit. This saddle shape profile makes the jet spread faster. It is found that the rectangular cross section gives maximum jet spread while triangular cross section gives minimum jet spread at $6D$ distance.

From the analysis it can be seen that the maximum turbulence intensity along the jet axis is also seen to decrease for non-circular jets as compared to circular jet. The location of maximum turbulence intensity is closer for non-circular jets (exception being square jet) than the circular jets. This indicates that the maximum mixing takes place in closer vicinity for non-circular jets. Hence it can be concluded that the non-circular jets especially rectangular jet is superior in performance than the circular jets when it comes to jet spread, mixing and turbulence.

Finally, non-circular jets are analyzed changing the twist rate of the pipe and changing the pipe length to observe the effect of twist rate. For rectangular pipe, it is seen that if twist rate is increased tangential velocity increases with increasing twist rate indicating more mixing for the higher twist rates. Amongst all the non-circular shapes, twist rate has the least effect on the triangular jet.

The twisted jet modifier pipe length has an opposite effect wherein, smaller the length of pipe higher is the tangential velocity. With increasing pipe length, at the same location, tangential velocity is decreasing in almost all the cases. 6cm pipe with the same twist rate is creating better turbulence and mixing than 12 *cm* and 18 *cm* pipes for all the non-circular jets.

Flow has been visualized to analyze the flow properly using velocity contour and streamline plot. From the velocity contour plot it has been seen that for the rectangular cross section, after the pipe exit flow is creating two different circular shape creating rotational motion. It ultimately creates saddle shape velocity profile which helps to create more turbulence and mixing. This same incident is evident from the streamline plot. This saddle shape velocity profile ultimately disappears with increasing twist rate which indicates more mixing for rectangular jet with increasing twist rate.

7.2 <u>Recommendations</u>

Here are some of the recommendations for the future expansion of the analysis:

1. Research work has been done considering the incompressible fluid. Compressible fluid flow can be analyzed in further study. In case of compressible flow, density will not be constant. Density effects will be present. Due to density variation, jet flow velocity would be much higher which would have further various compressibility effects on the flow characteristics. It would be interesting to see those effects in future study.
2. In case of future study, flat jet flow can be taken into consideration. It will create a flat spray characterized by a low flow rate and small size droplets which would be interesting to work on in future.
3. For the jet flow, use of diffuser can be considered in future. Using diffuser will ultimately slow down the flow but it might enhance the mixing characteristics.

Another advantage from these diffusers might be to circulate the flow in different directions.

4. In the present research, for the rectangular pipe, aspect ratio is 2.5. In the future study, aspect ratio can be changed to see the effects. Similarly, for all other non-circular jets, exit shape can be modified to observe the effects.

References

[1] Y. Tsuchiya and C, Horikoshi (1986), "On the spread of rectangular jets", Experiments in Fluids 4, 197-204.

[2] Chowdhury, T. (2004), "*EXPERIMENTAL STUDY OF SWIRLING COAXIAL JETS"*. Bangladesh University of Engineering & Technology.

[3] Shih, D., Tseng, D., Alkislar, M., Gogineni, D., Visbal, D., Lourenco, D. and Wilbur, M. (1999), "*Quantitative Flow Visualization"*.

[4] S.B. Müller, L. Kleiser, (2008), "Large-eddy simulation of vortex breakdown in compressible swirling jet flow", Computers & Fluids Volume 37, Issue 7, Pages 844-856.

[5] Zheng, X., Jian, X., Wei, J., & Wenzheng, D. (2016), "Numerical and Experimental Investigation of Near-Field Mixing in Parallel Dual Round Jets", *International Journal of Aerospace Engineering, 2016*.

[6] Peram, L., & Bommera, B. (2016), "Experimental Analysis on Incompressible circular and non-circular Fluid Jet through Passive Control Method", *IOSR Journal of Mechanical and Civil Engineering (IOSR-JMCE)*, 15-21. doi: 10.9790/1684-16053021521.

[7] Gutmark, E. J., & Grinstein, F. (1999), "FLOW CONTROL WITH NONCIRCULAR JETS", *Annu. Rev. Fluid Mech*.

[8] Hebbar, K. S., Sridhara, K., & Paranjpe, P. (1970, February), "Performance of Conical Jet Nozzles in Terms of Discharge Co-efficient", *Journal of the Aeronautical Society of India, 22*(1).

[9] Boguslawski, L. and Popiel, C. (1979), " Flow structure of the free round turbulent jet in the initial region", *Journal of Fluid Mechanics*, 90(03), p.531.

[10] Crighton, D. and Gaster, M. (1976), "Stability of slowly diverging jet flow", *Journal of Fluid Mechanics*, 77(02), p.397.

[11] Sforza, P. M.; Steiger, M. H.; Trentacoste, N, (1966), "Studies on three-

dimensional viscous jets", AIAA J. 4, 800- 806.

[12] Yevdjevich, V. M. (1966), "Diffusion of slot jets with finite length width ratios", Hydraulic Paper, Colorado State Univ. 2, 1-40.

[13] Miller, R.S. ,Madnia, C.K., and Givi, P., (1995), "Numerical Simulation of Non-circular jets. Computers and Fluids", Vol-24, No-1, pp. 1-25.

[14] Öçer, N.E., Taşar, G., Uzol, O., and Özgen, S., (2012), "Flow Structure and Turbulence in Near Fields of Circular and Noncircular Jets", Progress in Flight Physics 3 (2012) 41-52.

[15] duPlessis, M. P.; Wang, R. L.; Kahawita, R. (1974), "Investigation of the near-region of a   square jet", J. Fluids Eng. 96, 246-251.

[16] Islam, M. (1995), "*Flow Characteristics in the Near Field of a Circular Splined Jet",* M.Sc Thesis Dissertation. Bangladesh University of Engineering & Technology.

[17] Krothapalli, A., Baganoff, D., Karamcheti, K. (1981), "On the mixing of a rectangular jet" J. Fluid Mech. 107,201-220.

[18] Marsters, G. F. (1981), "Spanwise velocity distribution in jets from rectangular slots", AIAA J. 19, 148-152.

[19] Sfeir, A. A. (1976), "The velocity and temperature fields of rectangular jets", Int. J. Heat Mass Transf. 19, 1289-1297.

[20] Komori, S. and Ueda, H. (1985), "Turbulent flow structure in the near field of a swirling round free jet", *AIP: Physics of Fluid,* 28, 2075.

[21] Billant, P., Chomaz, J. and Huerre, P. (1998), "Experimental study of vortex breakdown in swirling jets", *Journal of Fluid Mechanics*, Volume - 376, pp.183-219.

[22] Loiseleux, T. and Chomaz, J. (2003), "Breaking of rotational symmetry in a swirling jet experiment", *AIP:Physics of Fluids*, 15(2), pp.511-523.

[23] Hossain, M. (2008), "*Experimental Study of Flow Characteristics in the Near Field of a Thermally Stratified Co-Axial Free Jet",* M.Sc. Thesis Dissertation.

Bangladesh University of Engineering & Technology.

[24] Parekh, D., Kibens, V., Glezer, A., Wiltse, J. and Smith, D. (1996), "Innovative jet flow control - Mixing enhancement experiments", *34th Aerospace Sciences Meeting and Exhibit,* AIAA paper 96-0308.

[25] Hashiehbaf, A. and Romano, G. (2013), "Particle image velocimetry investigation on mixing enhancement of non-circular sharp edge nozzles", *International Journal of Heat and Fluid Flow*, 44, pp.208-221.

[26] SMITH, B. and GLEZER, A. (2002), "Jet vectoring using synthetic jets". *Journal of Fluid Mechanics*, 458.

[27] Atmaca, M., Kurtulus, A., Aydin, M., Girgin, I. and Ezgi, C. (2016), "A Cfd And Experimental Study On Open Jet Flows", In: *ICCHMT 2016*. Cracow, Poland: ICCHMT 2016.

[28] Zhang, X. (2000), "Turbulence measurements of an inclined rectangular jet embedded in a turbulent boundary layer", *International Journal of Heat and Fluid Flow*, 21(3), pp.291-296.

[29] Gradeck, M., Kouachi, A., Dani, A., Arnoult, D. and Boréan, J. (2006), "Experimental and numerical study of the hydraulic jump of an impinging jet on a moving surface", *Experimental Thermal and Fluid Science*, 30(3), pp.193-201.

[30] Portoghese, F., Ferrante, L., Berruti, F., Briens, C. and Chan, E. (2008), "Effect of injection-nozzle operating parameters on the interaction between a gas–liquid jet and a gas–solid fluidized bed", *Powder Technology*, 184(1), pp.1-10.

[31] Alnahhal, M. and Panidis, T. (2009), "The effect of sidewalls on rectangular jets", *Experimental Thermal and Fluid Science*, 33(5), pp.838-851.

[32] Chong, T., Joseph, P. and Davies, P. (2009), "Design and performance of an open jet wind tunnel for aero-acoustic measurement", *Applied Acoustics*, 70(4), pp.605-614.

[33] Sharif, M. and Banerjee, A. (2009), "Numerical analysis of heat transfer due to confined slot-jet impingement on a moving plate", *Applied Thermal Engineering*, 29(2-3), pp.532-540.

[34] Lee, W., Park, Y., Kwon, K. and Taghavi, R. (2010), "Control of shear perturbation in coaxial swirling turbulent jets", *Aerospace Science and Technology*, 14(7), pp.472-486.

[35] Xu, P., Yu, B., Qiu, S., Poh, H. and Mujumdar, A. (2010), "Turbulent impinging jet heat transfer enhancement due to intermittent pulsation", *International Journal of Thermal Sciences*, 49(7), pp.1247-1252.

[36] Sung, M. and Mudawar, I. (2006), "Experimental and numerical investigation of single-phase heat transfer using a hybrid jet-impingement/micro-channel cooling scheme", *International Journal of Heat and Mass Transfer*, 49(3-4), pp.682-694.

[37] Mallinson, S., Reizes, J. and Hong, G. (2001), "An experimental and numerical study of synthetic jet flow", *The Aeronautical Journal*, pp.41-49.

[38] Narayanan, V., Seyed-Yagoobi, J. and Page, R. (2004), "An experimental study of fluid mechanics and heat transfer in an impinging slot jet flow", *International Journal of Heat and Mass Transfer*, 47(8-9), pp.1827-1845.

[39] Wygnanski, I. and Fiedler, H. (1969), "Some measurements in the self-preserving jet", *Journal of Fluid Mechanics*, 38(03), p.577.

[40] Patankar, S., Basu, D. and Alpay, S. (1977), "Prediction of the Three-Dimensional Velocity Field of a Deflected Turbulent Jet", *Journal of Fluids Engineering*, 99(4), p.758.

[41] Patankar, S., Liu, C. and Sparrow, E. (1977), "Fully Developed Flow and Heat Transfer in Ducts Having Streamwise-Periodic Variations of Cross-Sectional Area", *Journal of Heat Transfer*, 99(2), p.180.

[42] Leylek, J. and Zerkle, R. (1994), "Discrete-Jet Film Cooling: A Comparison of Computational Results With Experiments", *Journal of Turbomachinery*, 116(3), p.358.

[43] Garg, V. and Gaugler, R. (1997), "Effect of Velocity and Temperature Distribution at the Hole Exit on Film Cooling of Turbine Blades", *Journal of Turbormachinery*, [online] 119, pp.343-351.

[44] Wegner, B., Huai, Y. and Sadiki, A. (2004), "Comparative study of turbulent

mixing in jet in cross-flow configurations using LES", *International Journal of Heat and Fluid Flow*, 25(5), pp.767-775.

[45] Pathak, M., Dewan, A. and Dass, A. (2006), "Computational prediction of a slightly heated turbulent rectangular jet discharged into a narrow channel crossflow using two different turbulence models", *International Journal of Heat and Mass Transfer*, 49(21-22), pp.3914-3928.

[46] Needham, D., Riley, N. and Smith, J. (1988), "A jet in crossflow. *Journal of Fluid Mechanics",* 188(-1), p.159.

[47] Reichle, C. (2004), "Blower Assisted Heating and Defogging System for Small Aircrafts", US 7,017,828 B2.

[48] Payri, R., Molina, S., Salvador, F. and Gimeno, J. (2004), "A study of the relation between nozzle geometry, internal flow and sprays characteristics in diesel fuel injection systems", KSME International Journal, 18(7), pp.1222-1235.

[49] Nasif, G., Barron, R. and Balachandar, R. (2015), "THE APPLICATION OF JET IMPINGEMENT FOR PISTON COOLING", 11th International Conference on Heat Transfer, Fluid Mechanics and Thermodynamics. pp.481-486.

[50] Glynn, Colin & O'Donovan, Tadhg & Murray, D. (2005), "Jet Impingement Cooling", Proceedings of the 9th UK National Heat Transfer Conference.

[51] N. Vibhakar, N. (2012), "Studies on Radial Tipped Centrifugal Fan", Ph. D. Dissertation. Veer Narmad South Gujarat University, Surat.

[52] Hunt, J. (1973), "Mathematical Models of Turbulence", Journal of Fluid Mechanics, 57(04), p.826.

[53] Singh, O., Khilwani, R., Sreenivasulu, T. and Kannan, M. (2011) "PARAMETRIC STUDY OF CENTRIFUGAL FAN PERFORMANCE: EXPERIMENTS AND NUMERICAL SIMULATION", International Journal of Advances in Engineering & Technology, May 2011. IJAET, 1(2), pp.33-50.

[54] Fehse, K. and Neise, W. (1999), "Generation Mechanisms of Low-Frequency Centrifugal Fan Noise", AIAA Journal, 37(10), pp.1173-1179.

[55] W.R. Quinn, (2006), "Upstream nozzle shaping effects on near field flow in round turbulent free jets", Eur. J. Mech.-B/Fluids, 25 (3), pp. 279-301.

[56] Gupta, V. (2017), "*Electrical Energy Equipment: Fans and Blowers Energy Efficiency Guide for Industry in Aisa. FANS AND BLOWERS*", Academia.edu.

[57] Versteeg, Henk Kaarle; Malalasekera, Weeratunge (2007), "*An introduction to Computational Fluid Dynamics: The Finite Volume Method*", Pearson Education.

[58] Amiot, Larry (2017), "About TRACC." *Tracc.anl.gov*. N.p., 2017. Web. 11 Sept. 2017.

[59] R., Premnath (2017, "Qualitative Air Flow Modelling and Analysis Of Data Centre Air Conditioning As Multiple Jet Array", Ph.D. Thesis Dissertation. Division of Safety and Fire Engineering, School of Engineering, Cochin University of Science and Technology.

[60] Rajaratnam, N. (1976), "*Turbulent Jets*", Burlington: Elsevier, Elsevier Science, ISBN: 9780080869964.

[61] ELBANNA, H., S. GAHIN, and M. I. I. RASHED (1983), "Investigation Of Two Plane Parallel Jets", *AIAA Journal* 21.7 (1983): 986-991.

[62] Batchelor, G., Moffatt, H. and Worster, M. (2000), "Perspectives in Fluid Dynamics: A Collective Introduction to Current Research", Cambridge University Press.

[63] CARAZZO, G., KAMINSKI, E. and TAIT, S. (2006), "The route to self-similarity in turbulent jets and plumes", Journal of Fluid Mechanics, 547(-1), p.137.

[64] Deo, R., Mi, J. and Nathan, G. (2004), "An Investigation of the Influence of Nozzle Aspect Ratio on the Velocity Field of Turbulent Plane Jet", 15th Australasian Fluid Mechanics Conference. Sydney: University of Sydney, Australia.

[65] Pope, S. (2015), "Turbulent flows", Cambridge: Cambridge University Press.

[66] List, E. (1982), "Turbulent Jets and Plumes", Annual Review of Fluid Mechanics, 14(1), pp.189-212.

[67] Michele Mossa, Francesca De Serio (2016), "Rethinking the process of detrainment: jets in obstructed natural flows" *Scientific Reports* volume 6, Article number: 39103.

[68] Y.M.Shim, R.N.Sharma, P.J.Richards, (2013), "Proper orthogonal decomposition analysis of the flow field in a plane jet", Experimental thermal and fluid science. Volume 51, Pages 37-55

[69] Mohammad Jafari, Hossein Afshin, Bijan Farhanieh, Atta Sojoudi, (2016), "Numerical investigation of geometric parameter effects on the aerodynamic performance of a Bladeless fan", AEJ - Alexandria Engineering Journal, Volume 55, Issue 1, Pages 223-233.

[70] Yue. Z (1999), "Air jet velocity decay in ventilation applications", *Bulletin No.48*, Building services division, Royal Institute of Technology, Sweden.

[71] Mi, J., Nathan, G. and Luxton, R. (2000), "Centreline mixing characteristics of jets from nine differently shaped nozzles", Experiments in Fluids, 28(1), pp.93-94.

[72] Quinn, W. (1992), "Turbulent free jet flows issuing from sharp-edged rectangular slots: The influence of slot aspect ratio", Experimental Thermal and Fluid Science, 5(2), pp.203-215.

[73] Quinn, W. (2007), "Experimental study of the near field and transition region of a free jet issuing from a sharp-edged elliptic orifice plate", European Journal of Mechanics - B/Fluids, 26(4), pp.583-614.

[74] Aleyasin, S., Tachie, M. and Koupriyanov, M. (2017)", "Statistical Properties of Round, Square, and Elliptic Jets at Low and Moderate Reynolds Numbers", Journal of Fluids Engineering, 139(10), p.101206.

[75] Quinn, W. (2005), "Measurements in the near flow field of an isosceles triangular turbulent free jet", Experiments in Fluids, 39(1), pp.111-126.

[76] Jiang, T., Lin, X. and Yang, M. (2017), "Study of the Effect of Combustion Chamber Shapes on the Mixture Formation and Combustion Characteristic on CNG-DI Engine".

[77] Banapurmath, N., Chavan, A., Bansode, S., Patil, S., Naveen, G., Tonannavar, S., Keerthi, N. and Tandale, M. (2015), "Effect of Combustion Chamber Shapes on the Performance of Mahua and Neem Biodiesel Operated Diesel Engines", Journal of Petroleum and Environmental Biotechnology, 6(4).

[78] Carolus, T. and Stremel, M. (2002), "Blade Surface Pressure Fluctuations and Acoustic Radiation from an Axial Fan Rotor Due to Turbulent Inflow", Acta Acustica united with Acustica, 88(4), pp.472-482(11).

[79] Mrinal Kaushik, Rakesh Kumar, Humrutha G. (2015), "Review of Computational Fluid Dynamics Studies on Jets", American Journal of Fluid Dynamics, p-ISSN: 2168-4707 e-ISSN: 2168-4715;2015; 5(A): 1-11.

[80] Turner. (1973), "Buoyancy Effects in Fluids", pp. 167

[81] Morton, B. R., G. I. Taylor, and J. S. Turner. (1956), "Turbulent gravitational convection from maintained and instantaneous sources", Proc. R. Soc. London, Ser. A 234: 1–23.